Aus dem
CharitéCentrum für Chirurgische Medizin
Klinik für Allgemein- & Viszeralchirurgie, Campus Benjamin Franklin
Kommissarische Direktorin: Prof. Dr. med. Katharina Beyer

# Habilitationsschrift

# Prognostische Risikostratifikation des resektablen exokrinen Pankreaskarzinoms

zur Erlangung der Lehrbefähigung
für die Chirurgie

vorgelegt dem Fakultätsrat der Medizinischen Fakultät
Charité-Universitätsmedizin Berlin

von

**Dr. med. Florian Nino Loch**
**aus Neunkirchen/Saar**

**Eingereicht:** **01/2024**
**Dekan:** **Prof. Dr. Joachim Spranger**

**Inhaltverzeichnis**

**Abkürzungen**

| | |
|---|---|
| PDAC | duktales Adenokarzinom des Pankreas, engl. pancreatic ductal adenocarcinoma |
| AMS | Arteria mesenterica superior |
| TC | Truncus coeliacus |
| AHC | Arteria hepatica communis |
| PA | Pfortader |
| VMS | Vena mesenterica superior |
| NCCN | National Comprehensive Cancer Network® |
| ECOG | Eastern Cooperative Oncology Group |
| DMI | direkte mikroskopische Infiltration |
| AJCC | American Joint Committee on Cancer |
| CT | Computertomographie |
| MRT | Magnetresonanztomographie |
| EUS | Endosonographie, engl. endoscopic ultrasound |
| MALDI | Matrix–Assistierte Laser–Desorptions–Ionisierung |
| TOF-MS | Flugzeitmassenspektrometrie, engl. time-of-flight mass spectometry |
| MALDI-MSI | bildgebende MALDI-Massenspektrometrie, engl. matrix-assisted laser desorption ionization mass spectometry imaging |
| HE-Färbung | Hämatoxylin-Eosin-Färbung |
| PET-CT | Positronen-Emissions-Tomographie-CT |
| ICT | Immuncheckpoint-Therapie |
| ROC | Operationscharakteristik eines Beobachters, engl. Receiver Operating Characteristic |
| TMAs | Gewebe-Mikroarrays, engl. tissue microarrays |
| AJCC | American Joint Committee on Cancer |

| | |
|---|---|
| UICC | Union for International Cancer Control |

# 1. Einleitung

## 1.1 Epidemiologie und Prognose des Pankreaskarzinoms

Es treten weltweit treten jährlich nahezu 500000 neue Fälle von Pankreaskarzinomen auf.[1] Das stadienübergreifende relative 5-Jahres-Überleben liegt nach dieser Diagnose bei 10%.[2] Zum Zeitpunkt der Diagnosestellung sind lediglich 15-20% der Pankreaskarzinome kurativ resektabel und selbst nach kurativer onkologischer Tumorresektion beträgt das stadienübergreifende 5-Jahres-Überleben lediglich 23-27%.[3, 4, 5, 6] Das Pankreaskarzinom hat somit mit dem Mesotheliom die ungünstigste Prognose aller maligner Tumoren und ist geschlechterübergreifend die vierthäufigste Krebstodesursache in Deutschland.[2]

## 1.2 Pathologische Einteilung der Pankreaskarzinome

Maligne Neoplasien des Pankreas sind im Wesentlichen epithelialen Ursprungs, d. h. Karzinome. Diese malignen Neoplasien des Pankreas lassen sich histopathologisch weiter aufteilen in exokrinen und endokrinen Ursprungs. In der Gruppe der exokrinen Pankreaskarzinome finden sich wiederum duktale und azinäre Karzinome. Das (exokrine) duktale Adenokarzinom des Pankreas (engl. pancreatic ductal adenocarcinoma, PDAC) ist die mit Abstand häufigste maligne Neoplasie des Pankreas mit einem Anteil von ca. 90%.[7] Viele Studien zur Untersuchung maligner Neoplasien des Pankreas beschränken sich deshalb auf die Untersuchung des PDAC. Die Behandlung exokriner und endokriner Neoplasien des Pankreas unterscheidet sich deutlich.[8, 9]

## 1.3 Grundlagen der Behandlungskonzepte exokriner Pankreaskarzinome

Grundsätzlich ist ein wesentliches Ziel der Behandlung aller Patient:innen nach Diagnosestellung eines exokrinen Pankreaskarzinoms die maximale Verlängerung der Überlebenszeit. Die onkologische Tumorresektion kann in definierten Befundkonstellationen einen deutlichen prognostischen Vorteil herbeiführen und stellt die einzige potentiell kurative Behandlungsoption des exokrinen Pankreaskarzinoms dar. [9, 10] Sie ist somit ein anzustrebendes Behandlungsziel. Im Falle einer Fernmetastasierung ist in der Regel von einer Resektion des Primärtumors abzusehen, da hierdurch kein prognostischer Vorteil für Patient:innen entsteht.[9, 11] Zusätzliche Vorrausetzung für eine onkologische Resektion ist die anatomische Resektabilität des Primärtumors. In Abwesenheit von Fernmetastasierung ist durch multimodale Therapiekonzepte aus

neoadjuvanter (Radio-)Chemotherapie, operativer Tumorresektion und adjuvanter Chemotherapie das Ziel die Anzahl der für eine Operation zugänglichen Tumoren sowie die Prognose von Patient:innen zu maximieren.[9] Im Falle vorhandener Fernmetastasen wird i. d. R. eine palliative Chemotherapie durchgeführt.[9] Zur Festlegung des individuell geeigneten Behandlungsregimes sind somit grundlegende Fragen an die prätherapeutische Ausbreitungsdiagnostik, ob eine Fernmetastasierung vorliegt und der Primärtumor anatomisch resektabel ist.[9]

### 1.3.1 Vorhandensein von Fernmetastasen

Bei Vorliegen von bildmorphologisch erkennbaren Fernmetastasen eines exokrinen Pankreaskarzinoms soll eine Resektion des Primärtumors nicht erfolgen. Dies gilt für sowohl für das Vorhandensein von Peritonealkarzinose als auch nicht regionale Lymphknotenmetastasen und Organmetastasen. [9, 12] Grund hierfür ist, dass nach aktuellem Wissensstand bei Vorhandensein von Fernmastasen sich durch eine operative Tumorresektion die Prognose nicht verbessert.[11, 13]

Gegenstand aktueller Studien ist die Frage, ob konkrete Subgruppen metastasierter Tumoren von einer Tumorresektion profitieren könnten. So kann die Resektion des Primärtumors zusammen mit synchron vorhandenen Oligometastasen (≤ 3) sowie die Resektion metachroner Oligometastasen (≤ 3) im Rahmen prospektiver Studien mit multimodalem Therapiekonzept erfolgen. [9, 12, 14]

### 1.3.2 Anatomische Resektabilität des Primärtumors

Ziel der operativen Tumorresektion soll die vollständige Entfernung des Tumors im Gesunden sein.[9] Zur Einschätzung der Wahrscheinlichkeit dieses Ziel zu erreichen hat sich in Abhängigkeit der Involvierung umgebender Gefäße durch den Tumor international folgende Einteilung etabliert in primär resektabel, borderline (grenzwertig) resektabel und lokal fortgeschritten (nicht resektabel) [9, 12, 15, 16]:

1) Primär resektabel: Tumoren ohne Kontakt zu der Arteria mesenterica superior (AMS), dem Truncus coeliacus (TC) oder der Arteria hepatica communis (AHC). Tumorummauerung der Pfortader (PA) oder Vena mesenterica superior (VMS) von ≤ 180° unter Abwesenheit von Irregularitäten der Kontur.

2) Borderline resektabel: solide Tumorummauerung der PA oder VMS > 180° oder ≤ 180° mit Irregularitäten der Kontur oder venöser Thrombose mit intakter proximaler und distaler Vene mit sicherer Möglichkeit einer vollständigen Resektion und Rekonstruktion, Kontakt von solidem Tumor zur Vena cava inferior. Zudem bei Tumoren des Pankreaskopfes oder Processus uncinatus: Kontakt von solidem Tumor zur AMS über ≤ 180° der Gefäßzirkumferenz, zur AHC ohne Beteiligung des TC oder der Bifurkation der Arteria hepatica mit sicherer Möglichkeit einer vollständigen Resektion und Rekonstruktion oder zu einer lokalen arteriellen Normvariante. Bzw. bei Tumoren des Pankreaskorpus- und -schwanzes: Kontakt von solidem Tumor über ≤ 180° der Gefäßzirkumferenz des TC bzw. bei > 180° ohne Beteiligung der Aorta oder Arteria gastroduodenalis, welche intakt ist.

3) Nicht resektabel (lokal fortgeschritten): Verschluss (durch Thrombose oder Tumor) oder Tumorbeteiligung der PA oder VMS ohne Möglichkeit einer vollständigen Resektion und Rekonstruktion oder Kontakt von solidem Tumor zur AMS über > 180° der Gefäßzirkumferenz. Zudem bei Tumoren des Pankreaskopfes oder Processus uncinatus: Kontakt von solidem Tumor zum TC über > 180° der Gefäßzirkumferenz oder Kontakt des Tumors zum proximalsten in die PA drainierenden jejunalen Ast. Bei Tumoren des Pankreaskorpus und -schwanzes: Kontakt von solidem Tumor mit dem TC unter Beteiligung der Aorta.

### 1.3.3 Palliative und adjuvante Chemotherapie

Bei exokrinen Pankreaskarzinomen mit Fernmetastasen erfolgt in der Regel bis auf Ausnahmen von bestimmten Patient:innen, welche in o. g. Studienkonzepte bei Oligometastasierung (1.3.2) eigeschlossen sind, die Einleitung einer palliativen Chemotherapie. Nach operativer Tumorresektion sollte eine adjuvante Chemotherapie über sechs Monate erfolgen.[9, 12]

### 1.3.4 Neoadjuvante Therapie

Eine der Operation vorgeschaltete neoadjuvante Therapie kann einen prognostischen Vorteil bieten bei Patient:innen mit einem Pankreaskarzinom.[17] Einheitlich wird sie für das exokrine Pankreaskarzinom aktuell von dem National Comprehensive Cancer Network® (NCCN) als

auch von der aktuellen S3-Leitlinie bei anatomisch borderline resektablen und lokal fortgeschrittenen Tumoren empfohlen[9, 12] Grundlage hierfür ist, dass diese beiden Gruppen letztlich Primärtumore zusammenfassen sollen, die anatomisch nicht als nicht zuverlässig im Gesunden (borderline resektabel) bzw. nicht im Gesunden resektabel (lokal fortgeschritten) erachtet werden. Die Rationale für eine neoadjuvante Therapie in Bezug auf den Primärtumor ist in diesen Fällen eine potentielle Tumorverkleinerung mit erhöhter Wahrscheinlichkeit der vollständigen Resektion des Tumors im Gesunden bzw. dem Erreichen einer sekundären Resektabilität.[18, 19]

In der aktuellen S3-Leitlinie besteht für die neoadjuvante Therapie bei borderline resektablen exokrinen Pankreaskarzinomen die Empfehlung zur Durchführung einer Chemotherapie oder Radiochemotherapie und für lokal fortgeschrittene Karzinome zur Durchführung einer Chemotherapie.[9] Im Falle lokal fortgeschrittener Karzinome ist die initial durchgeführte Chemotherapie nur dann als neoadjuvant zu werten, wenn Tumoren unter ihr sekundär resektabel werden.

### 1.3.5 Das resektable exokrine Pankreaskarzinom

Zielsetzung der Resektion des exokrinen Pankreaskarzinoms soll die Resektion im Gesunden, d. h. vollständig, sein.[9] Die wesentlichste Grundvoraussetzung hierfür ist, dass der Tumor sich als primär oder im Rahmen eines multimodalen Therapiekonzeptes, d. h. nach neoadjuvanter Therapie, als letztendlich lokal im Gesunden resektabel erweist.

Auf Grundlage der Einteilung und Terminologie der anatomischen Resektabilität des Primärtumors (siehe 1.3.2) sind folgende Tumoren als letztendlich resektabel einzuordnen:

- primär resektable Karzinome
- primär oder sekundär resektable borderline resektable Karzinome
- sekundär resektable lokal fortgeschrittene Karzinome

Bei dem Vorhandensein einer Fernmetastasierung besteht jedoch international Konsens darüber, dass selbst bei chirurgisch potentiell möglicher Resektion des Primärtumors sowie aller vorhandenen erkennbaren Metastasen keine onkologische Operation erfolgen soll.[9, 12] Die empirische Empfehlungsgrundlage eine ausbleibende Verbesserung der Prognose von Patient:innen.[11, 13] Eine weitere Voraussetzung ist, dass der physische Zustand der Patient:innen eine onkologische Tumorresektion zulässt (i. d. R. Eastern Cooperative Oncology Group(ECOG)-Performance-Status $\geq 2$, ).[9, 20] Gegenstand aktueller Studien sind o. g. Fälle mit vorhandener Oligometastasierung (1.3.1).

### 1.4 Prognostische Risikostratifikation des resektablen exokrinen Pankreaskarzinoms

Innerhalb der Gruppe resektabler Pankreaskarzinome besteht eine prognostische Heterogenität. So gelten innerhalb dieser Gruppe beispielsweise der Nachweis von Tumor am Resektionsrand des onkologischen Operationsresektates (R1 & R2), regionale Lymphknotenmetastasen und ein deutlich erhöhtes perioperatives CA 19-9 als prognostisch ungünstige Parameter des resektablen Pankreaskarzinoms.[10, 21, 22, 23] Auch weitere prognostische Biomarker sind Gegenstand aktueller Forschung. [24, 25]

#### 1.4.1 Beteiligung der operativen Resektionsränder

Ziel der chirurgischen Therapie des exokrinen Pankreaskarzinoms ist die Resektion des Primärtumors im Gesunden (R0).[9] Dieser gegenüber steht eine Resektion, die nicht im Gesunden erfolgt. Bei dieser wurde bereits vor vielen Jahren die Unterteilung in ein makroskopisch erkennbares (R2) und lediglich mikroskopisch erkennbares (R1) Tumorresiduum am Resektionsrand eingeführt.[26] Ein makroskopisches Tumorresiduum (R2) führt hierbei zu einer deutlichen prognostischen Verschlechterung (medianes Gesamtüberleben 20 Monate (R0) vs. 10 Monate (R2) in Wagner et al., $p<0.01$).[10] Ein mikroskopisches Tumorresiduum wurde klassischerweise als direkte mikroskopische Infiltration (DMI) von Tumorzellen am Resektionsrand definiert (R1-DMI) und führt ebenfalls zu einer schlechteren Prognose im Vergleich zu der Resektion im Gesunden (medianes Gesamtüberleben 23 Monate (R0) vs. 15 Monate (R1-DMI) in Kimbrough et al., $p<0.01$).[27] Es gibt darüber hinaus Hinweise darauf, dass der Abstand des Tumors zum Resektionsrand auch über eine mikroskopische Tumorinfiltration (R1-DMI) hinaus prognostisch relevant ist.[21, 28] Es werden auch prognostische Unterschiede in Abhängigkeit der Lokalisation des Resektionsrandes mit mikroskopischer Tumorbeteiligung diskutiert.[29] Die differenzierte Untersuchung von operativen Resektionsrändern resezierter Tumore bietet somit das Potential einer präziseren prognostischen Risikostratifikation des Pankreaskarzinoms.

#### 1.4.2 Regionale Lymphknotenmetastasen

Regionale Lymphknotenmetastasen sind ein prognostischer Risikofaktor resektabler exokriner Pankreaskarzinome, der einen deutlichen negativen Einfluss auf die Prognose hat.[22] So war das mediane Gesamtüberleben 42,3 Monate ohne Lymphknotenmetastasen (pN-) und 17,4 Monate

mit Lymphknotenmetastasen (pN+) nach Tumorresektion bei Patient:innen mit exokrinen Pankreaskarzinom ($p<0.01$, in Morales-Oyarvide et al.)[30] Im Rahmen der lokregionären Tumorausbreitungsdiagnostik sind Computertomographie (CT), Magnetresonanztomographie (MRT) und Endosonographie (EUS) etablierte Verfahren.[9, 12] Für all diese Verfahren ist eine hohe diagnostische Genauigkeit beschrieben in Bezug auf die Diagnosestellung eines Pankreaskarzinoms mit Sensitivitäten und Spezifitäten >85%.[31] Das etablierteste Bildgebungsverfahren für das lokoregionäre Tumorstaging exokriner Pankreaskarzinome ist die CT.[12, 32] In Bezug auf das präoperative lokoregionäre Lymphknotenstaging des Pankreaskarzinoms zeigt die CT jedoch eine schwache diagnostische Wertigkeit, insbesondere bei niedriger Sensitivität (17% in Roche et al., 37% in Soriano et al.)[33, 34] Auch EUS und MRT weisen nur eine eingeschränkte Sensitivität auf (36% und 15% in Soriano et al.)[34] Das hierbei verwendete Malignitätskriterium in der präoperativen Beurteilung ist die Lymphknotengröße (> 10 mm).[33, 34] Insgesamt bleibt trotz der hohen prognostischen Relevanz regionaler Lymphknotenmetastasen die prätherapeutisches Einschätzung ihres Metastasierungszustandes mit etablierten Schnittbildgebungsverfahren eine Herausforderung.[35]

Im Rahmen weiterer Überlegungen bezüglich der Risikostratifikation exokriner Pankreaskarzinome anhand von Lymphknotenmetastasen ist es denkbar, dass eine direkte Infiltration von Lymphknoten durch exokrine Pankreaskarzinome prognostisch anders zu werten ist als eine „echte“ regionale Lymphknotenmetastase ohne jeglichen Tumorkontakt.[36] Eine isolierte regionale Lymphknotenmetastasierung eines exokrinen Pankreaskarzinoms durch eine solche direkte Tumorinvasion von Lymphknoten liegt regelmäßig vor (20% der Fälle mit ein oder zwei regionalen Lymphknotenmetastasen in Konstantinidis et al.)[37]

### 1.4.3 CA 19-9 und weitere Biomarker

Die Konzentration von CA19-9 im Serum sollte bei V. a. ein exokrines Pankreaskarzinom bestimmt werden.[9] Als Biomarker ist eine mediane Sensitivität und Spezifität von 79% und 82% beschrieben für die Diagnosestellung eines Pankreaskarzinoms.[38, 39] Erhöhte präoperative CA19-9-Konzentrationen sind assoziiert mit einer niedrigeren Resektionsrate und einem höheren Tumorstadium potentiell resektabler exokriner Pankreaskarzinome sowie einem verschlechtertem Langzeitüberleben nach Tumorresektion.[40, 41] Ein CA19-9-Anstieg im Langzeitverlauf nach kurativer Tumorresektion ist assoziiert mit dem Auftreten eines Tumorrezidivs.[42] Insgesamt ist CA19-9 somit ein wertvoller Biomarker exokriner Pankreaskarzinome. Limitationen sind falsch positive erhöhte Serumwerte von CA19-9, z. B. im Rahmen von Cholestase,

Entzündungen der Gallenwege, Pankreatitis sowie eine veränderte Sekretion in Lewis-Antigen negativen Patient:innen.[39]

Eine Untersuchung von Operationsresektaten ermöglicht darüber hinaus grundsätzlich die postoperative Analyse von prognostischen Gewebemarkern des exokrinen Pankreaskarzinoms.[24] Eine solche könnte auch prätherapeutisch im Rahmen von Biopsien stattfinden. Das NCCN empfiehlt die prätherapeutische Gewinnung einer Biopsie zur histologische Sicherung des exokrinen Pankreaskarzinoms vor Beginn einer neoadjuvanten Therapie.[12] Gewebemarker könnten so vor Therapiebeginn zur prognostischen Risikostratifikation beitragen. Zur Untersuchung von Gewebemarkern auf Proteinebene kommen verschiedene Verfahren zum Einsatz wie die Elektrophorese, Western Blotting, massenspektrometische Verfahren oder Immunhistochemie.[43] Es kommen zunehmend auch Kombinationsverfahren zur Anwendung, so z. B. die Matrix–Assistierte Laser–Desorptions–Ionisierung (MALDI) und Flugzeitmassenspektrometrie (engl. time-of-flight mass spectrometry, TOF-MS).[43] MALDI-TOF-MS kann zur Analyse von Gewebemarkern auf Proteinebene verwendet werden an durch Formalin-fixierten Paraffin-eingebetteten Gewebeschnitten. Es ist eine räumliche Auflösung von Proteinanalysen (engl. matrix-assisted laser desorption ionization mass spectometry imaging, MALDI-MSI) und der direkte Vergleich analysierter Areale mit histologischen Gewebeschnitten nach Hämatoxylin-Eosin-Färbung (HE-Färbung) möglich (siehe Abbildung 1).[44] Assoziationen analysierter Gewebemarker mit klinischen, histopathologischen und onkologischen Parametern können verglichen werden. Beispiele für Gewebemarker exokriner Pankreaskarzinome mit Hinweisen auf eine prognostische Bedeutung sind der Proliferationsmarker Ki-67, das mit einer Metastasierung im Zusammenhang stehende E-Cadherin und der regulatorisch mit dem Immunsystem interagierende PD-L1.[24]

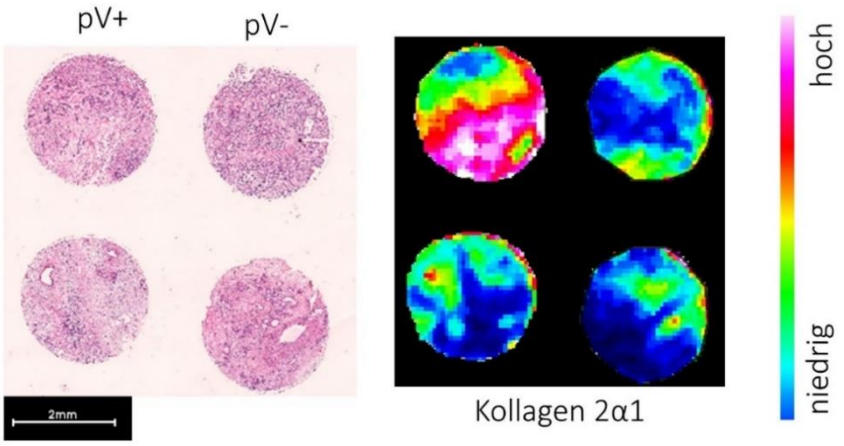


Abbildung 1: Räumliche Auflösung der Kollagen-Typ 2α1-Intensität mittels MALDI-MSI (rechts) und vergleichende Darstellung des korrespondierenden Gewebeschnittes nach HE-Färbung (links). Dargestellt sind Analysen von Resektionspräparaten zweier Patient:innen mit exokrinem Pankreaskarzinom mit (pV+) und ohne Gefäßinvasion (pV-). (Eigene Grafik.)

### 1.5 Therapeutische Implikationen der prognostischen Risikostratifikation des resektablen exokrinen Pankreaskarzinoms

Eine Hauptfunktion der präzisen Risikostratifikation des resektablen exokrinen Pankreaskarzinoms ist die bestmögliche Therapieplanung. Im Kontext der o. g. multimodalen Therapiekonzepte des resektablen exokrinen Pankreaskarzinoms könnte sie so zur Erweiterung der Indikationen für eine neoadjuvante Therapie sowie Anpassungen im intraoperativen Vorgehen und adjuvanter Therapiekonzepte beitragen.

Wie bereits in 1.3.4 erwähnt besteht einheitlich aktuell von dem NCCN als auch von der aktuellen S3-Leitlinie eine Indikation zur neoadjuvanten Therapie bei anatomisch borderline resektablen und lokal fortgeschrittenen exokrinen Pankreaskarzinomen.[9, 12] Hierdurch kann die Verkleinerung des Primärtumors und der damit erhöhten Wahrscheinlichkeit einer operativen Resektion im Gesunden bewirkt werden.[18, 19] In anderen gastrointestinalen Tumorentitäten hat sich gezeigt, dass eine neoadjuvante Therapie auch bei primär resektablen Tumoren die Prognose verbessern kann und ist bei diesen Entitäten etabliert.[45, 46] Die Kenntnis und prätherapeutische Bestimmung relevanter Risikofaktoren birgt das Potential zur Identifikation von Subgruppen anatomisch primär resektabler exokriner Pankreaskarzinome mit prognostischem Nachteil. So kann auch beim exokrinen Pankreaskarzinom geprüft werden, ob auf diese Weise identifizierte Subgruppen trotz anatomischer Resektabilität prognostisch von einer neoadjuvanten Therapie

profitieren. Ein onkologischer Grundgedanke hierbei ist auch, dass bei V. a. aggressivere Tumorbiologie bzw. okkulter fortgeschrittener Erkrankung eine neoadjuvante Therapie Tumoren aufzeigt, die unter der initialen systemischen Therapie lokal begrenzt und somit mit höherer Wahrscheinlichkeit kurativ therapierbar bleiben. Patient:innen mit exokrinen Pankreaskarzinomen aggressiver Tumorbiologie, bei denen es früh nach Diagnosestellung unter neoadjuvanter Therapie zu einer Metastasierung kommt, könnte eine onkologische Resektion mit entsprechender Morbidität kurz vor Lebensende erspart werden. Zudem würde eine unmittelbare systemische Therapie ursprünglich okkulter Fernmetastasierung durch die Neoadjuvanz stattfinden.[47, 48]

In diesem Zusammenhang gilt für die besonders etablierten negativen prognostischen Risikofaktoren einer regionalen Lymphknotenmetastasierung sowie der erhöhten prätherapeutischen CA19-9-Serumkonzentration (>500 U/ml) bereits, dass ein exokrines Pankreaskarzinom bei Vorhandensein einer dieser beiden Risikofaktoren trotz anatomischer Resektabilität als *biologisch* borderline resektabel einzustufen ist.[9, 20] Nach der aktuellen S3-Leitlinie kann das Vorhandensein einer dieser beiden Risikofaktoren somit eine Indikationsgrundlage für eine neoadjuvante Therapie darstellen, auch bei primärer anatomischer Resektabilität des Tumors. Die diagnostische Grundlage der regionalen Lymphknotenmetastasierung zur Einstufung des exokrinen Pankreaskarzinoms als biologisch borderline resektabel ist in diesem Kontext die Positronen-Emissions-Tomographie-CT (PET-CT) oder Biopsie.[9, 20] Perspektivisch könnten bei verbesserter diagnostischer Genauigkeit auch klassische Schnittbildverfahren zum Einsatz kommen.

Auch ein Einfluss prognostischer Faktoren auf adjuvante Therapiekonzepte des resektablen exokrinen Pankreaskarzinoms ist eine potentielle Perspektive, etwa im Spannungsfeld von Tumortoxizität und Begleitmorbidität von Cheomotherapieregimen (z. B. FOLFIRINOX vs. Gemcitabin).[49, 50] Zudem kann die Identifikation von Gewebemarkern über deren prognostische Aussagekraft hinaus als direktes Therapieziel dienen. So z. B. können mit dem Immunsystem interagierende Moleküle, sog. Immuncheckpoints (z. B. PD-L1), Ansatzpunkte einer immunmodulierenden Therapie sein, die einer Immunevasion des Tumors entgegenwirkt (Immuncheckpoint-Therapie, ICT).[51] Sowohl neoadjuvante, adjuvante als auch palliative Therapiekonzepte könnte potentiell um eine solche ICT ergänzt werden.[52, 53]

Die Weiterentwicklung prognostischer Risikofaktoren bildet auch eine potentielle Grundlage für die Anpassung des intraoperativen Vorgehens. So könnte z. B. eine Erweiterung der intraoperativen Schnellschnittuntersuchung des Resektionsrandes über eine DMI hinaus erweiterte Indikationen für eine Nachresektion bieten.[54]

### 1.6 Zielsetzung

Patient:innen haben nach der Diagnosestellung eines exokrinen Pankreaskarzinom eine deutlich eingeschränkt Prognose und die onkologische Resektion stellt gegenwärtig die einzige kurative Behandlungsmöglichkeit dar.[2, 9] Innerhalb der Gruppe der resektablen exokrinen Pankreaskarzinome zeigt sich eine prognostische Heterogenität. [10, 22, 23] Zur Identifikation von Subgruppen des resektablen exokrinen Pankreaskarzinoms in Abhängigkeit ihrer Prognose ist die Kenntnis und zuverlässige Identifikation prognostischer Merkmale nötig. Aus dieser prognostischen Risikostratifikation ergeben sich zahlreiche potentielle therapeutische Implikationen.

Das Ziel der vorliegenden Arbeit ist die die Herausarbeitung von Merkmalen prognostischer Heterogenität sowie die Präzisierung ihrer Identifizierung und somit die Weiterentwicklung der prognostischen Risikostratifikation des resektablen exokrinen Pankreaskarzinoms.

Diese Arbeit kann methodisch hierbei in drei Teile aufgeteilt werden:

1) Der erste Teil dieser Arbeit beschäftigt sich mit der Identifikation von Proteinen mit prognostischem Einfluss, die von Tumorzellen exokriner Pankreaskarzinome exprimiert werden **(Originalarbeit 1 und 2)**
2) Der zweite Teil dieser Arbeit beschäftigt sich mit der Identifikation und Präzisierung von aus der postoperativen pathologischen Aufarbeitung von Operationsresektaten hervorgehenden prognostischen Merkmalen **(Originalarbeit 3 und 4)**
3) Der dritte Teil der Arbeit beschäftigt sich mit der Evaluation und Präzisierung der Beurteilungskriterien des etablierten prognostischen Risikofaktors der regionalen Lymphnotenmetastasierung in der präoperativen Schnittbildgebung (**Originalarbeit 5)**

## 2. Eigene Arbeiten

### 2.1 Identifikation prognostischer Marker des resektablen exokrinen Pankreaskarzinoms mittels MALDI-MSI (Originalarbeit 1)

Die **Originalarbeit 1** identifiziert explorativ Proteine mit prognostischen Implikationen, welche von resektablen exokrinen Pankreaskarzinomen exprimiert werden, mittels MALDI–MSI als Analyseverfahren. Es ist hierbei die erste von den zwei Originalarbeiten dieser Schrift, die sich der Identifikation von Merkmalen mit prognostischem Einfluss auf der methodischen Ebene der Proteinexpressionsanalyse resektabler exokriner Pankreaskarzinome widmen.

**Florian N. Loch**, Oliver Klein, Katharina Beyer, Frederick Klauschen, Christian Schineis, Johannes C. Lauscher, Georgios A. Margonis, Claudius E. Degro, Wael Rayya, Carsten Kamphues.

Peptide Signatures for Prognostic Markers of Pancreatic Cancer by MALDI Mass Spectrometry Imaging. *Biology*, **2021**; 10:1033.

Der nachfolgende Text entspricht dem Originalabstract der o.g. Publikation *Peptide Signatures for Prognostic Markers of Pancreatic Cancer by MALDI Mass Spectrometry Imaging* übersetzt durch den Erstautor Florian N. Loch:

*„Trotz der insgesamt schlechten Prognose des Pankreaskarzinoms existiert Heterogenität im Verlauf der Tumorerkrankung, die aktuell nicht erfasst wird durch konventionelle Risikostratifikation. Somit bedarf es zusätzlicher Marker zur zuverlässigen Einschätzung der Prognose sowie multimodaler Therapiekonzepte. Wir weisen eine Machbarkeitsstudie vor zur Beurteilung der Umsetzbarkeit mittels MALDI-MSI spezifische Peptidsignaturen zu identifizieren, die mit prognostischen Parametern des Pankreaskarzinoms assoziiert sind. Bei 18 Patient:innen mit exokrinem Pankreaskarzinom nach Tumorresektion wurde MALDI-MSI angewendet, zusätzlich zur herkömmlicher histopathologischen Aufarbeitung. Eine Hauptkomponentenanalyse wurde durchgeführt zur explorativen Analyse unterschiedlicher Peptidsignaturen prognostisch relevanter histopathologischer Eigenschaften und eine anschließende Receiver Operating Characteristic (ROC, deutsch: Operationscharakteristik eines Beobachters), um die konkreten m/z-Werte zu identifizieren, die die prognostischen Subgruppen voneinander unterscheiden.*

*Aus 557 aufgetrennten m/z-Werten wurden unterschiedliche Peptidsignaturen für die prognostischen histopathologischen Eigenschaften Lymphgefäßinvasion (pL, 16 m/z-Werte, acht Proteine), Lymphknotenmetastasen (pN, zwei m/z-Werte, ein Protein) und Gefäßinvasion (pV, 4 m/z-Werte, zwei Proteine) identifiziert. Diese Ergebnisse zeigen, dass MALDI-MSI geeignet ist Peptidsignaturen mit prognostischer Relevanz zu identifizieren und kann so die Risikostratifikation ergänzen.“*

biology

MDPI

*Article*

# Peptide Signatures for Prognostic Markers of Pancreatic Cancer by MALDI Mass Spectrometry Imaging

**Florian N. Loch [1,*,†], Oliver Klein [2,†], Katharina Beyer [1], Frederick Klauschen [3,4], Christian Schineis [1], Johannes C. Lauscher [1], Georgios A. Margonis [5], Claudius E. Degro [1], Wael Rayya [1] and Carsten Kamphues [1]**

1 Department of Surgery, Charité—Universitätsmedizin Berlin, Corporate Member of Freie Universität Berlin and Humboldt-Universität zu Berlin, Hindenburgdamm 30, 12203 Berlin, Germany; katharina.beyer2@charite.de (K.B.); christian.schineis@charite.de (C.S.); johannes.lauscher@charite.de (J.C.L.); claudius-erwin.degro@charite.de (C.E.D.); wael.rayya@charite.de (W.R.); Carsten.kamphues@charite.de (C.K.)
2 Berlin Institute of Health, Charité—Universitätsmedizin Berlin, Center for Regenerative Therapies BCRT, Charitéplatz 1, 10117 Berlin, Germany; oliver.klein@charite.de
3 Institute for Pathology, Charité—Universitätsmedizin Berlin, Corporate Member of Freie Universität Berlin and Humboldt-Universität zu Berlin, Charitéplatz 1, 10117 Berlin, Germany; frederick.klauschen@charite.de
4 Institute for Pathology, Ludwig-Maximilians-Universität München, 80337 München, Germany
5 Department of Surgery, Memorial Sloan Kettering Cancer Center, New York, NY 10065, USA; margonig@mskcc.org
* Correspondence: florian.loch@charite.de; Tel.: +49-(0)30-450552712
† Authors contributed equally to this work.

**Simple Summary:** Pancreatic cancer remains one of the most lethal tumor entities worldwide given its overall 5-year survival after diagnosis of 9%. Thus, further understanding of molecular changes to improve individual prognostic assessment as well as diagnostic and therapeutic advancement is crucial. The aim of this study was to investigate the feasibility of Matrix-assisted laser desorption/ionization (MALDI) mass spectrometry imaging (MSI) to identify specific peptide signatures linked to established prognostic parameters of pancreatic cancer. In a patient cohort of 18 patients with exocrine pancreatic cancer after tumor resection, MALDI imaging analysis additional to histopathological assessment was performed. Applying this method to tissue sections of the tumors, we were able to identify discriminative peptide signatures corresponding to nine proteins for the prognostic histopathological features lymphatic vessel invasion, lymph node metastasis and angioinvasion. This demonstrates the technical feasibility of MALDI-MSI to identify peptide signatures with prognostic value through the workflows used in this study.

**Abstract:** Despite the overall poor prognosis of pancreatic cancer there is heterogeneity in clinical courses of tumors not assessed by conventional risk stratification. This yields the need of additional markers for proper assessment of prognosis and multimodal clinical management. We provide a proof of concept study evaluating the feasibility of Matrix-assisted laser desorption/ionization (MALDI) mass spectrometry imaging (MSI) to identify specific peptide signatures linked to prognostic parameters of pancreatic cancer. On 18 patients with exocrine pancreatic cancer after tumor resection, MALDI imaging analysis was performed additional to histopathological assessment. Principal component analysis (PCA) was used to explore discrimination of peptide signatures of prognostic histopathological features and receiver operator characteristic (ROC) to identify which specific $m/z$ values are the most discriminative between the prognostic subgroups of patients. Out of 557 aligned $m/z$ values discriminate peptide signatures for the prognostic histopathological features lymphatic vessel invasion (pL, 16 $m/z$ values, eight proteins), nodal metastasis (pN, two $m/z$ values, one protein) and angioinvasion (pV, 4 $m/z$ values, two proteins) were identified. These results yield proof of concept that MALDI-MSI of pancreatic cancer tissue is feasible to identify peptide signatures of prognostic relevance and can augment risk assessment.

**Keywords:** pancreatic cancer; peptide signatures; MALDI-MSI; risk stratification

check for updates

**Citation:** Loch, F.N.; Klein, O.; Beyer, K.; Klauschen, F.; Schineis, C.; Lauscher, J.C.; Margonis, G.A.; Degro, C.E.; Rayya, W.; Kamphues, C. Peptide Signatures for Prognostic Markers of Pancreatic Cancer by MALDI Mass Spectrometry Imaging. *Biology* **2021**, *10*, 1033. https://doi.org/10.3390/biology10101033

Academic Editors: Erxi Wu and Arnold Spek

Received: 13 August 2021
Accepted: 8 October 2021
Published: 12 October 2021

## 1. Introduction

Pancreatic cancer was diagnosed in 458,918 patients worldwide in 2018. Despite immense efforts to improve early detection and clinical management, the overall 5-year survival after diagnosis remains 9% [1]. At time of diagnosis the main proportion of patients has advanced stage disease, leaving only 15–20% qualified for potentially curative, resective surgery [2]. Even after successful resection of cancer of the pancreatic head the 5-year survival remains 21% [3]. There is, however, heterogeneity in clinical courses of tumors even within the same stage [4]. This indicates a pressing need to further augment clinical and histopathological staging in categorizing tumor malignancy, behavior and prognosis by additional prognostic markers for proper risk stratification and, consequently, clinical management of exocrine pancreatic cancer. In cases of resectable disease certain subgroups of patients need to be identified that are likely to benefit from neoadjuvant therapy due to aggressive tumor biology or occult metastatic disease. In cases of highly unfavorable tumor biology omitting surgery may be considered to spare hospitalization time at end of life period. In unresectable disease the further prognostic characterization contributes to the decision of the aggressiveness and toxicity of treatment.

Matrix-assisted laser desorption/ionization (MALDI) mass spectrometry imaging (MSI) is an emerging method for molecular analysis on tissue microarrays (TMAs) from obtained biopsies or surgical specimens which preserves the morphological integrity of the analyzed tissue. Therefore, it is enabled to assess the spatial distribution of proteomic analysis and allows further processing and staining of the TMA [5]. Due to its ability of untargeted peptide mapping, corresponding proteins observed do not need to be known in advance and therefore do not require molecule-specific tags [6,7]. Consequently, it allows the spatial correlation of peptide signatures with clinicopathological features. MALDI-MSI can be used to support tissue assessment in large formats and therefore has huge potential for routine clinical application and as pathology aid. A broad range of applications demonstrate that MALDI-MSI is feasible to, e.g., classify tumor subtypes [8,9], predicting therapeutic responses [10] or providing new biological insights into intratumor heterogeneity [9]. It has also been successfully applied to discover prognostic markers for recurrent vs. non-recurrent disease of early-stage high-grade serous ovarian cancer and risk stratification of neuroblastoma [11,12]. As for tissue analysis of pancreatic cancer, MALDI-MSI has so far been applied on pancreatic cryosections of genetically engineered mouse models to differentiate preneoplastic lesions (PanIN, IPMN) from healthy tissue and pancreatic ductal adenocarcinoma (PDAC) as well as to characterize the delivery and distribution of erlotinib in PDAC [13,14].

The aim of this study is to apply this method on formalin-fixed paraffin-embedded tumor tissue of patients with resected PDAC and find peptide signatures correlated to prognostic histopathological characteristics. Thus, to give proof of concept that MALDI-MSI is feasible to identify subgroups of patients with favorable and less favorable tumor biology in patients with PDAC.

## 2. Materials and Methods

### *2.1. Patient Cohort and Histopathological Assessment*

In this single center study approved by its local ethics committee, samples of 18 patients with histologically proven exocrine carcinoma of the pancreas that underwent primary oncologic surgery between January 2013 and March 2015 at the Department of Surgery, Campus Benjamin Franklin, Charité—University Medicine Berlin, Germany, were included after informed consent. Demographic and clinicopathological characteristics of the patients are shown in Table 1. Standard protocol of histopathological TNM staging of surgical specimens with additional variables of established prognostic relevance lymphatic vessel invasion (pL), angioinvasion (pV), perineural invasion (P) and histologic grade (Gx-4) was performed for conventional pathological assessment and risk stratification of tumors [15].

**Table 1.** Demographic and clinicopathological characteristics of patient cohort.

| **Patients** | ***n* = 18** |
|---|---|
| Age | |
| median age (years) | 67 |
| age range (years) | 36–77 |
| Sex | |
| Female | 8 (44%) |
| Male | 10 (56%) |
| Location of main tumor mass | |
| Pancreatic head | 14 (77%) |
| Pancreatic body | 1 (6%) |
| Pancreatic tail | 3 (17%) |
| Histopathological characteristics | |
| pT1 | 1 (6%) |
| pT2 | 1 (6%) |
| pT3 | 16 (88%) |
| pN+ | 12 (67%) |
| pN− | 6 (33%) |
| G1 | 1 (6%) |
| G2 | 11 (61%) |
| G3 | 5 (27%) |
| G4 | 1 (6%) |
| PN+ | 11 (61%) |
| pL+ | 8 (44%) |
| pL− | 10 (56%) |
| pV+ | 5 (27%) |
| pV− | 13 (73%) |
| Adenocarcinoma | 17 (94%) |
| Acinar cell carcinoma | 1 (6%) |

### *2.2. Procedure of MALDI-Imaging*

TMAs from formalin-fixed, paraffin-embedded tissue from patients diagnosed with exocrine pancreatic cancer were prepared at the Institute of Pathology, Charité—Medical University Berlin. For MALDI imaging, a 6-µm section from a paraffin block was prepared on the microtome and transferred to indium tin oxide slides (Bruker Daltonik, Bremen, Germany) by decreasing concentrations of ethanol (modified after Caprioli et al.) [5] and antigen recovery was performed (modified after Gustafsson et al.) [16]. An automatic spayer was used to apply Trypsin and matrix solutions (α-cyano-4-hydroxycinnamic acid, (HTX Sprayer). In total 550 µL trypsin solution (20 µg, 20 mM ammonium bicarbonate) was applied to the section. After incubating the tissue (2 h at 50 °C; humid chamber), the matrix solution (1 mL 7 g/L α-cyano-4-hydroxycinnamic acid in 50% acetonitrile and 1% trifluoroacetic acid) was applied also with the HTX sprayer (75 °C, estimation cycle 1.80).

### *2.3. MALDI Imaging Analysis*

Analyses were performed on 1–7 biologically independent cores of biopsies for each patient group (median 3.5). The tissue cores of the tumor used for analysis contain >80% of tumor cells. MALDI-MSI data acquisition was performed in reflector mode, detection range $m/z$ 800–3200, 500 laser shots per spot, sampling rate of 1.25 GS/s and grid width of 50 µm on Rapiflex MALDI-TOF using flexControl 3.0 and flexImaging 3.0 (Bruker Daltonik). A peptide calibration standard (Bruker Daltonik) was used for external calibration and spectra processed in flexAnalysis 3.0 (Bruker Daltonik). For the exclusion of possible contaminations such as sodium adducts or peptides, analysis of control areas outside the tissue was performed. Subsequent to the MALDI imaging experiments, the matrix was removed by applying 70% ethanol and the tissue sections were stained with haematoxylin and eosin (H&E) as a histological overview stain [5].

### 2.4. Data Processing

Statistical data was computed using the SCiLS Lab software (Version2021b, SCiLS GmbH, Bremen, Germany). MALDI-MSI raw data was imported into the SCiLS Lab software and then converted to the SCiLS Lab file format. Simultaneously, all data sets were preprocessed to ensure better comparability between the sample sets. Imported data was preprocessed by convolution baseline removal (width: 20) and total ion count (TIC) normalization. Segmentation pipelines were performed for peak-finding and their alignment as published previously [17–19]. The orthogonal matching pursuit (OMP) algorithm was used for the selection of peaks and top down segmentations were performed by bisecting k-means clustering, ±0.156 Da interval width, mean interval processing and medium smoothing strength [18–20]. As supervised approach receiver operating characteristic (ROC) analyses were performed to detect characteristic peptide values. ROC analysis was used for assessing the quality of all $m/z$ values within specific ROIs for discrimination between tumor tissues with respective prognostic histopathological features. For this method, the number of spectra in the ROIs of both groups should be approximately the same. Otherwise, 1500 randomly selected spectra per ROI/group were used. To determine statistical significance, discriminating $m/z$ values (peaks) with an AUC < 0.4 or > 0.6 were subsequently analyzed using the Wilcoxon rank sum test. A $p$-value of <0.001 was assumed as a potential marker. Figures were created using the SCiLS Lab software (Bruker, Bremen, Germany). Supervised principal component analysis (PCA) was conducted to define characteristic peptide signatures differentiating between tumor regions with >80% tumor cell content from groups in terms of absence or presence of prognostic histopathological features. The data was scaled for PCA in a level scaling model using settings to create five components, an interval width of ±0.3 Da, maximal interval processing mode, normalization to total ion count, no noise reduction.

### 2.5. Identification of Peptides by "Bottom-Up"-HPLC Mass Spectrometry

Complementary protein identification was performed on adjacent tissue sections to identify $m/z$ values by a "bottom-up"-nano liquid chromatography (nLC)-MS/MS approach as published previously [17]. In brief, tissue digestion (20 µg trypsin, 20 mM ammonium bicarbonate/acetonitrile 9:1) was performed via ImagePrep (Bruker Daltonik) followed bypeptide extraction for nUPLC-MS/MS analysis directly from adjacent tissue sections into 40 µL of 0.1% triflouroaceticacid (TFA; 15 min incubation at room temperature). Peptides were separated (60% acetonitrile/in 0.1% formic acid) using an analytical UPLC System (Thermo Dionex Ultimate 3000, Acclaim PepMap RSLC C18 column 75 µm × 15 cm; flow rate 200 nL/min, 70 min) and analyzed via Impact II (QTOF-MS, Bruker Daltonik). All raw spectra from the MS/MS measurement were converted to mascot generic files (.mgf) by the ProteinScape software [21]. Analysis of mass spectra was performed using the Mascot search engine (version 2.4, MatrixScience; UK) searching the UniPort database. The query was performed with the following set of parameters: (i) taxonomy: human; (ii) proteolytic enzyme: trypsin; (iii) peptide tolerance: 10 ppm; (iv) maximum of accepted missed cleavages: 1; (v) peptide charge: 2+, 3+, 4+; (vi) variable modification: oxidation (M); (vii) MS/MS tolerance: 0.8 Da; and (viii) MOWSE score > 25. Identification of MALDI-MSI $m/z$ values by using an LC-MS/MS reference list requires the accordance of more than one peptide (mass differences < 0.2 Da) to correctly assign the corresponding protein [22]. Peptides with lowest mass difference to the LC-MS/MS reference list value were assumed as a match.

## 3. Results

### 3.1. MALDI-MSI Data and Identification of Discriminative Peptide Signatures for Prognostic Histopathological Tumor Features

We evaluated the technical feasibility of MALDI-MSI to identify the peptide signature and potential discriminative peptide signatures of formalin-fixed, paraffin-embedded (FFPE) tissue sections of pancreatic cancer tissue of surgical specimens. In total, 557 aligned

$m/z$ values in the mass range for tryptic peptides ($m/z$ value range: 800–3200 were extracted from the analyzed tissue sections. In order to identify discriminative peptide signatures linked to prognostic histopathological tumor features (tumor size (pT), nodal metastasis (pN lymphatic vessel invasion (pL), vascular invasion (pV), perineural invasion (P) and histologic grade, Gx-4) principal compound analysis (PCA) was conducted on MALDI-MSI data from the tissue sections. PCA of MALDI-MSI data of tumor regions (>80% tumor cell content) showed a discrimination of peptide signatures of tumors in terms of absence or presence of the prognostic features lymphatic vessel invasion (pL+ vs. pL−), nodal metastasis (pN+ vs. pN−) and angioinvasion (pV+ vs. pV−) (Figure 1). The first principal component explained 54% of the variance. This demonstrates that unsupervised statistical approach results in discriminatory peptide signatures of tumors with lymphatic vessel invasion (pL+ vs. pL−), nodal metastasis (pN+ vs. pN−) and angioinvasion (pV+ vs. pV−) using MALDI-MSI data from pancreatic cancer tissue sections.

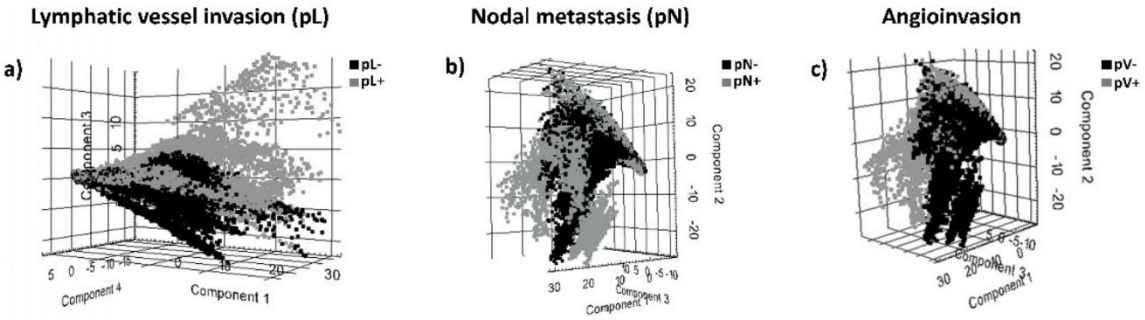


**Figure 1.** Principal component analysis (PCA) of MALDI-MSI data showing a discrimination of peptide signatures of tumors in terms of absence or presence of the prognostic histopathological features (**a**) lymphatic vessel invasion (pL+ vs. pL−), (**b**) nodal metastasis (pN+ vs. pN) and (**c**) angioinvasion (pV+ vs. pV−).

In total, MALDI-IMS derived 183 peptide values discriminative between subgroups of patients in terms of the prognostic features lymphatic vessel invasion (pL), nodal metastasis (pN) and angioinvasion (pL) from the 557 aligned $m/z$ values in the mass range for tryptic peptides in the analyzed tissue sections. The number of unique peptide values among the subgroups of patients with the respective prognostic feature and their overlap is shown in Figure 2.

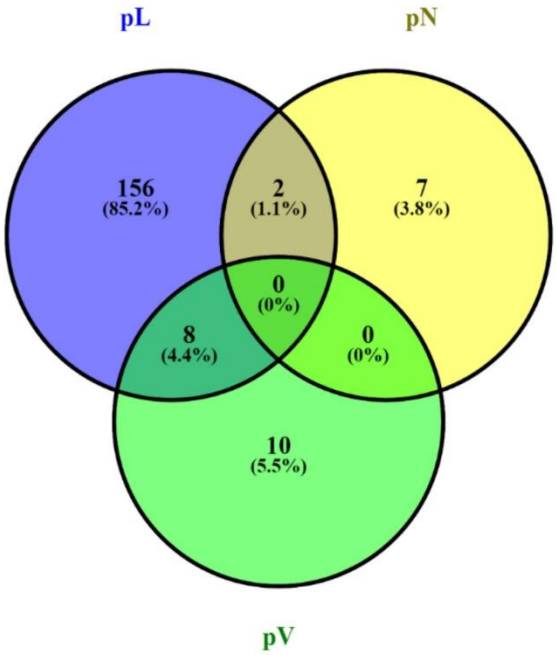


**Figure 2.** MALDI-IMS derived peptide values discriminative between the prognostic subgroups of lymphatic vessel invasion (pL), nodal metastasis (pN) and angioinvasion (pV) and their overlap. Discriminative peptide values: 156 peptides are unique to distinguish between tumors with lymphatic vessel invasion (pL+) and absence of lymphatic vessel invasion (pL−), seven peptides for nodal metastasis (pN+) and no nodal metastasis (pN−) and ten peptides for angioinvasion (pV+) and absence of angioinvasion (pV−).

### *3.2. Identification of Proteins Linked to Discriminative Peptide Signatures from Pancreatic Cancer Tissue Sections*

Univariate analysis of MALDI-MSI data has the potential to identify which specific $m/z$ values are the most discriminative between the prognostic subgroups of patients. Therefore, receiver operator characteristic (ROC) analyses were applied to the total 557 aligned $m/z$ peaks from tumor cell-rich areas in paired comparison of tissue sections of tumors with lymphatic vessel invasion (pL+) and absence of lymphatic vessel invasion (pL−), nodal metastasis (pN+) and without nodal metastasis (pN−) and angioinvasion (pV+) or absence of angioinvasion (pV−). Consequently, to identify the proteins corresponding to the discriminatory tryptic peptide fragments, we used a bottom-up nanoliquid chromatography-tandem mass spectrometry (nanoLC-MS/MS) approach in adjacent tissue sections. This analysis assigned 154 of the 557 $m/z$ values to peptides corresponding to proteins identified by nanoLC-MS/MS. Corresponding proteins to $m/z$ values are correctly identified when the validating approach (nanoLC-MS/MS in this case) identifies at least two peptides (detected in MALDI-MSI) from the same protein, whose spatial differential intensities are similar. This requisite was met for eight proteins (16 $m/z$ values), one protein (2 $m/z$ values) and two proteins (4 $m/z$ values) for the respective prognostic feature lymphatic vessel invasion (pL), nodal metastasis (pN) and angioinvasion (pV). The corresponding proteins show increased intensity distribution in the subgroup of patients with the prognostic characteristic of lymphatic vessel invasion (pL+, AUC > 0.6, $p < 0.001$) and angioinvasion (pV+; AUC > 0.6, $p < 0.001$). In contrast, the corresponding protein shows decreased intensity distribution in the subgroup of patients with nodal metastasis (pN+, AUC < 0.4, $p < 0.001$) (see Table 2).

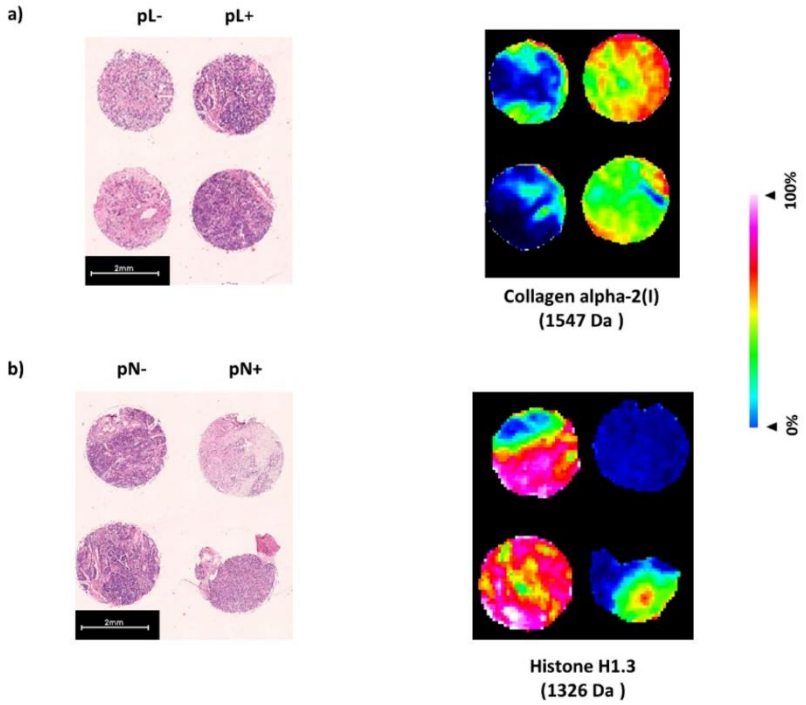


**Figure 3.** Differential spatial distribution and intensity of the subgroups with and without the respective prognostic histopathological feature (**a**) lymphatic vessel invasion, pL, (**b**) nodal metastasis, pN) for corresponding proteins. Peptide (1541 Da) from Collagen alpha-2(I) shows increased intensity distribution in patients with lymphatic vessel invasion (pL+) whereas peptide (1326 Da) from Histone H1.3 shows decreased intensity distribution in patients with nodal metastasis (pN+). For orientation hematoxylin and eosin stained tissue sections are show on the left.

## 4. Discussion

The prognosis of exocrine pancreatic cancer is generally poor. Only about 20% of patients qualify for curative, resective surgery at time of diagnosis [2]. Even after successful resection the survival rate remains on an unsatisfactory level of 21% leaving a survival rate of 9% of all patients with the disease after 5 years [3]. The therapeutic classification at diagnosis reaches from resectable to borderline-resectable to non-resectable, palliative disease.

Tumors are considered resectable in absence of infiltration of the coeliac trunk, the superior mesenteric artery and distant metastasis (other organs, peritoneal, distant lymph nodes). Yet, within the group of tumors considered resectable there is a large prognostic heterogeneity even within the same stage (IIa 16.5% to 36.8%, $p < 0.002$; IIb 0% to 59.8%, $p < 0.001$) [4]. This indicates a lack of understanding which patients after upfront tumor resection have favorable or unfavorable tumor biology. In clinical management, surgical resection of the tumor can fail in patients with biologically aggressive disease that do not benefit from extensive, high-morbidity resection at end-of-life period. Apart from the potential of increasing the resectability rate of pancreatic cancer in cases of borderline-resectability by neoadjuvant therapy, preoperative treatment is emerging for primarily resectable disease with the potential to improve prognosis [23]. In this context, exact understanding of tumor biology and risk stratification is crucial for deciding what patients may profit and which need to be precluded because of probable presence of more advanced disease and, consequently, exclusion from curative, surgical therapy after preoperative treatment. In non-resectable cases exact assessment of prognosis can contribute to the

choice of treatment regime in terms of toxicity to provide maximum life quality (e.g., FOLFORINOX vs. Gemcitabin-based).

In the performed analysis of this study, specific peptides linked to a signature of proteins for the prognostic histopathological characteristics lymphatic vessel invasion (pL), nodal metastasis (pN) and angioinvasion (pV) were found by MALDI-MSI. Therefore, we present a proof of concept for the technical feasibility of MALDI-MSI to describe prognostically relevant peptide signatures for the further risk stratification of pancreatic cancer beyond standard histopathological assessment and staging.

Additional to this general feasibility of MALDI-MSI, the identified proteins and their prognostic relevance were reviewed according to their concordance to pre-existing literature. All of the encountered peptides and correlated proteins were significantly associated with the respective histopathological characteristic when an increased intensity distribution was seen (AUC > 0.6, $p < 0.001$) except for a decreased intensity distribution of Histone H1.3 in tumors with nodal metastasis (pN+). In consideration of the fact that the exact prognostic role of the majority of these identified proteins is not yet fully resolved, in concordance to our findings Actin, cytoplasmic 1, Collagen alpha-2(I) chain, Collagen alpha-3(VI), Filamin-B and Myosin-11 have been associated with poor prognosis in pre-existing studies using different methods of molecular analysis such as Real-time PCR, western blotting, liquid chromatography-mass spectrometry and immunohistochemical staining [24–27] Furthermore, Valosin-containing protein (VCP) is known to be a prognosticator for poor prognosis in pancreatic cancer as well as other tumor entities and VCP inhibitors are currently being researched as potential therapeutic target for cancer therapy [28,29].

Noticeably, a large portion of the identified peptides is correlated to proteins that are part of the extracellular matrix (ECM). Generally, MALDI imaging experiments mainly address structural proteins, such as those located in the ECM, since methodically an enzymatic digestion of the surface of TMAs is performed. However, although stromal cells produce over 90% of the ECM mass [30], it was demonstrated that proteins of the ECM are highly expressed in pancreatic cancer cells [31] and elevated levels of ECM proteins derived from tumor cells of pancreatic cancer, but not those produced exclusively by stromal cells, tend to correlate with poor patient survival in pancreatic cancer [30]. The identified proteins are involved in cell migration (Collagen alpha-2(I) chain) [32], effected cancer cell motility (Actin) [33], promotion of metastasis (Valosin-containing protein) [34], cancer cell viability, angiogenesis (Collagen alpha-3(VI) chain) [35] and tumor progression (Collagen alpha-2(I) chain) [36].

In total, MALDI-MSI was able to successfully identify peptide signatures corresponding to altered intensity distribution of nine proteins from 18 patients with exocrine pancreatic cancer that were significantly correlated with poor prognostic parameters lymphatic vessel invasion (pL), nodal metastasis (pN) and angioinvasion (pV, $p < 0.001$). MALDI-MSI is an innovative technology in assisting risk classification taking into account tumor heterogeneity based on spatial peptide signatures [37]. In the presented pilot study, we could demonstrate that MALDI-MSI is feasible to identify peptide signatures of prognostic relevance and can augment risk assessment in pancreatic cancer. In subsequent large-scale studies, these peptide signatures in combination with, e.g., machine learning algorithms [8], leave-one-out cross-validation methods [38] or linear discriminant analysis [39] and deep learning approaches or convolutional neural network (CNN) [40] have to verify to these observations. Multiplex immunohistochemistry (IHC) as well as imaging Cytometry by time of flight (CyTOF) technologies [41] enable the spatial protein target analysis in tissue sections and, thus, represent capable tools to verify identified protein alterations from MALDI-MSI studies. In order to verify protein findings in large-scale cohorts a highly multiplexed IHC MALDI-MSI approach (up to 12-plex) is promising to confirm proteins from MALDI-MSI findings as parallel untargeted label-free investigation of small molecules [42].

The used workflows in this study are applicable to the analysis of larger sample cohorts. Thus, this work represents an important requisite for larger studies for intensified risk assessment of pancreatic cancer using MALDI-MSI.

## 5. Conclusions

Pancreatic cancer has a poor overall prognosis with tumor heterogeneity that is not sufficiently assessed by current conventional risk assessment. In the context of this poor prognosis, high-morbidity resection and toxicity of conservative treatment options an advancement of risk stratification is crucial. In conclusion, this proof of concept study showed the feasibility of MALDI-MSI to identify peptide signatures corresponding to prognostic features of pancreatic cancer.

**Author Contributions:** Conceptualization and methodology by C.K., F.K. and O.K.; data collection, formal analysis and investigation by C.K., F.K., O.K. and F.N.L. The manuscript draft was written by F.N.L., O.K. and C.K.; G.A.M., J.C.L., K.B., C.S., C.E.D. and W.R. provided intellectual input and advice on experiments and were part of the detailed review and editing of the manuscript draft. Funding acquisition was performed by C.K. All authors have read and agreed to the published version of the manuscript.

**Funding:** This work was supported by the foundation Stiftung Oskar-Helene-Heim, Berlin, Germany (#118895). This research was also funded by German Ministry for Education and Research in MSTAR (#031L0220A) and BCRT. We acknowledge support from the German Research Foundation (DFG) and the Open Access Publication Fund of Charité—Universitätsmedizin Berlin.

**Institutional Review Board Statement:** The study was conducted according to the guidelines of the Declaration of Helsinki, and approved by the Institutional Review Board of the Charité—Universitätsmedizin Berlin, corporate member of Freie Universität Berlin and Hum-boldt-Universität zu Berlin (#EA2/050/14 on the 14 June 2014).

**Informed Consent Statement:** Informed consent was obtained from all subjects involved in the study.

**Data Availability Statement:** The data presented in this study are available on request from the corresponding author. The data are not publicly available due to privacy.

**Conflicts of Interest:** The authors declare no conflict of interest.

## References

1. Rawla, P.; Sunkara, T.; Gaduputi, V. Epidemiology of Pancreatic Cancer: Global Trends, Etiology and Risk Factors. *World J. Oncol.* **2019**, *10*, 10–27. [CrossRef]
2. Du, T.; Bill, K.A.; Ford, J.; Barawi, M.; Hayward, R.D.; Alame, A.; Berri, R.N. The diagnosis and staging of pancreatic cancer: A comparison of endoscopic ultrasound and computed tomography with pancreas protocol. *Am. J. Surg.* **2018**, *215*, 472–475. [CrossRef]
3. Yeo, C.J.; Cameron, J.L.; Lillemoe, K.D.; Sitzmann, J.V.; Hruban, R.H.; Goodman, S.N.; Dooley, W.C.; Coleman, J.; Pitt, H.A. Pancreaticoduodenectomy for cancer of the head of the pancreas 201 patients. *Ann. Surg.* **1995**, *221*, 721–733. [CrossRef]
4. Hartwig, W.; Hackert, T.; Hinz, U.; Gluth, A.; Bergmann, F.; Strobel, O.; Büchler, M.W.; Werner, J. Pancreatic cancer surgery in the new millennium: Better prediction of outcome. *Ann. Surg.* **2011**, *254*, 311–319. [CrossRef]
5. Casadonte, R.; Caprioli, R.M. Proteomic analysis of formalin-fixed paraffin-embedded tissue by MALDI imaging mass spectrometry. *Nat. Protoc.* **2011**, *6*, 1695–1709. [CrossRef]
6. Cornett, D.S.; Reyzer, M.L.; Chaurand, P.; Caprioli, R.M. MALDI imaging mass spectrometry: Molecular snapshots of biochemical systems. *Nat. Methods* **2007**, *4*, 828–833. [CrossRef] [PubMed]
7. Walch, A.; Rauser, S.; Deininger, S.O.; Höfler, H. MALDI imaging mass spectrometry for direct tissue analysis: A new frontier for molecular histology. *Histochem. Cell Biol.* **2008**, *130*, 421–434. [CrossRef] [PubMed]
8. Kassuhn, W.; Klein, O.; Darb-Esfahani, S.; Lammert, H.; Handzik, S.; Taube, E.T.; Schmitt, W.D.; Keunecke, C.; Horst, D.; Dreher, F.; et al. Classification of Molecular Subtypes of High-Grade Serous Ovarian Cancer by MALDI-Imaging. *Cancers* **2021**, *13*, 1512. [CrossRef] [PubMed]
9. Klein, O.; Kanter, F.; Kulbe, H.; Jank, P.; Denkert, C.; Nebrich, G.; Schmitt, W.D.; Wu, Z.; Kunze, C.A.; Sehouli, J.; et al. MALDI-imaging for classification of epithelial ovarian cancer histotypes from a tissue microarray using machine learning methods. *Proteom. Clin. Appl.* **2019**, *13*, 1700181. [CrossRef] [PubMed]
10. Bauer, J.A.; Chakravarthy, A.B.; Rosenbluth, J.M.; Mi, D.; Seeley, E.H.; Granja-Ingram, N.D.M.; Olivares, M.G.; Kelley, M.C.; Mayer, I.A.; Meszoely, I.M.; et al. Identification of Markers of Taxane Sensitivity Using Proteomic and Genomic Analyses of Breast Tumors from Patients Receiving Neoadjuvant Paclitaxel and Radiation. *Clin. Cancer Res.* **2010**, *16*, 681–690. [CrossRef] [PubMed]
11. Kulbe, H.; Klein, O.; Wu, Z.; Taube, E.T.; Kassuhn, W.; Horst, D.; Darb-Esfahani, S.; Jank, P.; Abobaker, S.; Ringel, F.; et al. Discovery of prognostic markers for early-stage high-grade serous ovarian cancer by MALDI-Imaging. *Cancers* **2020**, *12*, 2000. [CrossRef] [PubMed]

12. Wu, Z.; Hundsdoerfer, P.; Schulte, J.H.; Astrahantseff, K.; Boral, S.; Schmelz, K.; Eggert, A.; Klein, O. Discovery of Spatial Peptide Signatures for Neuroblastoma Risk Assessment by MALDI Mass Spectrometry Imaging. *Cancers* **2021**, *13*, 3184. [CrossRef]
13. Grüner, B.M.; Hahne, H.; Mazur, P.K.; Trajkovic-Arsic, M.; Maier, S.; Esposito, I.; Kalideris, E.; Michalski, C.W.; Kleeff, J.; Rauser, S.; et al. MALDI imaging mass spectrometry for in situ proteomic analysis of preneoplastic lesions in pancreatic cancer. *PLoS ONE* **2012**, *7*, e39424. [CrossRef]
14. Grüner, B.M.; Winkelmann, I.; Feuchtinger, A.; Sun, N.; Balluff, B.; Teichmann, N.; Herner, A.; Kalideris, E.; Steiger, K.; Braren, R.; et al. Modeling therapy response and spatial tissue distribution of erlotinib in pancreatic cancer. *Mol. Cancer Ther.* **2016**, *15*, 1145–1152. [CrossRef]
15. National Comprehensive Cancer Network Website. NCCN Clinical Practice Guidelines in Oncology: Pancreatic Adenocarcinoma, Version 1.2015. Available online: www.nccn.org/professionals/physician_gls/pdf/pancreatic.pdf (accessed on 30 December 2014).
16. Gustafsson, O.J.; Briggs, M.T.; Condina, M.R.; Winderbaum, L.J.; Pelzing, M.; McColl, S.R.; Everest-Dass, A.V.; Packer, N.H.; Hoffmann, P. MALDI imaging mass spectrometry of N-linked glycans on formalin-fixed paraffin-embedded murine kidney. *Anal. Bioanal. Chem.* **2015**, *407*, 2127–2139. [CrossRef]
17. Klein, O.; Strohschein, K.; Nebrich, G.; Oetjen, J.; Trede, D.; Thiele, H.; Alexandrov, T.; Giavalisco, P.; Duda, G.N.; von Roth, P.; et al. MALDI imaging mass spectrometry: Discrimination of pathophysiological regions in traumatized skeletal muscle by characteristic peptide signatures. *Proteomics* **2014**, *14*, 2249–2260. [CrossRef]
18. Alexandrov, T.; Becker, M.; Guntinas-Lichius, O.; Ernst, G.; von Eggeling, F. MALDI-imaging segmentation is a powerful tool for spatial functional proteomic analysis of human larynx carcinoma. *J. Cancer Res. Clin. Oncol.* **2013**, *139*, 85–95. [CrossRef]
19. Alexandrov, T.; Becker, M.; Deininger, S.O.; Ernst, G.; Wehder, L.; Grasmair, M.; von Eggeling, F.; Thiele, H.; Maass, P. Spatial segmentation of imaging mass spectrometry data with edge-preserving image denoising and clustering. *J. Proteome Res.* **2010**, *9*, 6535–6546. [CrossRef] [PubMed]
20. Trede, D.; Schiffler, S.; Becker, M.; Wirtz, S.; Steinhorst, K.; Strehlow, J.; Aichler, M.; Kobarg, J.H.; Oetjen, J.; Dyatlov, A.; et al. Exploring three-dimensional matrix-assisted laser desorption/ionization imaging mass spectrometry data: Three-dimensional spatial segmentation of mouse kidney. *Anal. Chem.* **2012**, *84*, 6079–6087. [CrossRef] [PubMed]
21. Chambers, M.C.; Maclean, B.; Burke, R.; Amodei, D.; Ruderman, D.L.; Neumann, S.; Gatto, L.; Fischer, B.; Pratt, B.; Egertson, J.; et al. A cross-platform toolkit for mass spectrometry and proteomics. *Nat. Biotechnol.* **2012**, *30*, 918–920. [CrossRef] [PubMed]
22. Cillero-Pastor, B.; Heeren, R.M. Matrix-Assisted Laser Desorption Ionization Mass Spectrometry Imaging for Peptide and Protein Analyses: A Critical Review of On-Tissue Digestion. *J. Proteome Res.* **2013**, *13*, 325–333. [CrossRef]
23. Lim, K.H.; Chung, E.; Khan, A.; Cao, D.; Linehan, D.; Ben-Josef, E.; Wang-Gilliam, A. Neoadjuvant therapy of pancreatic cancer: The emerging paradigm? *Oncologist* **2012**, *17*, 192–200. [CrossRef]
24. Guo, C.; Liu, S.; Wang, J.; Sun, M.Z.; Greenaway, F.T. ACTB in cancer. *Clin. Chim. Acta* **2013**, *417*, 39–44. [CrossRef] [PubMed]
25. Wu, J.; Liu, J.; Wei, X.; Yu, Q.; Niu, X.; Tang, S.; Song, L. A feature-based analysis identifies COL1A2 as a regulator in pancreatic cancer. *J. Enzyme Inhib. Med. Chem.* **2019**, *34*, 420–428. [CrossRef] [PubMed]
26. Svoronos, C.; Tsoulfas, G.; Souvatzi, M.; Chatzitheoklitos, E. Prognostic value of COL6A3 in pancreatic adenocarcinoma. *Ann. Hepato-Biliary-Pancreat. Surg.* **2020**, *24*, 52–56. [CrossRef] [PubMed]
27. Iguchi, Y.; Ishihara, S.; Uchida, Y.; Tajima, K.; Mizutani, T.; Kawabata, K.; Haga, H. Filamin B enhances the invasiveness of cancer cells into 3D collagen matrices. *Cell Struct. Funct.* **2015**, *40*, 61–67. [CrossRef] [PubMed]
28. Yamamoto, S.; Tomita, Y.; Hoshida, Y.; Nagano, H.; Dono, K.; Umeshita, K.; Sakon, M.; Ishikawa, O.; Ohigashi, H.; Nakamori, S.; et al. Increased expression of valosin-containing protein (p97) is associated with lymph node metastasis and prognosis of pancreatic ductal adenocarcinoma. *Ann. Surg. Oncol.* **2004**, *11*, 165–172. [CrossRef] [PubMed]
29. Bastola, P.; Neums, L.; Schoenen, F.J.; Chien, J. VCP inhibitors induce endoplasmic reticulum stress, cause cell cycle arrest, trigger caspase-mediated cell death and synergistically kill ovarian cancer cells in combination with Salubrinal. *Mol. Oncol.* **2016**, *10*, 1559–1574. [CrossRef]
30. Tian, C.; Clauser, K.R.; Öhlund, D.; Rickelt, S.; Huang, Y.; Gupta, M.; Mani, D.R.; Carr, S.A.; Tuveson, D.A.; Hynes, R.O. Proteomic analyses of ECM during pancreatic ductal adenocarcinoma progression reveal different contributions by tumor and stromal cells. *Proc. Natl. Acad. Sci. USA* **2019**, *116*, 19609–19618. [CrossRef]
31. Ting, D.T.; Wittner, B.S.; Ligorio, M.; Vincent, J.N.; Shah, A.M.; Miyamoto, D.T.; Aceto, N.; Bersani, F.; Brannigan, B.W.; Xega, K.; et al. Single-cell RNA sequencing identifies extracellular matrix gene expression by pancreatic circulating tumor cells. *Cell Rep.* **2014**, *8*, 1905–1918. [CrossRef] [PubMed]
32. Ji, J.; Zhao, L.; Budhu, A.; Forgues, M.; Jia, H.L.; Qin, L.X.; Yu, J.; Shi, X.; Tang, Z.; Wang, X.W. Let-7g targets collagen type I alpha2 and inhibits cell migration in hepatocellular carcinoma. *J. Hepatol.* **2010**, *52*, 690–697. [CrossRef]
33. Olson, M.F.; Sahai, E. The actin cytoskeleton in cancer cell motility. *Clin. Exp. Metastasis* **2009**, *26*, 273. [CrossRef] [PubMed]
34. Long, X.H.; Zhou, Y.F.; Lan, M.; Huang, S.H.; Liu, Z.L.; Shu, Y. Valosin-containing protein promotes metastasis of osteosarcoma through autophagy induction and anoikis inhibition via the ERK/NF-κβ/beclin-1 signaling pathway. *Oncol. Lett.* **2019**, *18*, 3823–3829. [CrossRef] [PubMed]
35. Huang, Y.; Li, G.; Wang, K.; Mu, Z.; Xie, Q.; Qu, H.; Lv, H.; Hu, B. Collagen Type VI Alpha 3 Chain Promotes Epithelial-Mesenchymal Transition in Bladder Cancer Cells via Transforming Growth Factor β (TGF-β)/Smad Pathway. *Med. Sci. Monit.* **2018**, *24*, 5346–5354. [CrossRef] [PubMed]

36. Wu, Y.H.; Chang, T.H.; Huang, Y.F.; Huang, H.D.; Chou, C.Y. COL1A1 promotes tumor progression and predicts poor clinical outcome in ovarian cancer. *Oncogene* **2014**, *33*, 3432–3440. [CrossRef]
37. Aichler, M.; Walch, A. MALDI Imaging mass spectrometry: Current frontiers and perspectives in pathology research and practice. *Lab. Investig.* **2015**, *95*, 422–431. [CrossRef]
38. Winderbaum, L.; Koch, I.; Mittal, P.; Hoffmann, P. Classification of MALDI-MS imaging data of tissue microarrays using canonical correlation analysis-based variable selection. *Proteomics* **2016**, *16*, 1731–1735. [CrossRef]
39. Boskamp, T.; Lachmund, D.; Oetjen, J.; Hernandez, Y.C.; Trede, D.; Maass, P.; Casadonte, R.; Kriegsmann, J.; Warth, A.; Dienemann, H.; et al. A new classification method for MALDI imaging mass spectrometry data acquired on formalin-fixed paraffin-embedded tissue samples. *Biochim. Biophys. Acta* **2017**, *1865*, 916–926. [CrossRef]
40. Behrmann, J.; Etmann, C.; Boskamp, T.; Casadonte, R.; Kriegsmann, J.; Maass, P. Deep learning for tumor classification in imaging mass spectrometry. *Bioinformatics* **2017**, *34*, 1215–1223. [CrossRef]
41. Ali, H.R.; Jackson, H.W.; Zanotelli, V.R.T.; Danenberg, E.; Fischer, J.R.; Bardwell, H.; Provenzano, E.; Rueda, O.M.; Chin, S.; Aparicio, S.; et al. Imaging mass cytometry and multiplatform genomics define the phenogenomic landscape of breast cancer. *Nat. Cancer* **2020**, *1*, 163–175. [CrossRef]
42. Yagnik, G.; Liu, Z.; Rothschild, K.J.; Lim, M.J. Highly multiplexed immunohistochemical MALDI-MS imaging of biomarkers in tissues. *J. Am. Soc. Mass Spectrom.* **2021**, *32*, 977–988. [CrossRef] [PubMed]

## 2.2. Identifikation von prognostisch relevanten Immuncheckpoints resektabler exokriner Pankreaskarzinome (Originalarbeit 2)

Die Ergebnisse der **Originalarbeit 1** werden durch die folgende Arbeit ergänzt, die eine weitere Analyse des prognostischen Einflusses von durch Tumoren exprimierte Proteine darstellt bei Patient:innen mit resektablen exokrinen Pankreaskarzinomen. Es wurde hierbei in der folgenden **Originalarbeit 2** der prognostische Einfluss der Expression konkreter Immuncheckpoint-Proteine untersucht.

**Florian N. Loch**, Carsten Kamphues, Katharina Beyer, Christian Schineis, Wael Rayya, Johannes C. Lauscher, David Horst, Mihnea P. Dragomir, Simon Schallenberg.

The Immune Checkpoint Landscape in Tumor Cells of Pancreatic Ductal Adenocarcinoma. *International Journal of Molecular Sciences.* **2023**; 24:2160.

Der nachfolgende Text entspricht dem Originalabstract der o.g. Publikation *The Immune Checkpoint Landscape in Tumor Cells of Pancreatic Ductal Adenocarcinoma* übersetzt durch den Erstautor Florian N. Loch:

*„Die ICT hat in der Behandlung multipler solider Tumore bereits vielversprechendes Potential gezeigt. Beim PDAC ist der Einsatz der ICT jedoch noch begrenzt. Die Kenntnis der vorhandenen Immuncheckpoints ist die Grundlage zur Etablierung einer wirkungsvollen ICT. Ziel dieser Studie ist es Expressionsprofile von Immuncheckpoints der Tumorzellen des PDAC zu erstellen. Hierzu erfolgte die Untersuchung von Tumorzellen aus Gewebe-Mikroarrays (engl. tissue microarrays, TMAs) aus zentralem und peripherem Tumorgewebe von 68 Patient:innen mit histologisch bestätigtem PDAC nach Tumorresektion in Bezug auf Expression von TIM3, IDO, B7H4, LAG3, VISTA und PD-L1 mittels Immunhistochemie.*

*Das Vorhandensein der jeweiligen Immuncheckpoints wurde dann mit dem Gesamtüberleben verglichen. Das Vorhandensein von VISTA und PD-L1 war mit einem kürzeren Gesamtüberleben assoziiert (medianes Gesamtüberleben 22 Monate vs. 7 Monate und 22 Monate vs. 11 Monate, $p<0.05$). Für das Vorhandensein von TIM3, IDO, B7H4 und LAG3 wurde kein Unterschied im Gesamtüberleben gefunden. Die Analyse des Gesamtüberlebens kombinierter Subgruppen aus VISTA und PD-L1 (VISTA und PD-L1 negativ, VISTA positiv und PD-L1 negativ,*

*VISTA negativ und PD-L1 positiv sowie VISTA und PD-L1 positiv) zeigte insgesamt einen statistisch signifikanten Unterschied. Diese Ergebnisse implizieren, dass VISTA und PD-L1 prognostische Relevanz haben und potentielle Ziele einer ICT darstellen.“*

International Journal of
*Molecular Sciences*

MDPI

*Article*

# The Immune Checkpoint Landscape in Tumor Cells of Pancreatic Ductal Adenocarcinoma

**Florian N. Loch [1,*], Carsten Kamphues [2], Katharina Beyer [1], Christian Schineis [1], Wael Rayya [1], Johannes C. Lauscher [1], David Horst [3], Mihnea P. Dragomir [3,4,5,†] and Simon Schallenberg [3,†]**

1 Department of Surgery, Charité—Universitätsmedizin Berlin, Corporate Member of Freie Universität Berlin and Humboldt-Universität zu Berlin, 12203 Berlin, Germany
2 Department of Surgery, Park-Klinik Weißensee, 13086 Berlin, Germany
3 Institute of Pathology, Charité—Universitätsmedizin Berlin, Corporate Member of Freie Universität Berlin and Humboldt-Universität zu Berlin, 10117 Berlin, Germany
4 Berlin Institute of Health at Charité, Charitéplatz 1, 10117 Berlin, Germany
5 German Cancer Research Center (DKFZ), German Cancer Consortium (DKTK), Partner Site Berlin, 69210 Heidelberg, Germany
* Correspondence: florian.loch@charite.de; Tel.: +49-(0)30-450552722
† These authors contributed equally to this work.

**Abstract:** Immune checkpoint therapy (ICT) has shown promising potential in the treatment of multiple solid tumors. However, the role of ICT in pancreatic ductal adenocarcinoma (PDAC) remains limited. Patterns of immune checkpoints (ICs) in PDAC represent the basis for establishing a potent ICT. The aim of this study is to create a profile of IC expression and its prognostic relevance in cancer cells of PDAC. Therefore, tumor cells from peripheral and central tissue microarray (TMA) spots from histologically confirmed PDAC of 68 patients after tumor resection were investigated in terms of expressions of TIM3, IDO, B7H4, LAG3, VISTA, and PD-L1 using immunohistochemistry. The presence of the respective ICs was compared to overall survival (OS). The presence of VISTA and PD-L1 significantly correlates with shorter OS (median OS: 22 months vs. 7 months and 22 months vs. 11 months, respectively, $p < 0.05$). For the presence of TIM3, IDO, B7H4, and LAG3, no difference in OS was observed ($p > 0.05$). The analysis of OS of combined subgroups for VISTA and PD-L1 (VISTA and PD-L1 neg., VISTA pos. and PD-L1 neg., VISTA neg. and PD-L1 pos., and VISTA and PD-L1 pos.) yielded overall statistical significance difference ($p = 0.02$). These results suggest that the presence of VISTA and PD-L1 is of prognostic relevance and potentially qualifies them as targets for ICT.

**Keywords:** pancreatic ductal adenocarcinoma; immune checkpoints; survival; immune checkpoint inhibitors; immune checkpoint treatment



**Citation:** Loch, F.N.; Kamphues, C.; Beyer, K.; Schineis, C.; Rayya, W.; Lauscher, J.C.; Horst, D.; Dragomir, M.P.; Schallenberg, S. The Immune Checkpoint Landscape in Tumor Cells of Pancreatic Ductal Adenocarcinoma. *Int. J. Mol. Sci.* **2023**, *24*, 2160. https://doi.org/10.3390/ijms24032160

Academic Editor: Asfar S. Azmi

Received: 21 November 2022
Revised: 8 January 2023
Accepted: 18 January 2023
Published: 21 January 2023



## 1. Introduction

Immune checkpoints (ICs) are molecules involved in the stimulation and inhibition of the interaction of antigen-presenting cells (APC) and cells of the immune system, and thus they play a crucial role in the regulation of immune responses. The interaction between cancer cells and immune cells through ICs in the tumor microenvironment (TME) inhibits immunosurveillance and mediates the immune escape of the tumor. Thereby, ICs promote tumor development, growth, invasion and metastasis [1]. More specifically, the interaction of ICs in the TME caused by produced soluble ligands or as membrane-bound ligands of an APC—such as a cancer cells and receptors of immune cells, mainly CD4+ helper T-cells, and CD8+ effector T-cells—ultimately suppresses immune responses [2]. By inhibiting these interactions, immune checkpoint therapy (ICT) with immune checkpoint inhibitors (ICI) has shown outstanding potential in the treatment of multiple solid tumors [3]. Programmed cell death protein (PD-1) and programmed death-ligand (PD-L1) inhibitors are most established and have been approved for the therapy of advanced melanoma, metastatic non-small cell lung cancer and multiple other types of cancer [3].

Approximately 466,000 patients die yearly from pancreatic ductal adenocarcinoma (PDAC) worldwide [4], and the overall 5-year survival after diagnosis remains 9%, despite tremendous efforts to improve early detection and clinical management [5,6]. However, despite its aggressiveness, the role of ICIs in PDAC has not been thoroughly elicited, and thus currently remains limited [7]. An understanding of the IC patterns of a specific tumor entity and their clinical relevance represents the basis for the development, identification and establishment of a respective potent ICT. The ICs—PD-L1, Indoleamine 2, 3-Dioxygenase (IDO) and V-set domain-containing T-cell activation inhibitor 1 (B7H4)—are known to potentially be expressed in cancer cells with the capability to inhibit immune responses by interaction with immune cells [2,8,9]. Studies investigating the role of the ICs T-cell immunoglobulin and mucin domain 3 (TIM3), lymphocyte-activation gene 3 (LAG3) and V-domain immunoglobulin suppressor of T-cell activation (VISTA) mainly focus on their expression on immune cells, especially T-cells, in the TME [2,10–13]. However, there are indications that TIM3, LAG3 and VISTA expressions in cancer cells lead to an immunosuppressive TME, is of prognostic relevance, and thus a potential target for future ICIs [14–16].

Thus, the aim of this study is to understand the landscape of IC in resected PDAC by investigating the presence of TIM3, IDO, B7H4, LAG3, VISTA, and PD-L1 in cancer cells and to determine their prognostic relevance in terms of overall survival (OS).

## 2. Results

### 2.1. Demographics, Clinicopathological Characteristics and Survival of Patient Cohort

The demographic and clinicopathological characteristics of the patient cohort are shown in Table 1. Median survival of the entire patient cohort was 17 months (CI: 9.9–24.1, range 1–118). The one-year, three-year, and five-year survival rates of the entire patient cohort were 60.3%, 26.5% and 19.1%, respectively.

**Table 1.** Demographic and clinicopathological characteristics.

| **Patients** | ***n* = 68** |
|---|---|
| **Age** | |
| Median age (years) | 72 |
| Age range | 35–86 |
| **Sex** | |
| Female | 30 (44.1%) |
| Male | 38 (55.9%) |
| **Location of main tumor mass** | |
| Pancreatic head | 55 (80.9%) |
| Pancreatic body | 1 (1.5%) |
| Pancreatic tail | 8 (11.8%) |
| Overlapping | 4 (5.9%) |
| **Histopathological characteristics** | |
| pT1 | 3 (4.4%) |
| pT2 | 16 (23.5%) |
| pT3 | 49 (72.1%) |
| pN0 | 13 (19.1%) |
| pN+ (pN1 andand pN2) | 55 (80.9%) |
| R0 | 56 (82.4%) |
| R1 | 12 (17.6%) |
| G1 | 2 (2.9%) |
| G2 | 39 (57.4%) |
| G3 | 26 (38.2%) |
| G4 | 1 (1.5%) |
| PN0 | 19 (27.9%) |

**Table 1.** *Cont.*

| Patients | *n* = 68 |
|---|---|
| PN1 | 49 (72.1%) |
| pL0 | 34 (50.0%) |
| pL1 | 34 (50.0%) |
| pV0 | 47 (69.1%) |
| pV1 | 21 (30.9%) |

R: resection margin; G: grading; PN: perineural invasion; pL: lymphatic vessel invasion; pV: angioinvasion.

Table 2 shows hazard ratios for OS in univariate and multivariate analysis for the respective demographic and pathological characteristics. For the nodal involvement characteristics (pN+ vs. pN0), resection margin (R1 vs. R0) and angioinvasion (pV1 vs. pV0), hazard ratios showed significance in univariate and multivariate analyses ($p < 0.05$). The hazard ratio of lymphatic vessel invasion (pL1 vs. pL0) showed significance only in the univariate analysis ($p < 0.05$).

**Table 2.** Univariate and multivariate hazard ratios of demographic and pathological characteristics for OS.

| | Univariate | | | Multivariate | | |
|---|---|---|---|---|---|---|
| | **HR** | **CI 95%** | ***p*-Value** | **HR** | **CI 95%** | ***p*-Value** |
| Age (>65 vs. <65 years) | 1.95 | 0.98–3.87 | 0.06 | 1.96 | 0.96–4.01 | 0.06 |
| Sex (male vs. female) | 1.49 | 0.86–2.57 | 0.15 | | | |
| T stage (pT3–4 vs. pT1/2) | 1.57 | 0.83.2.99 | 0.17 | | | |
| Nodal involvement (pN+ vs. pN0) | 5.09 | 2.01–12.92 | <0.01 | 4.06 | 1.56–10.6 | <0.01 |
| Resection margin (R1 vs. R0) | 3.00 | 1.50–5.60 | <0.01 | 2.16 | 1.06–4.43 | 0.04 |
| Grading (G3–4 vs. G1–2) | 1.37 | 0.80–2.34 | 0.25 | | | |
| Perineural invasion (Pn1 vs. Pn0) | 1.61 | 0.88–2.96 | 0.13 | | | |
| Lymphatic vessel invasion (pL1 vs. pL0) | 1.87 | 1.09–3.20 | 0.02 | 1.21 | 0.66–2.21 | 0.55 |
| Angioinvasion (pV1 vs. pV0) | 2.52 | 1.43–4.43 | <0.01 | 2.30 | 1.24–4.28 | <0.01 |

HR: hazard ratio; CI 95%: 95% confidence interval.

### *2.2. Presence of TIM3, IDO, B7H4, LAG3, VISTA and PD-L1 in Cancer Cells of PDAC*

At least one of the ICs—TIM3, IDO, B7H4, LAG3, VISTA or PD-L1—was present in cancers cells in 66.2% (n = 45) of resected tumors. IDO was most frequently present (n = 28, 41.2%), and TIM 3 was least frequently present (n = 11, 16.2%). Table 3 shows the presence of the respective ICs in the entire study group, as well as individually in the subgroups of survivors and non-survivors. VISTA and PD-L1 were present in cancer cells of 30.9% (n = 17), and 38.2% (n = 21) of the resected tumors in the subgroup of non-survivors and only in 7.7% (n = 1) and 15.4% (n = 2) of tumors in the subgroup of survivors, respectively. Representative examples of presence and absence of TIM3, IDO, B7H4, LAG3, VISTA and PD-L1 in immunohistochemical (IHC) staining are presented in Figure 1A–L.

**Table 3.** Presence of the ICs in all patients, the subgroup of survivors and subgroup of non-survivors.

| IC | All Patients | Survivors | Non-Survivors |
|---|---|---|---|
| TIM3 | 16.2% (*n* = 11) | 7.7% (*n* = 1) | 18.2% (*n* = 10) |
| IDO | 41.2% (*n* = 28) | 30.8% (*n* = 4) | 43.6% (*n* = 24) |
| B7H4 | 22.1% (*n* = 15) | 15.4% (*n* = 2) | 23.6% (*n* = 13) |
| LAG3 | 20.6% (*n* = 14) | 15.4% (*n* = 2) | 21.8% (*n* = 12) |
| VISTA | 26.5% (*n* = 18) | 7.7% (*n* = 1) | 30.9% (*n* = 17) |
| PD-L1 | 33.8% (*n* = 23) | 15.4% (*n* = 2) | 38.2% (*n* = 21) |
| Any IC | 66.2% (*n* = 45) | 61.5% (*n* = 8) | 67.3% (*n* = 37) |

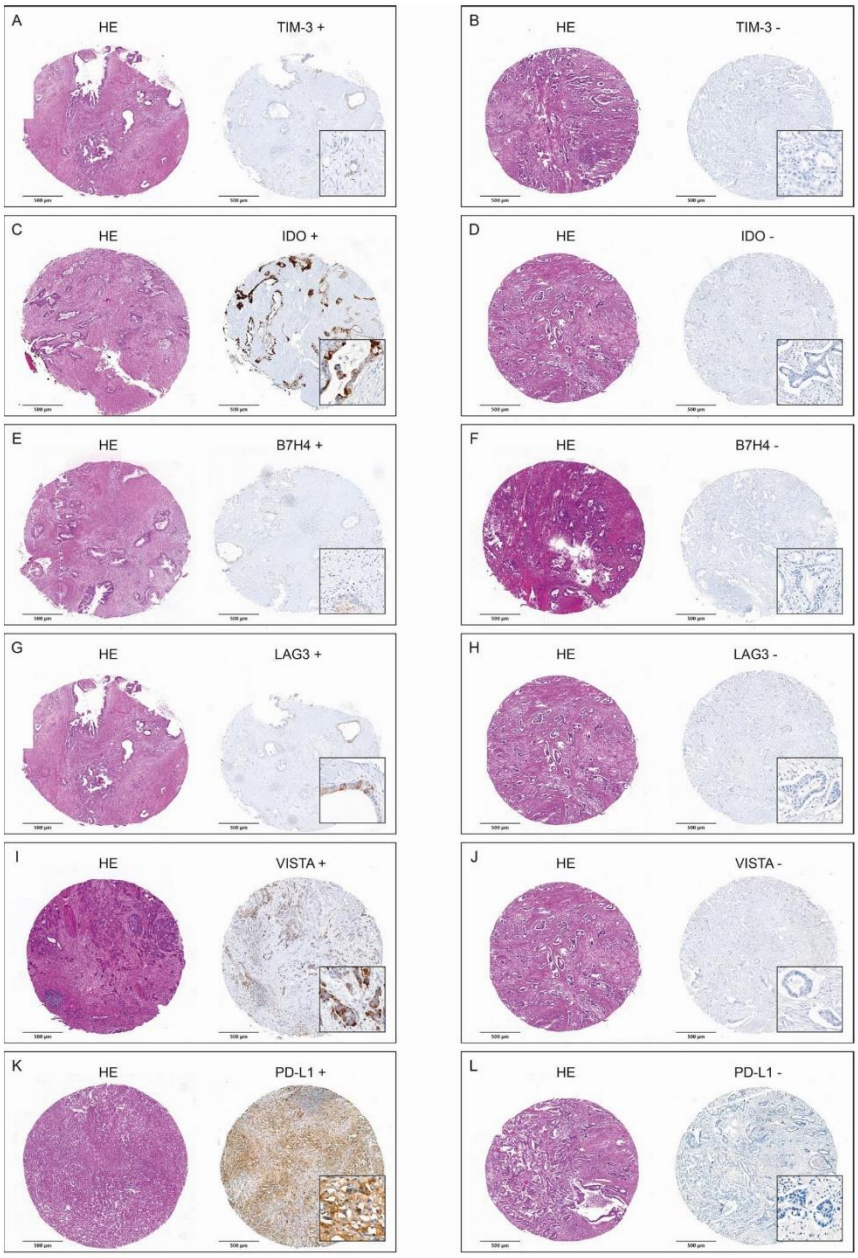


**Figure 1.** H&E-stained tumor spots and corresponding positive and negative IHC stainings of TIM3 (**A**,**B**), IDO (**C**,**D**), B7H4 (**E**,**F**), LAG3 (**G**,**H**), VISTA (**I**,**J**), and PD-L1 (**K**,**L**).

### *2.3. Correlation of Overall Survival and TIM3, IDO, B7H4, LAG3, VISTA, and PD-L1 in Cancer Cells of PDAC*

#### 2.3.1. General Analysis

Figure 2 shows the result of individual survival analyses for the expression of TIM3 (Figure 2a), IDO (Figure 2b), B7H4 (Figure 2c), LAG3 (Figure 2d), VISTA (Figure 2e), and PD-L1 (Figure 2f) on tumor cells. The presence of VISTA and PD-L1 significantly correlates with shorter OS (median OS in VISTA neg. subgroup 22 months (CI: 12.9–31.1 months) vs. 7 months (CI: 3.5–13.9) in VISTA pos. subgroup, $p = 0.01$, and 22 months (CI: 10.2–33.8)

in PD-L1 neg. subgroup vs. 11 months (CI: 5.1–16.9) in PD-L1 pos. subgroup, $p = 0.04$). For the presence of TIM3, IDO, B7H4 and LAG3 in tumor cells, no difference in OS was observed ($p > 0.05$).

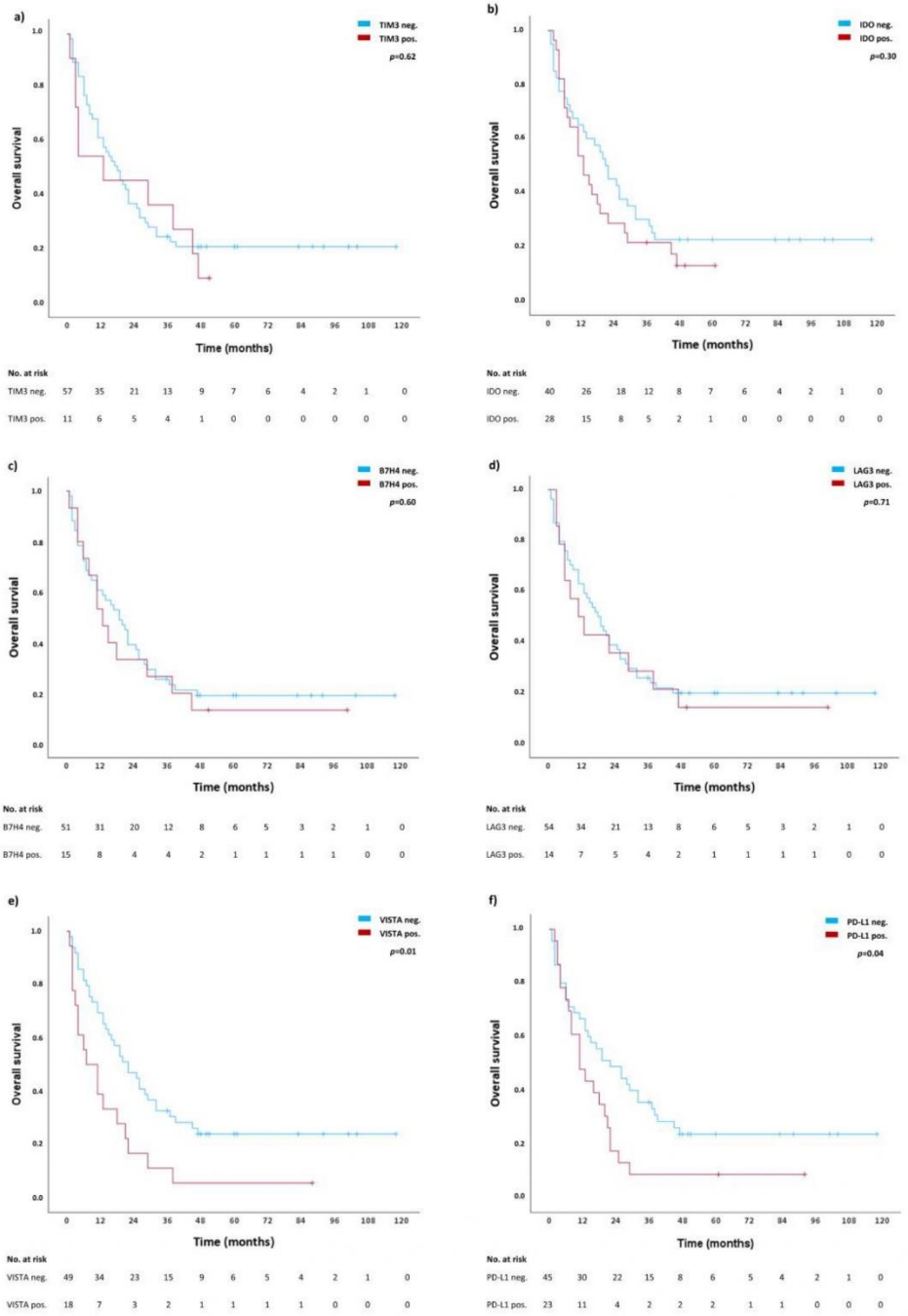


**Figure 2.** Individual survival analyses for TIM3 (**a**), IDO (**b**), B7H4 (**c**), LAG3 (**d**), VISTA (**e**), and PD-L1 (**f**). Blue lines represent survival curves in absence of the respective ICs, whereas red lines represent survival curves in presence of the respective IC. Tick marks indicate censoring.

#### 2.3.2. Combined Analysis of Significantly Correlated Immune Checkpoints VISTA and PD-L1

For VISTA and PD-L1 an in-depth subgroup analysis was performed correlating the absence of both VISTA and PD-L1 (VISTA neg., PD-L1 neg.), the presence of either VISTA (VISTA pos., PD-L1 neg.) or PD-L1 (VISTA neg., PD-L1 neg.) or both VISTA and PD-L1 (VISTA pos., PD-L1 pos.) with OS. Table 4 shows the presence of the respective combination of ICs in patients as well as one-year, three-year and five-year survival rates for each subgroup. The OS rates of the subgroup VISTA neg., PD-L1 neg. are the highest, whereas the OS rates of the subgroup VISTA pos., PD-L1 pos. are the lowest, intermediated by the subgroups with one of the ICs being present (VISTA pos., PD-L1 neg. and VISTA neg., PD-L1 pos.). Figure 3 shows the survival curves of OS for the combined analysis for all four subgroups with overall statistical significance difference ($p = 0.02$). Consistent with the survival rates, the survival curves of the subgroup VISTA neg., PD-L1 neg. and the subgroup VISTA pos., PD-L1 pos. diverge the most and are intermediated by subgroups with positivity for one of the ICs (VISTA pos., PD-L1 neg. and VISTA neg., PD-L1 pos.).

**Table 4.** Presence of the ICs of the formed subgroups and their respective one-year, three-year and five-year survival rates.

| ICs | All Patients | One-Year SR | Three-Year SR | Five-Year SR |
|---|---|---|---|---|
| VISTA neg., PD-L1 neg. | 52.9% ($n = 36$) | 77.8% | 38.9% | 26.9% |
| VISTA pos., PD-L1 neg. | 11.8% ($n = 8$) | 25.0% | 25.0% | 12.5% |
| VISTA neg., PD-L1 pos. | 19.1% ($n = 13$) | 46.2% | 15.4% | 15.4% |
| VISTA pos., PD-L1 pos. | 14.7% ($n = 10$) | 50.0% | 0.0% | 0.0% |

SR: survival rate.

### *2.4. Heterogeneity of VISTA and PD-L1 in Cancer Cells of PDAC*

For the two ICs that significantly correlated with shorter OS, we analyzed their distribution across the different spots of the TMA and compared their expressions between tumor periphery vs. tumor center. For VISTA, we observed an intratumoral heterogeneity: Of the 18 patients expressing VISTA, two (11.1%) were positive in all spots (100%), one patient (5.6%) in 66.7% of the spots, four patients (22.2%) in 50% of the spots, two patients (11.1%) in 33.3% of the spots, and the majority (n = 9, 50%) in one of six spots (16.67%, Figure 4A). PD-L1 had a higher degree of homogeneity regarding its expression: Eight patients (34.8%) showed positivity in 100% of the analyzed spots, four patients (17.4%) in 83.3% of the spots, three patients (13.0%) in 66.7% of the spots, three (13.0%) in 50.0% of the spots, another three (13.0%) in 33.3% of the spots, and only two patients (8.7%) in 16.7% of the spots (Figure 4B).

The expressions of VISTA and PD-L1 were also compared to the average expression of spots localized at the periphery of the tumor vs. average expression of spots localized in the center of the tumor. This paired analysis showed no difference in the expressions of VISTA ($p = 0.52$, Figure 4C) or PD-L1 ($p = 0.14$, Figure 4D) in the periphery vs. the center of PDAC.

Additionally, survival analyses were performed for subgroups of VISTA and PD-L1 expression (1) only in the periphery and (2) only the center of tumors as well as (3) expression in both, the periphery and the center of the tumor. For PD-L1 there was no significant impact on OS for these individual subgroups ($p > 0.05$). VISTA expression in the center only and in both the center and the periphery of tumors showed a significant correlation with shorter OS ($p < 0.05$), whereas expression only in the periphery of tumors does not correlate with shorter OS (Table 5). Two of the eighteen patients (11.1%) expressing VISTA were excluded from this analysis due to absence of peripheral tumor spots in the TMA.

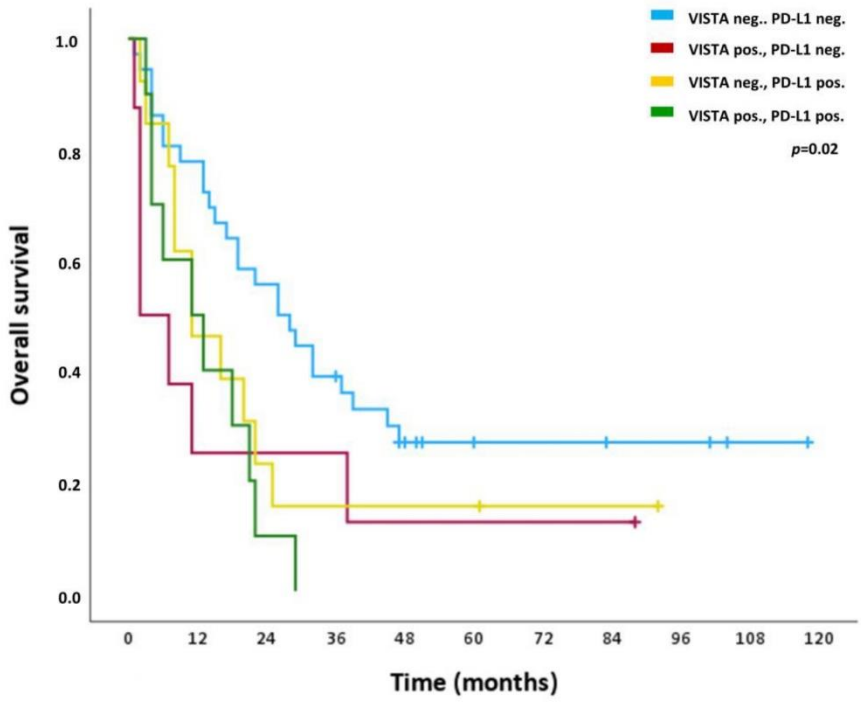


| No. at risk | | | | | | | | | | | |
|---|---|---|---|---|---|---|---|---|---|---|---|
| VISTA neg. PD-L1 neg. | 36 | 28 | 20 | 13 | 7 | 5 | 4 | 3 | 2 | 1 | 0 |
| VISTA pos. PD-L1 neg. | 8 | 2 | 2 | 2 | 1 | 1 | 1 | 1 | 0 | 0 | 0 |
| VISTA neg. PD-L1 pos. | 13 | 6 | 3 | 2 | 2 | 2 | 1 | 0 | 0 | 0 | 0 |
| VISTA pos. PD-L1 pos. | 10 | 5 | 1 | 0 | 0 | 0 | 0 | 0 | 0 | 0 | 0 |

**Figure 3.** Overall survival (OS) of the subgroups VISTA neg. and PD-1 neg. (blue line), VISTA pos. and PD-L1-neg. (red line), VISTA neg. and PD-L1 pos. (turquoise line), and VISTA pos. and PD-L1 pos. (purple line). Tick marks indicate censoring.

**Table 5.** Expression of VISTA in the periphery, the center or both regions of tumors and respective survival rates.

| Localization of VISTA Expression | Patients | Log-Rank *p*-Value | Median Survival No Expression vs. Expression |
|---|---|---|---|
| Periphery only | 22.2% ($n$ = 4) | $p$ = 0.97 | 19 months (CI: 11.5–26.5) vs. 11 months (CI: 0.0–24.7) |
| Center only | 44.4% ($n$ = 8) | $p$ = 0.01 | 19 months (CI: 12.8–25.2) vs. 4 months (CI: 0.0–9.5) |
| Periphery and center | 22.2% ($n$ = 4) | $p$ < 0.01 | 19 months (CI: 13.4–24.6) vs. 2 months |

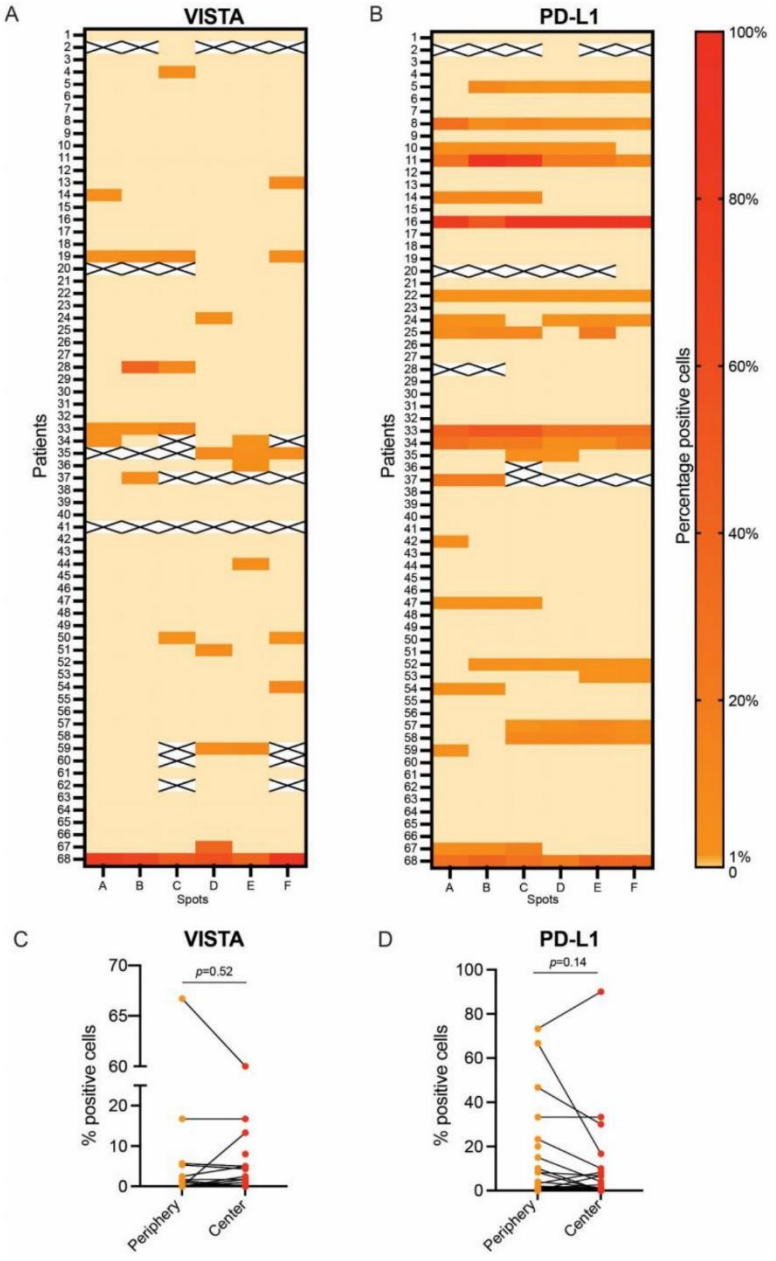


**Figure 4.** Intratumoral heterogeneity of VISTA and PD-L1 expression: percentage of VISTA expression in tumor cells across the entire PDAC cohort (**A**) and percentage of PD-L1 expression in tumor cells across the entire PDAC cohort (**B**). Paired comparison of VISTA expression in spots of tumor periphery vs. spots of tumor center (**C**) and paired comparison of PD-L1 expression in spots from tumor periphery vs. spots from tumor center (**D**).

## 3. Discussion

From a mutational point of view, PDAC is a very homogenous malignant disease. This cancer type is defined by frequent *KRAS*, *TP53*, and *SMAD4* mutations [17], making DNA sequencing data far less valuable for patient prognosis and therapy selection. Hence, our

aim was to discover new markers that can stratify patients with PDAC and reveal new potential therapeutic targets.

ICs are established prognostic and therapeutic targets in multiple malignancies [18] and thousands of clinical trials are ongoing to broaden our arsenal of inhibitors for multiple cancer types, including PDAC [19]. The only ICT approved for PDAC is the agnostic approval of anti-PD1 for tumors that are MSI-H/dMMR. PDACs with MSI-H/dMMR represent only 0.8–2% of all PDACs, and even for these tumors, the response rate is limited [7]. PDAC is perceived as a "cold" malignancy from an immunological point of view with a low mutational burden making ICT very challenging. Therefore, we believe that a deeper biological understanding of ICs in these tumors is crucial and future therapeutic regimes are likely to contain combinations of ICTs that target multiple immune checkpoint proteins.

We used a well-annotated cohort of PDAC patients, for whom we had long-term survival data, and analyzed the expression levels of TIM3, IDO, B7H4, LAG3, VISTA and PD-L1 in cancer cells by IHC to obtain an overview of IC expression in this neoplasia. We observed that PD-L1- and VISTA-positive tumors are associated with shorter OS. Regarding PD-L1 expression, our results are in line with previous studies. In a cohort of 373 patients with PDAC, Linag et al. showed that PD-L1 positivity in tumor cells is associated with shorter OS and progression-free survival. Additionally, they observed a borderline association between PD-L1 positivity and lymph node metastases [20]. In a more recent paper, this observation was also confirmed: PD-L1 positivity in tumor cells in PDAC, but not in immune cells, correlates with a shorter OS [21].

The role of VISTA as a prognostic marker in PDAC is much more controversial. In a large study, Hou et al. analyzed the expression of VISTA in two cohorts of PDAC. They observed that high VISTA expression is borderline associated with longer OS compared with the low expression of VISTA in both cohorts. It is important to note that Hou et al. methodologically divided VISTA into high-expression vs. low-expression groups and not positive vs. negative, which was the case in this study [22]. The results of the subgroup analysis of our study show a loss of significance regarding the negative effect on OS for expression of VISTA in $\geq$10% of tumor cells (Supplementary Table S2). This is because, in our study, the negative effect on median survival does not increase with a higher percentage of positive tumor cells, whereas the number of cases in which VISTA is present to such a high extent decreases. Additionally, our results show that VISTA expression is heterogeneous within tumors and only has an impact on OS in cases where it is present in the center of the tumor. For VISTA, in contrast to PD-L1, there is currently no consensus regarding what staining interpretation is the most clinically relevant, and this point needs to be addressed in future studies. However, our results underline the importance of sampling multiple regions in order to discover VISTA positivity and indicate that the center of tumors may present a TME, in which VISTA expression on tumor cells has a prognostic impact, in contrast to the periphery of tumors. Hou et al. also analyzed the expression of VISTA in immune cells and endothelial cells but did not observe any differences in OS [22].

Another study, complementary to ours, analyzed the expressions of IDO, VISTA, LAG3, and TIM3 in tumor-infiltrating lymphocytes in PDAC patients from the PANCALYZE study cohort. Here, Popp et al. observed that a high expression of IDO, but not of VISTA, LAG3, and TIM3, is associated with a prolonged OS [10]. In our study, however, a significant negative effect on survival in presence of IDO in $\geq$10% and <50% of tumor cells was found (Supplementary Table S2, median survival 19 months (CI: 12.4–25.6) vs. 4 months (CI: 0.0–13.2), $p = 0.016$). This agrees with existing studies that identify a strong expression of IDO in cancer cells as a negative prognostic factor [23]. These complementary data point out the versatile role that IC molecules can play and the differences in their significance between immune cells and tumor cells.

Finally, by performing a combined analysis, we observed that negativity in both VISTA and PD-L1 characterizes a subgroup of patients with significantly longer OS, while positivity in both is associated with the worst OS.

Our study has limitations that need to be reported. Firstly, we want to stress that all samples come from only one center, Charité—Universitätsmedizin Berlin. Secondly, the study was retrospectively performed and lacks information regarding tumor recurrence and disease-free survival. Third, no DNA-sequencing data were available in the study cohort. It is of potential clinical interest to see if there are any associations between the type of *KRAS* or *TP53* mutations and the expression of the various immune checkpoints. Fourthly, post-translational modifications (e.g., glycosylation) may influence the binding between ICs and the corresponding antibodies used in this study and can potentially lead to false-negative results [24]. Such potential false-negative results can be detected using multiple antibodies for each marker and by removing post-translational modifications before staining. This will be addressed in future studies of a less explorative nature.

These results open multiple interesting avenues of exploration for future studies. We believe that there is a subtle interplay between immune cells, tumor cells, and nerve cells in PDAC. To maximize the potential of anticancer immunotherapy in the future, factors complementary to ICs that influence the complex interplay of immune cells in the TME need to also be taken into account [25,26]. We hypothesize that the VISTA pos./PD-L1 pos. subgroup is characterized also by specific subtypes of mutations in *TP53* and *KRAS*, and by a specific TME defined by various types of specialized immune cells and regulatory nerve fibers [27]. We will address these points in subsequent studies.

## 4. Materials and Methods

### *4.1. Patient Cohort*

In this retrospective, single-center study approved by the institutional ethics committee (#EA2/031/21), samples from formalin-fixed, paraffin-embedded (FFPE) specimens of 68 patients with histologically confirmed PDAC—who underwent oncologic pancreatic resection between September 2009 and September 2020 in the Department of Surgery, Campus Benjamin Franklin, Charité—Universitätsmedizin Berlin—were included following informed consent. Of 93 patients, five patients that died within 30 days postoperatively, nine patients with metastatic disease at the time of surgery, seven patients with neuroendocrine tumors (NET) in the final histopathology report, two patients with tumors of duodenal origin, and two patients that had no follow-up after surgery as they were not living in Germany were excluded from this study ($n$ = 25). Patients' demographic and clinicopathological characteristics are presented in Table 1. The follow-up of patients in terms of OS was performed until death or for a median of 61 months (range: 36–118 months, censored cases, referred to as "survivors" in Results).

### *4.2. Surgery*

All patients underwent oncologic pancreatic resection (pylorus-preserving pancreaticoduodenectomy, Whipple procedure, left-sided pancreatic resection or total pancreatectomy) according to the current guidelines after surgery was indicated by an interdisciplinary tumor board. One patient received neoadjuvant chemotherapy prior to tumor resection.

### *4.3. Tissue-Microarrays and Immunohistochemistry*

FFPE specimens of resected PDAC were collected from the archive of the Institute of Pathology at the Charité—Universitätsmedizin Berlin, Campus Mitte and Campus Benjamin Franklin, Berlin, Germany. For the purpose of this study, tumor specimens were reviewed by two study pathologists (S.S. and M.P.D.) with 6 and 2 years of experience, respectively, in the histopathology of the pancreas, regarding cancer subtype, grading, pTNM-classification, vascular, lymphatic, and perineural invasion according to the 8th edition of the TNM classification (AJCC). They annotated the tumor area and excluded non-tumor regions, including necrosis and artefacts. For tissue microarray (TMA) construction, from each tumor, a total of six 2 mm tissue cores were punched out from high-tumor-purity regions of the tumor, three of them from different areas of the periphery of the tumor, and three from different areas of the tumor center; these were embedded in empty recipient

paraffin blocks. For IHC analysis, the TMA blocks were cut into 4 µm sections. The sections were incubated in a CC1 mild buffer (Ventana Medical Systems, Tucson, AZ, USA) for 30 min at 100 °C or in protease 1 for 8 min. Afterwards, the sections were stained with an anti-B7H4 antibody (D1M8I, Cell Signaling, Danvers, Massachusetts, United States, 1:300), anti-IDO antibody (D5J4E, Cell Signaling, 1:100), anti-LAG3 antibody (D2G40; 1:300; Cell Signaling Technology), anti-PD-L1 antibody (E1L3N, Cell Signaling, 1:200), anti-TIM-3 antibody (D5D5R; 1:100; Cell Signaling Technology), and anti-VISTA antibody (D1L2G; 1:100; Cell Signaling Technology) for 60 min at room temperature, before being visualized using the avidin–biotin complex method and DAB. For this purpose, the BenchMark XT immunostainer (Ventana Medical Systems, Tucson, AZ, USA) was used. A detailed list of these applied antibodies is presented in Supplementary Table S1. For the counterstaining of cell nuclei, sections were incubated with hematoxylin and bluing reagent (Ventana Medical Systems, Tucson, AZ) for 12 min. In this way, for each patient, six IHC stainings from the respective TMA were prepared for IHC evaluation (three from the center and three from the periphery of each tumor). As usual in TMA processing, there is a certain loss of stainings (~10%). In our cohort, the overall median of stainings for each IC per patient was 6.0 (range 0–6, total of 2321 stainings). One patient had no IHC staining of VISTA, and three patients had no IHC staining of B7H4. The stainings were analyzed using an Olympus BX50 microscope (Olympus Europe). Histological images were acquired with the digital slide scanner, PANNORAMIC 1000 (3DHISTECH).

### *4.4. Evaluation of Immunohistochemistry and Threshold Selection*

Evaluations of all IHC stainings were performed individually by the two study pathologists. The tumor cells on each staining were evaluated in terms of presence of the ICs: TIM-3, IDO, B7H4, IDO, LAG3, VISTA and PD-L1. For each respective IC, the ratio of visible positive cancer cells to total cancer cells per staining in percentage (%) was calculated. The tumor of a patient was classified as IC-positive if the respective IC was visible in at least 1% of cancer cells on at least one staining of the respective case. Discrepancies between the two study pathologists were discussed, and if no consensus was found, a third pathologist was consulted. Subsequently, to analyze the increasing expression levels, four subgroups were formed: ICs were visible in $\geq$ 1%, $\geq$ 1% and <10%, $\geq$ 10% and <50% and $\geq$ 50% of total cancers cells. The tumor of a patient was assigned to one of these subgroups when an IC was visible in the respective percentage of total cancers per staining on at least one of staining of the respective case (Supplementary Table S2). For ICs that significantly correlated with OS, intratumoral heterogeneity was evaluated via an analysis of distribution of expressed ICs across the different spots of the TMA of each individual tumor, generally, and regarding tumor center vs. tumor periphery.

### *4.5. Statistics*

For our statistical analysis, we utilized SPSS version 28.0 (IBM Corp. Released 2021. IBM SPSS Statistics for Windows, Version 28.0. Armonk, NY, USA: IBM Corp.) Overall-survival (OS) Kaplan–Meier curves were plotted and compared using the log-rank test. For medians of OS, 95% confidence intervals (CI) were calculated. Cox proportional-hazards regression model was used for the calculation of univariate and multivariate hazard ratios for OS. Univariate variables with a trend towards significance ($p < 0.10$) and after testing of the proportional hazards assumption were used for analysis in the multivariate model. For the analysis of intratumoral heterogeneity of IC expression, we averaged the respective IC expression of all spots located in the periphery and in the center of the respective tumor and performed a paired t-test to test for differences. A $p$-value of <0.05 was considered a statistically significant difference. Graphics were designed using CorelDRAW® Graphic Suite 2021 (Corel Corporation, Ottawa, ON, Canada) and GraphPad Prism Version 9.3.1 (GraphPad Software, San Diego, CA, USA).

## 5. Conclusions

The results of our study suggest that the presence of VISTA and PD-L1 in cancer cells of PDAC is of prognostic relevance and potentially qualifies them as targets for ICT. Further studies investigating the exact interplay between immune cells, tumor cells and nerve cells in PDAC, as well as their mutational subtypes in the TME, are warranted.

**Supplementary Materials:** The following supporting information can be downloaded at: https://www.mdpi.com/article/10.3390/ijms24032160/s1.

**Author Contributions:** Conceptualization, F.N.L., C.K., M.P.D. and S.S.; methodology, F.N.L., C.K., M.P.D. and S.S.; software, F.N.L., C.K., M.P.D. and S.S.; validation, C.K.; formal analysis, F.N.L., C.K., M.P.D. and S.S.; investigation, M.P.D. and S.S.; resources, F.N.L., C.K., M.P.D. and S.S.; data curation, F.N.L., C.K., M.P.D. and S.S.; writing—original draft preparation, F.N.L., C.K., M.P.D. and S.S.; writing—review and editing, K.B., W.R., C.S., J.C.L. and D.H.; visualization, F.N.L., M.P.D. and S.S.; supervision, C.K., K.B. and D.H.; project administration, F.N.L., C.K., M.P.D. and S.S. All authors have read and agreed to the published version of the manuscript.

**Funding:** The work of M.P.D. is supported by Berlin Institute of Health, Junior Clinician Scientist Program, DKTK Berlin Young Investigator Grant 2022, Berliner Krebsgesellschaft (DRFF202204). We acknowledge support from the German Research Foundation (DFG) and the Open Access Publication Fund of Charité—Universitätsmedizin Berlin, corporate member of Freie Universität Berlin and Humboldt-Universität zu Berlin.

**Institutional Review Board Statement:** The study was conducted in accordance with the Declaration of Helsinki, and approved by the ethics committee of the Charité—Universitätsmedizin Berlin, corporate member of Freie Universität Berlin and Humboldt-Universität zu Berlin (#EA2/031/21 on the 5 March 2021).

**Informed Consent Statement:** Informed consent was obtained from all subjects involved in the study.

**Data Availability Statement:** The datasets used and/or analyzed during the current study are available upon reasonable request pending approval by the local data security authorities.

**Conflicts of Interest:** The authors declare no conflict of interest.

## References

1. Beatty, G.L.; Gladney, W.L. Immune escape mechanisms as a guide for cancer immunotherapy. *Clin. Cancer Res.* **2015**, *21*, 687–692. [CrossRef] [PubMed]
2. Pardoll, D. The blockade of immune checkpoints in cancer immunotherapy. *Nat. Rev. Cancer* **2012**, *12*, 252–264. [CrossRef] [PubMed]
3. Sharma, P.; Siddiqui, B.A.; Anandhan, S.; Yadav, S.S.; Subudhi, S.K.; Gao, J.; Goswami, S.; Allison, J.P. The next decade of immune checkpoint therapy. *Cancer Discov.* **2012**, *11*, 838–857. [CrossRef] [PubMed]
4. Sung, H.; Ferlay, J.; Siegel, R.L.; Laversanne, M.; Soerjomataram, I.; Jemal, A.; Bray, F. CA Global cancer statistics 2020. GLOBOCAN estimates of incidence and mortality worldwide for 36 cancers in 185 countries. *Cancer J. Clin.* **2021**, *71*, 209–249. [CrossRef] [PubMed]
5. Rawla, P.; Sunkara, T.; Gaduputi, V. Epidemiology of Pancreatic Cancer: Global Trends, Etiology and Risk Factors. *World J. Oncol.* **2019**, *10*, 10–27. [CrossRef]
6. Jun, U.; Kanno, A.; Ikeda, E.; Ando, K.; Nagai, H.; Miwata, T.; Kawasaki, Y.; Tada, Y.; Yokoyama, K.; Numao, N.; et al. Pancreatic Ductal Adenocarcinoma: Epidemiology and Risk Factors. *Diagnostics* **2021**, *11*, 562. [CrossRef]
7. Bian, J.; Almhanna, K. Pancreatic cancer and immune checkpoint inhibitors-still a long way to go. *Transl. Gastroenterol. Hepatol.* **2021**, *6*, 6. [CrossRef]
8. Wang, M.; Liu, Y.; Cheng, Y.; Wei, Y.; Wei, X. Immune checkpoint blockade and its combination therapy with small-molecule inhibitors for cancer treatment. *Biochim. Biophys. Acta Rev. Cancer* **2019**, *1871*, 199–224. [CrossRef]
9. Sun, Y.; Wang, Y.; Zhao, J.; Gu, M.; Giscombe, R.; Lefvert, A.K.; Wang, X. B7-H3 and B7-H4 expression in non-small-cell lung cancer. *Lung Cancer* **2006**, *53*, 143–151. [CrossRef]
10. Popp, F.C.; Capino, I.; Bartels, J.; Damanakis, A.; Li, J.; Datta, R.R.; Löser, H.; Zhao, Y.; Quaas, A.; Lohneis, P.; et al. Expression of Immune Checkpoint Regulators IDO, VISTA, LAG3, and TIM3 in Resected Pancreatic Ductal Adenocarcinoma. *Cancers* **2021**, *13*, 2689. [CrossRef]
11. Chocarro, L.; Blanco, E.; Zuazo, M.; Arasanz, H.; Bocanegra, A.; Fernández-Rubio, L.; Morente, P.; Fernández-Hinojal, G.; Echaide, M.; Garnica, M.; et al. Understanding LAG-3 Signaling. *Int. J. Mol. Sci.* **2021**, *22*, 5282. [CrossRef] [PubMed]

12. Seifert, L.; Plesca, I.; Müller, L.; Sommer, U.; Heiduk, M.; von Renesse, J.; Digomann, D.; Glück, J.; Klimova, A.; Weitz, J.; et al. LAG-3-Expressing Tumor-Infiltrating T Cells Are Associated with Reduced Disease-Free Survival in Pancreatic Cancer. *Cancers* **2021**, *13*, 1297. [CrossRef] [PubMed]
13. Kryczek, I.; Zou, L.; Rodriguez, P.; Zhu, G.; Wei, S.; Mottram, P.; Brumlik, M.; Cheng, P.; Curiel, T.; Myers, L.; et al. B7-H4 expression identifies a novel suppressive macrophage population in human ovarian carcinoma. *J. Exp. Med.* **2006**, *203*, 871–881. [CrossRef] [PubMed]
14. Cao, Y.; Zhou, X.; Huang, X.; Li, Q.; Gao, L.; Jiang, L.; Huang, M.; Zhou, J. Tim-3 expression in cervical cancer promotes tumor metastasis. *PLoS ONE* **2013**, *8*, e53834. [CrossRef]
15. Klümper, N.; Ralser, D.J.; Bawden, E.G.; Landsberg, J.; Zarbl, R.; Kristiansen, G.; Toma, M.; Ritter, M.; Hölzel, M.; Ellinger, J.; et al. LAG3 (LAG-3, CD223) DNA methylation correlates with LAG3 expression by tumor and immune cells, immune cell infiltration, and overall survival in clear cell renal cell carcinoma. *J. Immunother. Cancer* **2020**, *8*, e000552. [CrossRef] [PubMed]
16. Mulati, K.; Hamanishi, J.; Matsumura, N.; Chamoto, K.; Mise, N.; Abiko, K.; Baba, T.; Yamaguchi, K.; Horikawa, N.; Murakami, R.; et al. VISTA expressed in tumour cells regulates T cell function. *Br. J. Cancer* **2019**, *120*, 115–127. [CrossRef] [PubMed]
17. Cancer Genome Atlas Research Network. Integrated Genomic Characterization of Pancreatic Ductal Adenocarcinoma. *Cancer Cell* **2017**, *32*, 185–203.e13. [CrossRef] [PubMed]
18. He, X.; Xu, C. Immune checkpoint signaling and cancer immunotherapy. *Cell Res.* **2020**, *30*, 660–669. [CrossRef]
19. Gaikwad, S.; Agrawal, M.Y.; Kaushik, I.; Ramachandran, S.; Srivastava, S.K. Immune checkpoint proteins: Signaling mechanisms and molecular interactions in cancer immunotherapy. *Semin. Cancer Biol.* **2022**, *86*, 137–150. [CrossRef]
20. Liang, X.; Sun, J.; Wu, H.; Luo, Y.; Wang, L.; Lu, J.; Zhang, Z.; Guo, J.; Liang, Z.; Liu, T. PD-L1 in pancreatic ductal adenocarcinoma: A retrospective analysis of 373 Chinese patients using an in vitro diagnostic assay. *Diagn. Pathol.* **2018**, *13*, 5. [CrossRef]
21. Zhang, Y.; Chen, X.; Mo, S.; Ma, H.; Lu, Z.; Yu, S.; Chen, J. PD-L1 and PD-L2 expression in pancreatic ductal adenocarcinoma and their correlation with immune infiltrates and DNA damage response molecules. *J. Pathol. Clin. Res.* **2022**, *8*, 257–267. [CrossRef] [PubMed]
22. Hou, Z.; Pan, Y.; Fei, Q.; Lin, Y.; Zhou, Y.; Liu, Y.; Guan, H.; Yu, X.; Lin, X.; Lu, F.; et al. Prognostic significance and therapeutic potential of the immune checkpoint VISTA in pancreatic cancer. *J. Cancer Res. Clin. Oncol.* **2021**, *147*, 517–531. [CrossRef] [PubMed]
23. Meireson, A.; Devos, M.; Brochez, L. IDO Expression in Cancer: Different Compartment, Different Functionality? *Front. Immunol.* **2020**, *11*, 531491. [CrossRef] [PubMed]
24. Lee, H.H.; Wang, Y.N.; Xia, W.; Chen, H.; Rau, K.M.; Ye, L.; Wei, Y.; Chou, C.K.; Wang, S.C.; Yan, M.; et al. Removal of N-Linked Glycosylation Enhances PD-L1 Detection and Predicts Anti-PD-1/PD-L1 Therapeutic Efficacy. *Cancer Cell* **2019**, *36*, 168–178. [CrossRef] [PubMed]
25. Huang, X.; Tang, T.; Zhang, G.; Hong, Z.; Xu, J.; Yadav, D.K.; Bai, X.; Liang, T. Genomic investigation of co-targeting tumor immune microenvironment and immune checkpoints in pan-cancer immunotherapy. *NPJ Precis. Oncol.* **2020**, *4*, 29. [CrossRef]
26. Huang, X.; Tang, T.; Wang, X.; Bai, X.; Liang, T. Calreticulin couples with immune checkpoints in pancreatic cancer. *Clin. Transl. Med.* **2020**, *10*, 36–44. [CrossRef]
27. Dragomir, M.P.; Moisoiu, V.; Manaila, R.; Pardini, B.; Knutsen, E.; Anfossi, S.; Amit, M.; Calin, G.A. A Holistic Perspective: Exosomes Shuttle between Nerves and Immune Cells in the Tumor Microenvironment. *J. Clin. Med.* **2020**, *9*, 3529. [CrossRef]

### 2.3 Analyse des Einflusses chirurgischer Resektionsränder resektabler exokriner Pankreaskopfkarzinome auf das Gesamtüberleben sowie das Auftreten von Fernmetastasen (Originalarbeit 3)

Eine prognostischen Risikostratifikation resektabler exokriner Pankreaskarzinome erfolgt auch anhand von prognostischen Merkmalen, die aus der postoperativen pathologischen Aufarbeitung chirurgischer Operationsresektate hervorgehen. Die **Originalarbeit 3** untersucht als ein solches Merkmal systematisch den Einfluss der Entfernung sowie der Lokalisation von Tumorzellen zu den chirurgischen Resektionsrändern. Wie die **Originalarbeit 1 und 2** widmet sie sich so der prognostischen Risikostratifikation resektabler exokriner Pankreaskarzinome und ergänzt sie auf dieser weiteren methodischen Ebene.

**Florian N. Loch**, Carsten Kamphues, Freschta Rieger, Katharina Beyer, Wael Rayya, Christian Schineis, Frederick Klauschen, David Horst, Simon Schallenberg, Mihnea P.Dragomir.

Stepwise analysis of resection margin impact on survival and distant metastasis in pancreatic head ductal adenocarcinoma. *International Journal of Surgical Pathology*. **2024**; Epub ahead of print: https://doi.org/10.1177/10668969241229342.

Der nachfolgende Text entspricht dem Originalabstract der o.g. Publikation *Stepwise analysis of resection margin impact on survival and distant metastasis in pancreatic head ductal adenocarcinoma* übersetzt durch den Erstautor Florian N. Loch:

*„Die prognostische Bedeutung von Tumorzellen des PDAC des Pankreaskopfes mit DMI oder von Tumorzellen in unmittelbarer Nähe eines Resektionsrandes (≤ 1 mm) ist weiterhin nicht eindeutig. Diese monozentrischen retrospektive Studie schloss Resektate von 75 Patient:innen ein, die zwischen Februar 2013 und Juli 2020 eine onkologischer Tumorresektion eines PDAC des Pankreaskopfes erhielten. Es erfolgte die erneute Vermessung des Abstandes von Tumoren zu den jeweiligen Resektionsrändern unabhängig voneinander durch zwei Pathologen. Der Einfluss der DMI sowie von Tumorzellen im Abstand von ≤ 1 mm eines Resektionsrandes auf das Gesamtüberleben und die Entwicklung von Lungen- und Lebermetastasen wurde analysiert, für alle Resektionsränder zusammengefasst sowie individuell für einzelne Resektionsränder. DMI eines Resektionsrandes war signifikant mit einem kürzeren Gesamtüberleben assoziiert (Median 5 vs. 19 Monate, p=0.02). Das Vorhandensein von Tumorzellen im Abstand von ≤*

*1 mm eines Resektionsrandes zeigte eine Tendenz zur Signifikanz (Median 9 Monaten vs. 21 Monate, p=0.09). In der individuellen Analyse zeigte sich bei DMI sowie Tumorzellen im Abstand von ≤ 1 mm zur Pankreasabsetzungsebene (medialer Resektionsrand) ein negativer Einfluss auf das Gesamtüberleben (Median 4 vs. 19 Monate und 6 vs. 19 Monate, p<0.05), der sich individuell für keine anderen Resektionsränder zeigte. Eine ausschließliche Einbeziehung des Resektionsrandes durch Tumorzellen im Abstand von ≤ 1 mm zur Gefäßrinne resultierte in einer kürzeren Zeit bis zur Entwicklung von Lebermetastasen (p=0.05). Bei DMI des retropankreatischen Resektionsrandes oder der Gefäßrinne zeigte sich eine kürzere Zeit bis zur Entwicklung von Lungenmetastasen (p<0.05). Potentielle klinische Erwägungen schließen eine erweiterte intraoperative Beurteilung der Pankreasabsetzungebene (1 mm) sowie eine Intensivierung der präoperativen Risikoeinschätzung einer R1-Resektion als eine Grundlage für eine neoadjuvante Therapie ein.“*

*Original Article*

# Stepwise Analysis of Resection Margin Impact on Survival and Distant Metastasis in Pancreatic Head Ductal Adenocarcinoma

International Journal of Surgical Pathology
1–12

DOI: 10.1177/10668969241229342
journals.sagepub.com/home/ijs


**Florian N. Loch, MD[1], Carsten Kamphues, MD[2], Freschta Rieger, MD[2], Katharina Beyer, MD[1], Wael Rayya, MD[1], Christian Schineis, MD[1], Frederick Klauschen, MD[3,4,5,6,7], David Horst, MD[3], Simon Schallenberg, MD[3], and Mihnea P. Dragomir, MD, PhD[3,4,8]**

## Abstract

The prognostic role of tumor cells in pancreatic ductal adenocarcinoma (PDAC) of the pancreatic head with direct microscopic infiltration (DMI) or in close proximity (≤1 mm) to the resection margin (RM) remains unclear. This single-center, retrospective study included specimens from 75 patients who underwent oncological resection of pancreatic head PDAC between February 2013 and July 2020. Two pathologists independently re-measured the distance between tumors and the multiple RMs. The impact of RM involvement for DMI, tumor cells within ≤1 mm, in general, and for individual RMs on overall survival (OS) and development of distant pulmonary (PM) and hepatic (HM) metastasis was analyzed. DMI of RMs was significantly associated with a shorter OS (median 5 vs 19 months, $P = .02$). The presence of tumor cells within ≤1 mm of RMs yielded a negative impact on OS with a trend toward significance (median 9 vs 21 months, $P = .09$). DMI and tumor cells within ≤1 mm of the pancreatic transection margin (PRM), individually, had a significant negative impact on OS (median 4 vs 19 months and 6 vs 19 months, $P < .05$), but not for any other individual RM. RM involvement of ≤1 mm of only the vascular circumferential resection margin (VCRM) resulted in a shorter time to HM development ($P = 0.05$). DMI of the posterior circumferential resection margin (PCRM) and VCRM, individually, showed shorter time to PM ($P < .05$). Potential clinical considerations include extended intraoperative evaluation of the PRM (1 mm) and intensified preoperative prediction of R1 resection as a basis for neoadjuvant therapy.

## Keywords

pancreatic cancer, resection margins, histopathology, risk stratification, neoadjuvant therapy

[1]Department of Surgery, Charité—Universitätsmedizin Berlin, Corporate Member of Freie Universität Berlin and Humboldt-Universität zu Berlin, Berlin, Germany
[2]Department of Surgery, Park-Klinik Weißensee, Berlin, Germany
[3]Institute of Pathology, Charité—Universitätsmedizin Berlin, Corporate Member of Freie Universität Berlin and Humboldt-Universität zu Berlin, Berlin, Germany
[4]German Cancer Consortium (DKTK), German Cancer Research Center (DKFZ), Heidelberg, Germany
[5]BIFOLD - The Berlin Institute for the Foundations of Learning and Data, Berlin, Germany
[6]Institute of Pathology, Ludwig-Maximilians-University Munich, München, Germany
[7]German Cancer Consortium (DKTK), German Cancer Research Center (DKFZ), Heidelberg, Germany
[8]Berlin Institute of Health at Charité, Berlin, Germany

Mihnea P. Dragomir and Simon Schallenberg contributed equally as last authors.

**Corresponding Author:**
Florian N. Loch, Department of Surgery, Charité—Universitätsmedizin Berlin, Corporate Member of Freie Universität Berlin and Humboldt-Universität zu Berlin, 12203 Berlin, Germany.
Email: Florian.Loch@charite.de

## Introduction

Pancreatic ductal adenocarcinoma (PDAC) is one of the deadliest malignancies, with an overall 5-year survival rate of only 9%, resulting in approximately 466 000 related deaths worldwide each year.[1,2] It is predicted that pancreatic cancer will become the second most frequent cause of cancer-related death in the United States by 2040.[3] Currently, oncologic resection is the only curative therapeutic approach. However, at the time of diagnosis, only about 20% of patients are eligible for oncologic resection. Even after tumor resection, overall 5-year survival rates remain as low as 20% to 27%.[4–6] Therefore, precise pre-operative and postoperative therapeutic decision making is crucial under such unfavorable prognostic circumstances.

The histopathological examination of the surgical specimen from oncologic resection is substantial in determining postoperative prognosis. It is well established that residual disease in the form of direct microscopic infiltration (DMI) of a resection margin (RM) has poor prognostic influence.[7] However, is not clear what role tumor cells play when they are not directly infiltrating an RM but are in close proximity of it (≤1 mm) or further away (>1 mm). Furthermore, it is necessary to determine the impact of tumor cells infiltrating and being in proximity to different RMs.[7] During oncologic resection of the pancreatic head the surgical specimen has circumferential resection margins (CRMs): anterior (ACRM), posterior (PCRM), and vascular (VCRM), as well as a pancreatic transection margin (PRM). In resectable PDAC located in the pancreatic head, tumor involvement of an RM is almost exclusively located within the circumference of the PRM and the CRMs, whereas tumor involvement in the bile duct, gastric or duodenal, and jejunal transection margins is rare.[8]

The purpose of this study is to incrementally analyze the impact of the distance and location of RMs on the survival and development of distant metastasis in PDAC of the pancreatic head.

## Material and Methods

### Patient Cohort

This retrospective single-center study included consecutive patients who underwent curative oncologic resection of the pancreatic head between February 2013 and July 2020 at the Department of Surgery, Campus Benjamin Franklin, Charité—Universitätsmedizin Berlin, and had histologically confirmed PDAC. Exclusion criteria were metastatic disease at the time of surgery (n = 4), retrospective nondeterminability of all RMs (n = 2), death within 30 days postoperatively (n = 6), and loss to follow up due to the patient residing outside of Germany (n = 1). After applying these exclusion criteria, a total of 75 patients (100%) were included in the study (Table 1). Overall survival (OS) was followed up for all patients until death or in censored cases for a median time of 63.5 months (range 39–109 months, n = 16, 21%). The development of distant hepatic and pulmonary metastasis was followed up for 54 patients (72%) either until metastasis or for a median time of 16.0 months (range 2–55 months).

**Table 1.** Demographic and Pathological Characteristics of the Patient Cohort.

| Patients | n = 75 |
|---|---|
| **Age** | |
| Median age (years) | 71 |
| Age range | 51–86 |
| **Sex** | |
| Female | 34 (45%) |
| Male | 41 (55%) |
| **Histopathological characteristics** | |
| pT1 | 9 (12%) |
| pT2 | 44 (59%) |
| pT3 | 21 (28%) |
| pT4 | 1 (1%) |
| pN0 | 15 (25%) |
| pN + (pN1 & pN2) | 60 (80%) |
| G1 | 1 (1%) |
| G2 | 46 (63%) |
| G3 | 28 (36%) |
| Pn0 | 13 (17%) |
| Pn1 | 62 (83%) |
| pL0 | 37 (49%) |
| pL1 | 38 (51%) |
| pV0 | 57 (76%) |
| pV1 | 18 (24%) |

Abbreviations: G, grading; pL, lymphovascular invasion; pV: vascular invasion; Pn, perineural invasion.

This study was approved by the ethics committee of the Charité—Universitätsmedizin Berlin (No. EA4/020/19), and written informed consent was waived due to the retrospective study design.

### Surgery

All patients included in this study underwent curative oncologic resection of the pancreatic head, either through pylorus-preserving pancreaticoduodenectomy (n = 48, 64%), Whipple procedure (n = 25, 33%), or total pancreatectomy (n = 2, 3%) as recommended by the interdisciplinary tumor board. Two patients (3%) had undergone neoadjuvant chemotherapy prior to tumor resection.

### Sample Gross Examination and Macroscopic Examination

The gross examination of all specimens from oncologic resection was performed in a standardized fashion, as

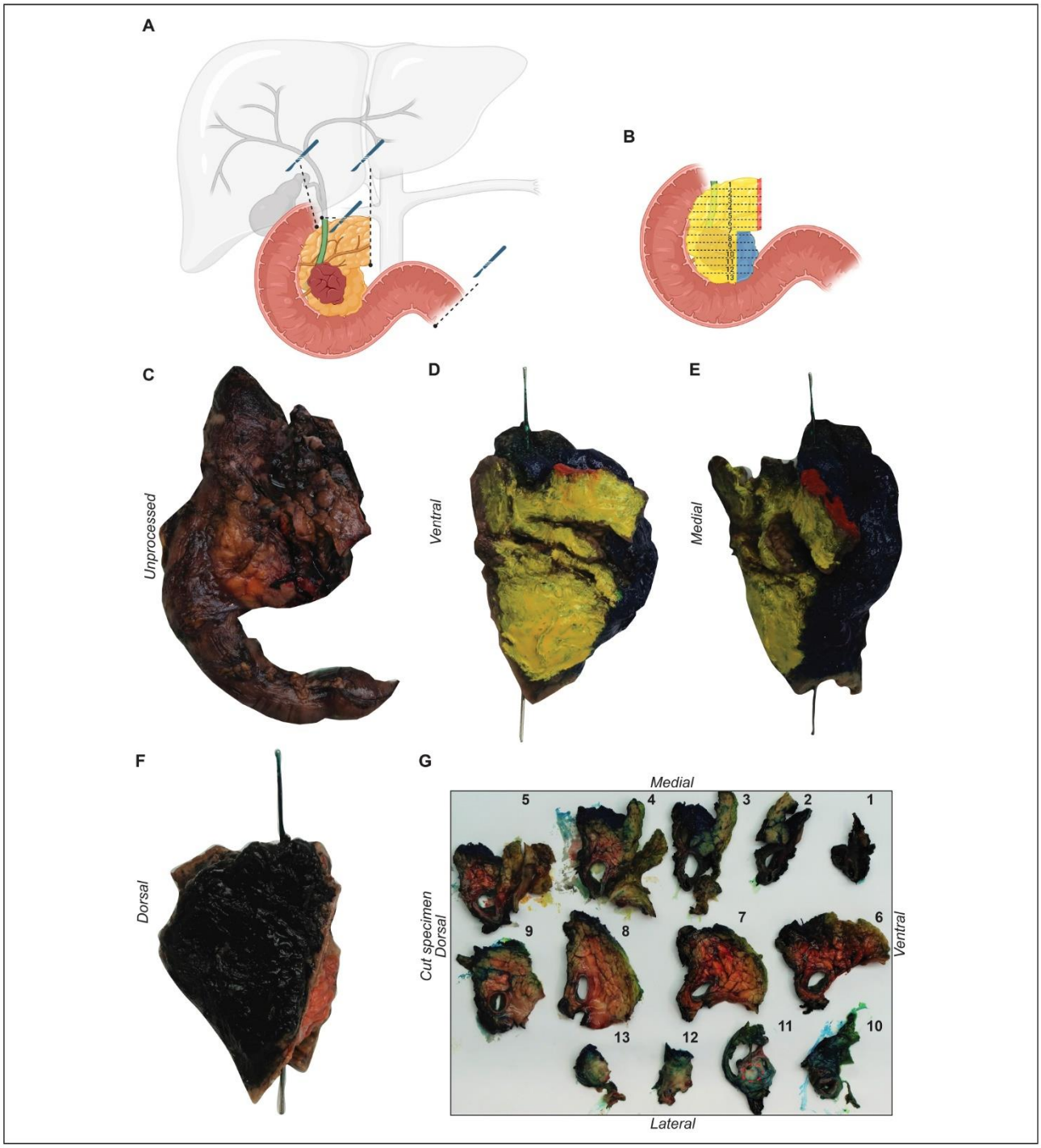


**Figure 1.** Tumor gross examination of a specimen obtained from oncological resection of the pancreatic head. (A) Depiction of the transection margins: pancreatic transection margin, distal bile duct, gastric/duodenal, and jejunal transection margin. (B) Graphical representation of the axial sectioning of the specimen from cranial to caudal. An unprocessed specimen of the pancreatic head, (C) and the same specimen stained according to our protocols: anterior—yellow (D) vascular margin—blue (E), posterior—black (F). (G) The specimen sectioned from cranial to caudal, with the tumor located in the uncinate process.

recently described and demonstrated in Figure 1A and B.[9] The specimens were fixed in 10% buffered formalin before gross examination. The anatomical elements (pylorus, duodenum, pancreas, bile duct) were measured, and the macroscopic appearance of the specimen was described (Figure 1C). The specimens were then marked using tissue dyes. Briefly, the ACRM of the pancreas was marked yellow (Figure 1D), the VCRM blue (Figure 1E),

the PCRM black (Figure 1F), the PRM red, and the bile duct lumen until the major duodenal papilla was marked green.

Next, the 4 transection margins (gastric/oral duodenal, aboral jejunal, pancreatic, and bile duct transection margin) were each embedded in 4 separate tissue-embedding cassettes. The remaining specimen was sliced in 5 mm sections from cranial to caudal perpendicular to the duodenal lumen (Figure 1G). Afterwards, a precise inspection of the slices was conducted to locate, describe, and measure the tumor. At this point, the macroscopic minimal distance of the tumor to the CRMs (ACRM, VCRM, and PCRM) and the PRM was determined and measured. The cranial and caudal ends of the specimen were further sliced and completely embedded. Next, the proximity of the tumors to the CRMs and the PRM were prepared and embedded. A minimum of 4 cassettes were prepared, 1 for each margin. Finally, all peripancreatic lymph nodes were detected and further embedded. An average of 20 tissue-embedding cassettes was prepared for each specimen. The embedded tissue blocks were cut into 2µm thick sections, and stained with hematoxylin and eosin (H&E), and one tissue block containing tumor tissue was stained with periodic acid-Schiff (PAS). Standard histological examination was performed according to the eighth edition of the TNM classification (AJCC) and included: T-stage, N-stage, grading (G1–3), lymphovascular (pL) and vascular invasion (pV), perineural invasion (Pn) and resection status. During routine diagnosis at our institution we considered a margin positive only if tumor cells were present in the colored surface of the specimen. Macroscopic residual disease (R2) was not present in any of the patients included in this study.

### *Microscopic Examination and R-Status Evaluation*

For the purpose of this study, all included specimens were re-evaluated. For the re-evaluation of the RM status and the minimal distance between tumors to CRMs and PRM, all slides were retrieved from the archive of the Institute of Pathology, Charité—Universitätsmedizin Berlin. Two pathologists (MPD and SS) independently remeasured the distance between the tumor and the respective margins in 1 mm increments. In case of discrepancies these were further discussed with a senior pathologist from the Institute of Pathology, Charité—Universitätsmedizin Berlin. In cases of re-resections of the PRM, the specimens from the re-resection were used. None of the specimens included in this study showed tumor cells in the pyloric/duodenal, jejunal, or bile duct transection margins. In 2 specimens (2.7%), the ACRM, VCRM, and PCRM could not be re-evaluated and information regarding the DMI of these margins was retrieved from the original histopathology reports. Beyond DMI, these margins were excluded from further analysis within this study. When reported or referred to as results of this study, in a summarizing manner the PCRM, VCRM, ACRM, and PRM will be referred to as RMs for convenience.

### *Statistics*

We compared the impact of different criteria of RM involvement on OS, as well as the development of distant hepatic and pulmonary metastases using Kaplan-Meier curves. The curves were compared using the log-rank test, and 95% confidence intervals (CI) were calculated for medians of OS. If there was a significant difference in survival analysis, we analyzed the association of the respective criterion of RM involvement with demographic and histopathological characteristics using the $\chi^2$ test. A $P$ value of $\leq .05$ was considered statistically significant, while $P$ values between .05 and .10 were considered a trend toward significance. Statistical analyses were performed using SPSS version 29.0 (IBM Corp. Released 2022. IBM SPSS Statistics for Windows, Version 29.0. Armonk, NY, USA: IBM Corp.).

## Results

### *Demographic and Pathological Characteristics of Patient Cohort*

The demographic and pathological characteristics of the patient cohort included in this study are presented in Table 1. The median OS of the entire patient cohort was 18 months (range 1–109, CI: 12.1–23.9). One-year, 3-year, and 5-year survival rates for the entire patient cohort were 61%, 27%, and 21%, respectively.

### *Distribution of Involved Resection Margins*

Table 2 summarizes the specimens with DMI and presence of tumor cells within ≤1mm of an RM in terms of the total number of specimens as well as the involved RMs. Ten patients (13.3%) had tumors with DMI of at least 1 RM (Figure 2A-C). Of these 10 tumors, 8 (80.0%) showed DMI of only 1 RM (PCRM, n = 2, 20.0%; VCRM, n = 2, 20.0%; PRM, n = 4, 40.0%) and 2 tumors (20.0%) showed DMI of 2 RMs (PCRM & VCRM and PRM & VCRM).

Tumors in 47 patients (62.7%) showed the presence of tumor cells within ≤1mm of at least 1 RM (Figure 2D-G). Tumors in 27 patients (36.0%) showed the presence of tumor cells within ≤1mm of only 1 RM.

Table 3 summarizes the specimens that only showed the presence of tumor cells in >1 mm from any RM (n = 26, 34.7%). For the incremental analysis of the closest distance of tumor cells to any of the RMs (eg, specimens in which the distance of the tumor cells that showed the closest presence to any RM was at least >1mm but within 2 mm of the respective RM) subgroups were created in steps of 1 mm.

**Table 2.** Distribution of Tumors With Direct Microscopic Infiltration and the Presence of Tumor Cells Within ≤ 1mm of the Specimen's Circumference.

| Location of Involved RM | Number of Tumors |
|---|---|
| **Microscopic infiltration** | |
| Any RM | n = 10 (13%) |
| PCRM | n = 2 (3%) |
| VCRM | n = 2 (3%) |
| ACRM | – |
| PRM | n = 4 (5%) |
| PCRM & VCRM | n = 1 (1%) |
| PRM & VCRM | n = 1 (1%) |
| **Presence of tumor cells within ≤1mm** | |
| Any RM | n = 47 (63%) |
| PCRM | n = 20 (27%) |
| VCRM | n = 30 (40%) |
| ACRM | n = 16 (21%) |
| PRM | n = 7 (9%) |
| **Presence of tumor cells within ≤1mm of only one RM** | |
| PCRM | n = 8 (11%) |
| VCRM | n = 11 (15%) |
| ACRM | n = 6 (8%) |
| PRM | n = 2 (3%) |

Abbreviations: ACRM: anterior circumferential resection margin; PCRM: posterior circumferential resection margin; PRM: pancreatic transection margin; RM: resection margin; VCRM: vascular circumferential resection margin.

## Influence of Margin Involvement on Overall Survival

*Influence of Direct Microscopic Infiltration of Resection Margins on Overall Survival.* Survival analysis showed that DMI of an RM was significantly associated with a shorter OS ($P = .02$). Median OS in the group of patients with DMI of an RM was 5 months (CI: 1.9–8.1) versus 19 months (CI: 14.1–23.9) in the group of patients without DMI of an RM (Figure 3). DMI of an RM was significantly associated with male gender ($P = .02$). No significant association was found between DMI of a, RM and age (>65 years), advanced T stage (pT3/4), nodal metastasis (pN+), lymphovascular invasion (pL1), perineural invasion (Pn1), vascular invasion (pV1), or higher grade (G3) ($P > .05$, for all associations).

To further distinguish the effect of DMI on OS, subgroup survival analysis was performed with respect to the location of DMI for each RM, individually. In this individual subgroup analysis, DMI of the PRM yielded a significantly shorter OS (median 4 months [CI: 1.9–6.1] versus 19 months [CI: 14.5–23.5], $P = .02$). For the individual DMI of other RMs (PCRM and VCRM), this subgroup survival analysis did not yield significance ($P = .86$ and .08, respectively). No significant association of PRM DMI with other demographic or histopathological characteristics was observed (gender, age >65 years, pT3/4, pN+, pL1, Pn1, pV1, G3; $p > 0.05$).

*Influence of Presence of Tumors Cells Within ≤1 mm of Resection Margins on Overall Survival.* Moreover, survival analyses were performed to investigate the influence of the presence of tumor cells within ≤1 mm of any RM on OS, as well as the presence of tumor cells within ≤1 mm of a specific RM, individually (Figure 4). The analysis regarding tumor cells within ≤1 mm of any RM showed a negative impact on OS with a trend toward significance (median OS 9 months [CI: 0.0–19.1] versus 21 months [CI: 13.5–28.5], $P = .09$).

When analyzing the presence of tumor cells within ≤1 mm of a specific RM, individually, a significant impact on OS was seen for the PRM (median OS 6 months [CI: 0.9–11.1] versus 19 months [14.5–23.5], $P = .01$, Figure 4, dark blue line) and a trend toward significance for the PCRM (6 months [CI: 1.6–10.4] versus 19 months [12.8–25.2], $P = .09$, Figure 4, orange line). No difference in OS was seen for tumor cells within ≤1 mm of the VCRM and ACRM ($P = .32$ and .85, respectively). For the presence of tumor cells within ≤1 mm of the PRM a significant association was seen with male gender ($P = .01$) but not with other demographic or histopathological characteristics (age >65 years, pT3/4, pN+, pL1, Pn1, pV1, G3; $P > .05$).

To further endorse the impact of tumor cells within ≤1 mm of a specific RM, subgroup survival analysis was performed for the subset of specimens with tumor cells within ≤1 mm of only one specific RM (n = 27, 36%) for each RM, individually, compared to specimens with no tumor cells within ≤1 mm of any RM (n = 26, 35%). Also in this analysis, a significant impact on OS was seen for the PRM (median OS 2 vs 21 months (CI: 13.5–28.5), $P < .01$) but not for any other specific RM ($P > .05$). No significant association with demographic or other histopathological characteristics (gender, age >65 years, pT3/4, pN+, pL1, Pn1, pV1, G3; $P > .05$) was observed for PRM in this analysis.

## Determination of a Prognostically Safe Distance to Resection Margins

To examine the impact of tumor distance of to the circumference beyond the presence of tumor within ≤1 mm of an RM or DMI, and to potentially determine a prognostically "safe distance" to the circumference, subgroups were formed for the incremental analysis of the closest distance of tumor cells to any RM in steps of 1 mm (see Table 3).

Survival analysis of these subgroups was performed and is presented in Figure 5. The shortest OS was seen in the group of tumors with DMI of one RM (Figure 5A, thick red line, 5-year survival rate 0%) and most patients survived over time in the subgroup of tumors with >5 mm distance to all RMs (Figure 5A, thick blue line, 5-year survival rate 60%). These 2 groups are intermediate to all

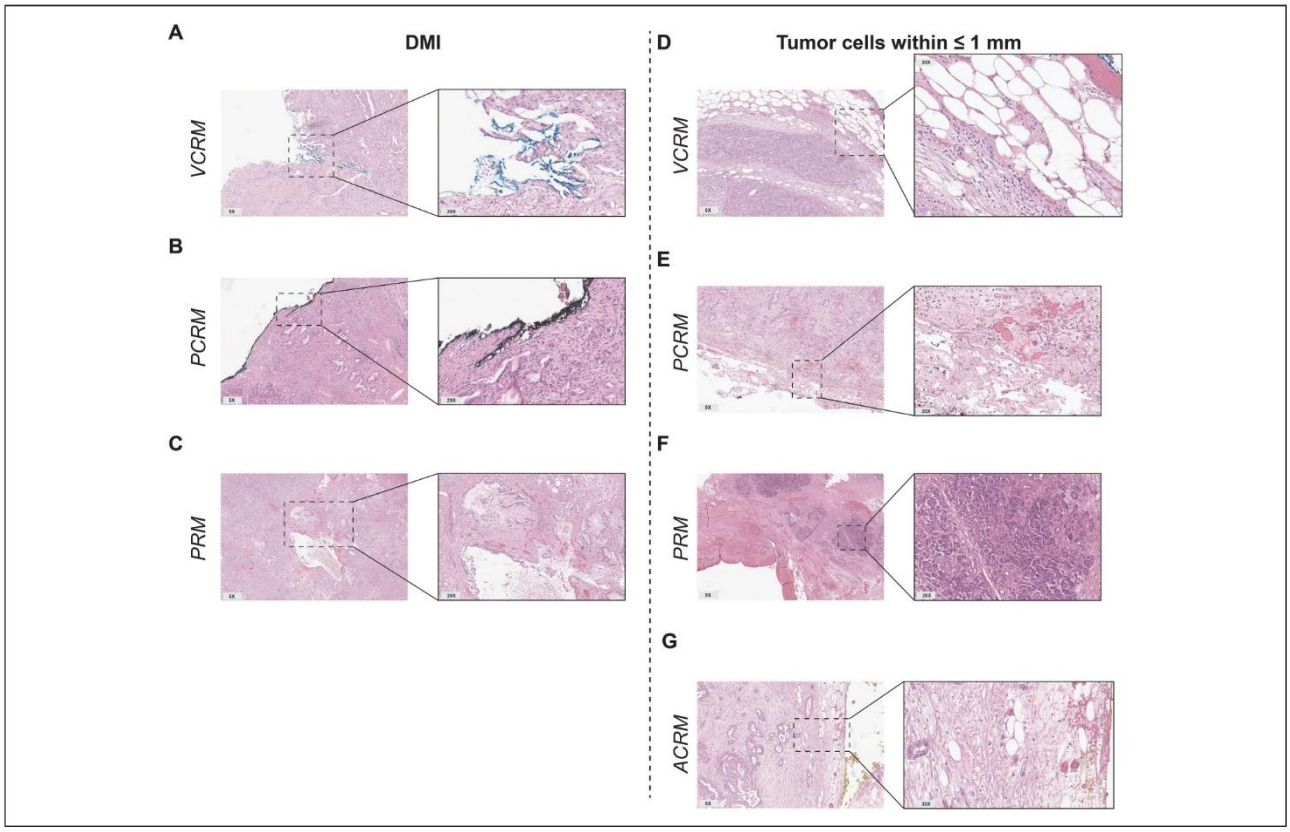


**Figure 2.** Microscopic examination of the resection margins. Representative H&E images showing tumor cells with DMI into the VCRM (A), PCRM (B), and PRM (C), and the presence of tumor cells within ≤1mm of the VCRM (D), PCRM (E), PRM (F), and ACRM (G). Abbreviations: ACRM, anterior circumferential resection margin; DMI, direct microscopic infiltration; PCRM, posterior circumferential resection margin; PRM, pancreatic transection margin; VCRM, vascular circumferential resection margin.

**Table 3.** Subgroups in Steps of 1 mm for Incremental Analysis of Closest Distance to an RM.

| Distance | Number of Tumors |
|---|---|
| Closest to RM in any distance >1 mm | n = 26 (35%) |
| Closest to RM > 1 mm & ≤2 mm | n = 10 (13%) |
| Closest to RM > 2 mm & ≤3 mm | n = 5 (7%) |
| Closest to RM > 3 mm & ≤4 mm | n = 3 (4%) |
| Closest to RM > 4 mm & ≤5 mm | n = 3 (4%) |
| Distance to all RMs > 5 mm | n = 5 (7%) |

Abbreviation: RM, resection margin.

other subgroups in the incremental analysis of the closest tumor distance to an RM (thin lines). However ,these intermediate subgroups, show only small differences, yielding no significant difference in OS between all groups (closest distance to an RM ≤ 1 mm but no DMI, > 1 mm & ≤2 mm, > 2 mm & ≤3 mm, >3 mm & ≤4 mm and >4 mm & ≤5 mm, 5-year survival rate ≤33% in all subgroups, $P = .17$).

After combining the intermediate subgroups of closest distance to an RM from ≤1 mm (no DMI) to ≤5 mm (≥0.1 mm–≤5mm), survival analysis yields overall significance in the difference in OS of the 3 subgroups (Figure 5B, $P = .03$).

## *Resection Margins and Development of Metastatic Disease*

Regarding distant hepatic and pulmonary metastases, 41% (n = 22) developed distant metastases. Hepatic metastases developed in 28% of the patients (n = 15) and pulmonary metastasis in 22% (n = 12). Five of these patients (9%) developed both hepatic and pulmonary metastases. The median time to liver metastasis was 3 (range 1–40) and 19 months (range 2–35) to pulmonary metastasis. Patients with liver metastases showed a significantly shorter OS compared to patients without metastases (median OS 18 months [CI: 4.1–31.9] vs 25 months [CI: 13.8–36.2], $P = .02$). No difference in OS was seen in patients with pulmonary metastases compared to patients without metastases ($P > .05$).

As previously presented for OS, we subsequently analyzed the impact of the different degrees of tumor distance to RMs in general and for the involvement of specific RMs

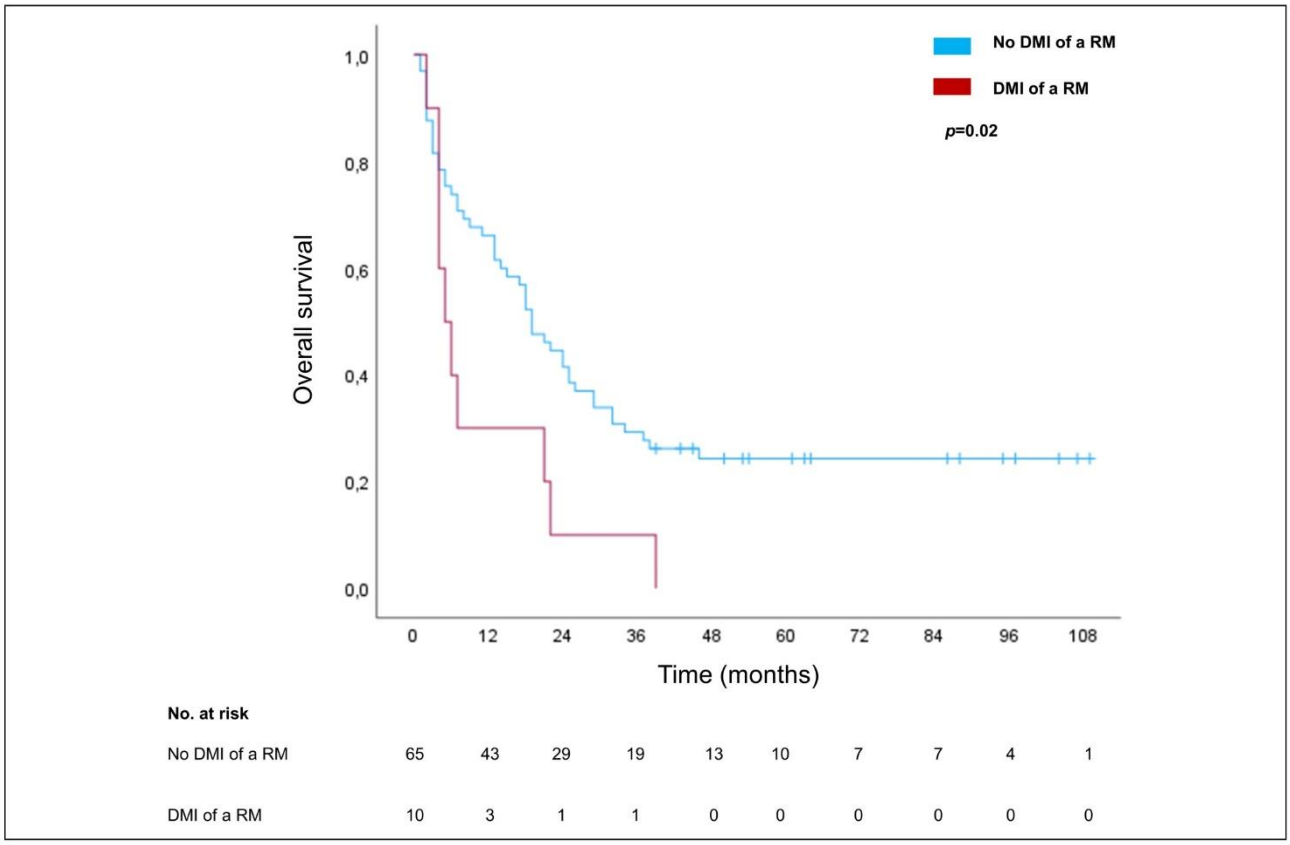


**Figure 3.** Survival analysis for DMI of an RM. The blue line represents the survival curve in the absence of DMI and the red line represents the survival curve in the presence of DMI of an RM. Tick marks indicate censoring. Abbreviations: DMI, direct microscopic infiltration; RM, resection margin.

individually on the development of hepatic and pulmonary metastasis. Among tumors that showed tumor cells within ≤1 mm of only one RM, the presence of tumor cells within ≤1 mm of only the VCRM led to a significantly shorter time to development of liver metastasis (50% of patients vs 5% of patients at 4 months, $P = .05$), whereas no difference was seen for any other RM ($P > .05$). Specifically, DMI of the PCRM and VCRM, showed significantly shorter time to pulmonary metastasis compared to no DMI of the respective RM (50% vs 2% and 100% vs 2% at 7 months, $P < .05$).

## Discussion

The prognostic significance of residual disease after resection of malignant tumors is well established, and R-classification was added to histopathological TNM classification decades ago.[10] Since then, histopathological R-classification has been divided into microscopic residual disease (R1) and macroscopic residual disease (R2).[11] Traditionally, microscopic residual disease was defined as the presence of tumor cells directly within a resection margin on microscopic examination (DMI). Furthermore, in other malignancies, a negative prognostic role of tumor cells in the close proximity to resection margins (≤1 mm) has been demonstrated in addition to tumor cells directly infiltrating an RM.[12] These findings suggest that limiting histopathological examination and reporting to conventional R1 status of DMI may lead to occult residual disease. In the context of PDAC, this aspect is of paramount interest given its poor prognosis and thus, the imperative need to detect residual disease alongside reactive glands of associated chronic pancreatitis in a highly desmoplastic stromal reaction with diffuse infiltration. Additionally, given the complex anatomy in which the pancreatic head is embedded, the prognostic impact of margin involvement by PDAC may differ depending on the location of the involved margin.

In the present study, survival analysis of DMI of an RM was associated with a shorter OS. This represents the basis of the traditional R1 classification and is consistent with the existing literature.[13–15] The OS analysis of the presence of tumor cells within ≤1 mm of an RM showed a negative impact with a trend toward significance. The significance of the presence of tumor cells within ≤1 mm of an RM in PDAC specimens remains equivocal in the existing

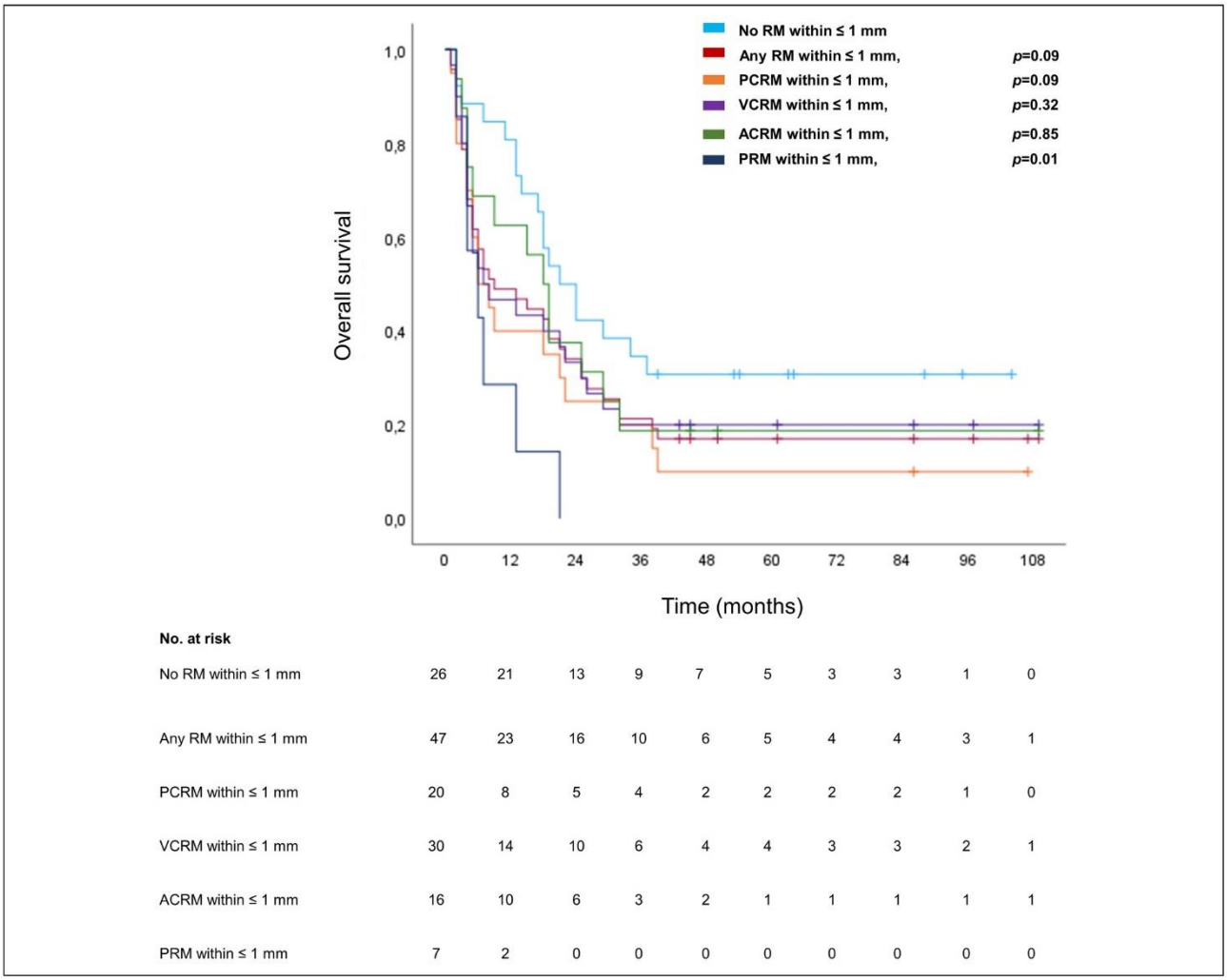


**Figure 4.** Survival analyses for the presence of tumor cells within ≤1 mm of RMs. The light blue line represents the survival curve in the absence of tumor cells within ≤1 mm of any RM; the red line represents specimens with tumor cells within ≤1 mm present at any RM; the orange line represents specimens with tumor cells within ≤1 mm of the PCRM; the purple line represents specimens with tumor cells within ≤1 mm of the VCRM; the green line represents specimens with tumor cells within ≤1 mm of the ACRM; and the dark blue line represents specimens with tumor cells within ≤1 mm of the PRM. Tick marks indicate censoring. *P* values refer to comparison of group of patients with presence versus absence of tumor cells within ≤1 mm of the specific RM analyzed. Abbreviations: ACRM, anterior circumferential resection margin; DMI, direct microscopic infiltration; PCRM, posterior circumferential resection margin; PRM, pancreatic transection margin; RM, resection margin; VCRM, vascular circumferential resection margin.

literature. In a large study by Ghaneh *et al*, a negative impact on OS was seen for patients with conventional R1 resection status (DMI) but not for <1 mm positive RMs compared to patients with RM negative tumors (>1mm, median OS 18.7 and 25.4 months vs 24.9 months, $P<.01$).[7] Sugiura *et al* also did not observe a negative impact of the presence of tumor cells within ≤1 mm of an RM compared to RMs with >1 mm tumor clearance (median OS 30.4 vs 26.0 months, $P>.05$). In contrast, Jamieson *et al* showed a significant negative impact on OS for microscopic evidence of tumor ≤1 mm of an RM compared to tumor clearance >1 mm of RMs (median OS 15.4 vs 26.5 months, $P=.01$).[8] A negative impact on OS was also seen by Strobel *et al* between R0, R1 (<1 mm), and R1 (DMI) status (41.6, 27.5, and 23.4 months, $P<.01$).[16] Although final clarification appears to be pending, based on the existing data the Royal College of Pathologists as well as the American Joint Committee on Cancer (AJCC) consider tumor cells within 1 mm of a margin in PDAC as microscopic residual disease (R1).[17,18]

We also performed survival analyses of the individual RMs of the pancreatic head. For DMI as well as of tumor cells within ≤1 mm of an individual margin a significant impact on OS was seen for the PRM but not for any other margin. These results are consistent with the subgroup survival analysis of specimens in which tumor

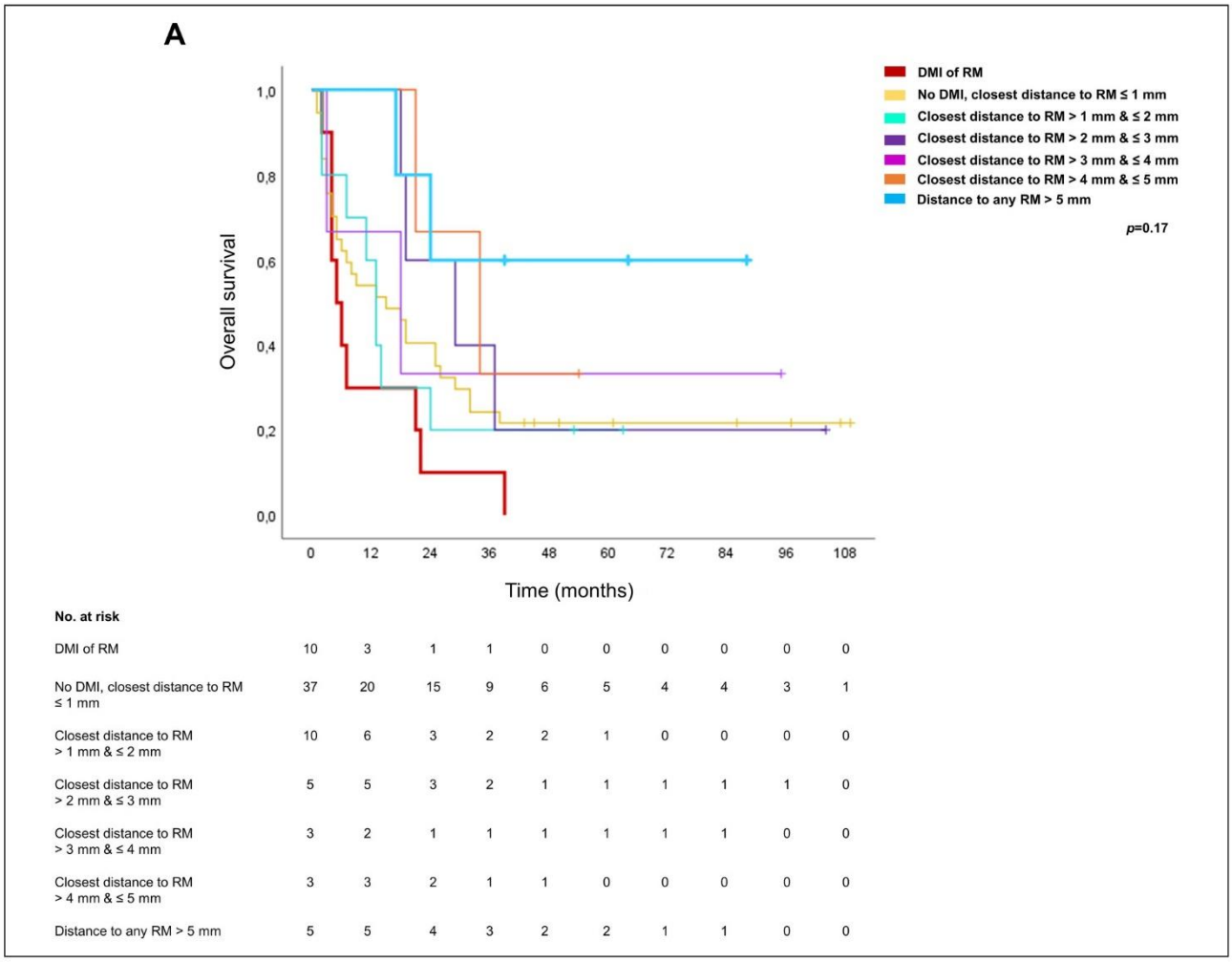


**Figure 5.** Survival analysis of subgroups formed by incremental analysis of the distance of tumor cells to the closest RM. (A) Survival analysis of all subgroups formed: DMI (thick red line), no DMI & closest RM ≤ 1 mm (yellow line), closest RM > 1 mm & ≤2 mm (turquoise line), >2 mm & ≤3 mm (purple line), >3 mm & ≤4 mm (pink line), >4 mm & ≤5 mm (orange) and >5 mm (thick light blue line). (B) Subgroup survival analysis : DMI (thick red line), distance to all RMs > 5 mm (thick blue line) and summary of all intermediate subgroups (≥0.1 to ≤5 mm, green line). Tick marks indicate censoring. Abbreviations: DMI, direct microscopic infiltration; RM, resection margin. (continued)

cells were present within ≤1 mm of only one specific RM. In this context, Tummer *et al* found no statistically significant association with OS for the location of an R1 margin using a 1 mm definition for R1.[19] Ghaneh *et al* found a negative impact on OS for PCRM DMI.[7] Similarly, Demir *et al* found a worse median OS for PCRM margin involvement compared to VCRM (median OS: 14.8 vs 31.0 months, $P = .02$). Thus, the findings of this study regarding the impact of VCRM and ACRM involvement are consistent with these data. For PCRM involvement of ≤1 mm, our data show a trend toward significance ($P = .09$). Additionally, our findings emphasize the prognostic impact of the PRM.

Subsequent to survival analyses of margin involvement (DMI and ≤1 mm), the impact of tumor distance >1 mm was examined in order to potentially identify a subset of patients with a higher survival rate and thereby determine a prognostically "safe distance." Only small differences between distances were seen and OS analysis of all incremental subgroups of 1 mm from DMI to distance >5 mm did not reach significance. However, the survival rate in the subgroup of patients with margin clearance >5 mm, stood out (5-year survival rate 60%), and combining the intermediate subgroups as one (≥0.1 to ≤5 mm) yields overall significance in the difference of OS of the 3 subgroups formed, whereas no difference in OS was seen for clearance from 1 to 3 mm and clearance of 3 to 5 mm ($P = 0.73$). Similarly, Liu *et al* found a better OS for clearance of >5 mm than of >1 to ≤5 mm ($P = .02$) whereas no difference in OS was seen for clearance from 1 to 3 mm and clearance of 3 to 5 mm ($P = .73$).[20] However, Liu *et al* only examined the distance to the superior mesenteric

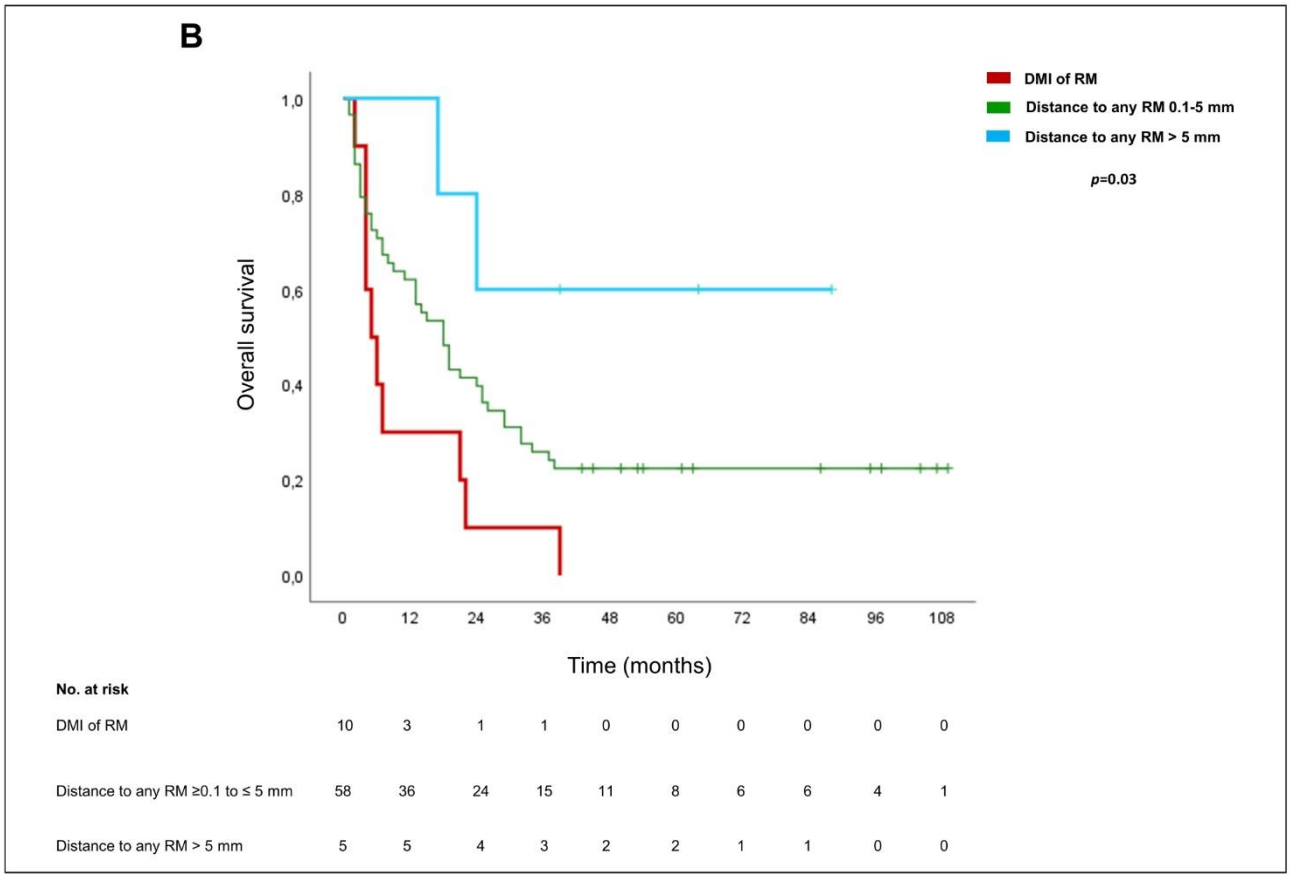


**Figure 5.** Continued.

artery (SMA) and all patients included in their study had received neoadjuvant therapy.

When analyzing the impact of margin involvement on the development of distant hepatic and pulmonary metastases, tumors with malignant cells within ≤1 mm of only the VCRM resulted in a significantly shorter time to liver metastasis. Individual DMI of the PCRM and VCRM showed significantly shorter time to pulmonary metastasis compared to no DMI of the respective RM. Similarly, Liu *et al* observed a higher rate of distant metastasis in patients with tumor involvement of ≤1 mm of the superior mesenteric artery compared to >1 mm, and Tummer *et al* noticed a shorter time from diagnosis to distant metastasis after R1 resection without specifying the site of margin involvement (≤1 mm).[19,20] Portal vein invasion has also been seen to be associated with a higher incidence of distant metastasis.[21]

Although the results of our study are encouraging, our present study has limitations. First, we did not subdivide the VCRM into SMA margin and superior mesenteric vein margin, which limits the interpretation of the individual impact of the superior mesenteric vessels involvement. Also, the size of our study cohort and, consequently the size of the subgroups formed is limited. For instance, only 2 of the patients included in this study (3%) received neoadjuvant therapy, not allowing a sufficient subgroup analysis of this subgroup. However, strict inclusion criteria were applied and specimens from each patient were re-examined for the purpose of this study by 2 pathologists independently with respect to the distance between the tumor and the respective margins. Future larger multi-institutional studies with further subdivision of margins would improve the statistical power of these results and allow a more precise differentiation of the margin impact on prognosis. The results of the survival analysis of the larger subgroup of patients after primary surgery (97%) are summarized in Supplemental Table S1.

Nevertheless, the results presented provide suggestions for clinical implications. Intraoperative histopathological examination of frozen sections of the PRM during oncologic resection of the pancreatic head is considered standard in specialized centers. Our results suggest that intraoperative evaluation of the PRM not only for DMI but also for tumor cells within ≤1 mm as a basis for margin revision may hold the potential to improve resections with margin clearance >1 mm of the PRM and thereby improve prognosis.[22] Currently, we perform frozen sections using OCT (optimal cutting temperature)

as embedding media. Next, the tissue is frozen a −20°C to −15°C using a cryostat. The quality of the analysis is best for small tissue samples ideally up to 5 mm in diameter. The tissue is cut into 4 to 7 microns thick slides. Finally, the slides are stained with H&E. This procedure leads to multiple possible artifacts, such as ice crystals, overfreezing, and underfreezing, often making analysis difficult. In order to perform a more precise analysis of PRM the use of molecular biology techniques holds potential in the near future. Indeed, molecular based analysis of the intraoperative RM using methylation data would be of great use, as shown in recent studies on formalin fixed paraffin embedded (FFPE) samples using machine learning classifiers that can automatically detect PDAC.[23] In order to transfer this technique into the intraoperative setting nanopore sequencing of targeted DNA methylation regions needs to be employed. Moreover, preoperative imaging criteria as surrogate parameters for predicting margin positive resection (R1) in resectable PDAC should receive more attention.[24] In this way, preoperative prediction of R1 resection may represent a sufficient basis to guide neoadjuvant therapy to improve prognosis and R0 resection rates.[25–27]

In conclusion, the present study underlines the utmost importance of accurate histopathological preparation and examination of PDAC specimens including a differentiated analysis of each margin individually and its exact distance from the tumor not only as a basis for future studies but also for considerations in contemporary clinical decision making.

## Author Contributions

FNL, CK, SS, and MPD were involved in conceptualization, methodology, and project administration; FNL, FR, SS, and MPD in software and visualization; FNL, CK, SS, and MPD in validation; FNL, CK, FR, SS, and MPD in formal analysis, investigation, and writing—original draft preparation; FNL, CK, KB, WR, CS, FK, DH, SS, and MPD in resources; FNL and FR in data curation; and CK, KB, WR, CS, FK, and DH in supervision.

## Data Availability Statement

The datasets used and/or analyzed during the current study are available upon reasonable request pending approval by the local data security authorities.

## Declaration of Conflicting Interests

The author(s) declared no potential conflicts of interest with respect to the research, authorship, and/or publication of this article: The work of MPD was supported by Berlin Institute of Health (Junior Clinician Scientist Program) and DKTK Berlin (Young Investigator Grant 2022). The work of SS was supported by the Federal Ministry of Education and Research (BMBF).

## Ethical Approval

The study was conducted in accordance with the Declaration of Helsinki. It was approved by the local ethics committee (No. EA4/020/19).

## Funding

The author(s) disclosed receipt of the following financial support for the research, authorship, and/or publication of this article: This work was supported by the Bundesministerium für Bildung und Forschung, (grant number 16LW0239K).

## Informed Consent

The written informed consent was waived due to the retrospective study design.

## Trial Registration

Not applicable, because this article does not contain any clinical trials.

## ORCID iDs

Florian N. Loch https://orcid.org/0000-0003-1513-8339
Christian Schineis https://orcid.org/0000-0001-9189-6751

## Supplemental Material

Supplemental material for this article is available online.

## References

1. Rawla P, Sunkara T, Gaduputi V. Epidemiology of pancreatic cancer: global trends, etiology and risk factors. *World J Oncol*. 2019;10(1):10-27.
2. Ushio J, Kanno A, Ikeda E, et al. Pancreatic ductal adenocarcinoma: epidemiology and risk factors. *Diagnostics*. 2021;11(3):562.
3. Rahib L, Wehner MR, Matrisian LM, Nead KT. Estimated projection of US cancer incidence and death to 2040. *JAMA Netw Open*. 2021;4(4):e214708.
4. Du T, Bill KA, Ford J, et al. The diagnosis and staging of pancreatic cancer: a comparison of endoscopic ultrasound and computed tomography with pancreas protocol. *Am J Surg*. 2018;215(3):472-475.
5. Lewis R, Drebin JA, Callery MP, et al. A contemporary analysis of survival for resected pancreatic ductal adenocarcinoma. *HPB (Oxford)*. 2013;15(1):49-60.
6. Belfiori G, Crippa S, Francesca A, et al. Long-term survivors after upfront resection for pancreatic ductal adenocarcinoma: an actual 5-year analysis of disease-specific and post-recurrence survival. *Ann Surg Oncol*. 2021;28(13):8249-8260.
7. Ghaneh P, Kleeff J, Halloran CM, et al. The impact of positive resection margins on survival and recurrence following resection and adjuvant chemotherapy for pancreatic ductal adenocarcinoma. *Ann Surg*. 2019;269(3):520-529.
8. Jamieson NB, Foulis AK, Oien KA, et al. Positive mobilization margins alone do not influence survival following pancreatico-duodenectomy for pancreatic ductal adenocarcinoma. *Ann Surg*. 2010;251(6):1003-1010.

9. Speichinger F, Dragomir MP, Schallenberg S, et al. Rethinking the TNM classification regarding direct lymph node invasion in pancreatic ductal adenocarcinoma. *Cancers (Basel)*. 2022;14(1):201.
10. Wittekind C, Compton C, Quirke P, et al. A uniform residual tumor (R) classification: integration of the R classification and the circumferential margin status. *Cancer*. 2009;115(15): 3483-3488.
11. Hermanek P, Sobin LH. *TNM Classification of Malignant Tumors*. 4th edn. Springer; 1987.
12. Birbeck KF, Macklin CP, Tiffin NJ, et al. Rates of circumferential resection margin involvement vary between surgeons and predict outcomes in rectal cancer surgery. *Ann Surg*. 2002;235(4):449.
13. Chang DK, Johns AL, Merrett ND, et al. Margin clearance and outcome in resected pancreatic cancer. *J Clin Oncol*. 2009;27(17):2855-2862.
14. Raut CP, Tseng JF, Sun CC, et al. Impact of resection status on pattern of failure and survival after pancreaticoduodenectomy for pancreatic adenocarcinoma. *Ann Surg*. 2007;246(1):52-60.
15. Kimbrough CW S, Hill CR, Martin RC, McMasters KM, Scoggins CR. Tumor–positive resection margins reflect an aggressive tumor biology in pancreatic cancer. *J Surg Oncol*. 2013;107(6):602-607.
16. Strobel O, Hank T, Hinz U, et al. Pancreatic cancer surgery: the new R-Status counts. *Ann Surgery*. 2017;265(3):565-573.
17. Campbell F, Foulis AK, Verbeke CC. *Dataset for the Histopathological Reporting of Carcinomas of the Pancreas, Ampulla of Vater and Common Bile Duct*. The Royal College of Pathologists; 2010.
18. Amin MB, Edge S, Greene F, et al. *AJCC Cancer Staging Manual*. 8th edn. Springer; 2017.
19. Tummers WS, Groen JV, Sibinga Mulder BG, et al. Impact of resection margin status on recurrence and survival in pancreatic cancer surgery. *Br J Surg*. 2019;106(8):1055-1065.
20. Liu L, Katz MH, Lee SM, et al. Superior mesenteric artery margin of posttherapy pancreaticoduodenectomy and prognosis in patients with pancreatic ductal adenocarcinoma. *Am J Surg Pathol*. 2015;39(10):1395-1403.
21. Mierke F, Hempel S, Distler M, et al. Impact of portal vein involvement from pancreatic cancer on metastatic pattern after surgical resection. *Ann Surg Oncol*. 2016;23(S5):730-736.
22. Birgin E, Rasbach E, Téoule P, Rückert F, Reissfelder C, Rahbari NN. Impact of intraoperative margin clearance on survival following pancreatoduodenectomy for pancreatic cancer: a systematic review and meta-analysis. *Sci Rep*. 2020;10(1):22178.
23. Dragomir MP, Calina TG, Perez E, et al. DNA methylation-based classifier differentiates intrahepatic pancreato-biliary tumours. *EBioMedicine*. 2023;93:104657.
24. Cassinotto C, Dohan A, Zogopoulos G, et al. Pancreatic adenocarcinoma: a simple CT score for predicting margin-positive resection in patients with resectable disease. *Eur J Radiol*. 2017;95:33-38.
25. Zhang E, Wang L, Shaikh T, et al. Neoadjuvant chemoradiation impacts the prognostic effect of surgical margin status in pancreatic adenocarcinoma. *Ann Surg Oncol*. 2022;29(1): 354-363.
26. Chopra A, Zenati M, Hogg ME, et al. Impact of neoadjuvant therapy on survival following margin-positive resection for pancreatic cancer. *Ann Surg Oncol*. 2021;28(12):7759-7769.
27. Torgeson A, Garrido-Laguna I, Tao R, Cannon GM, Scaife CL, Lloyd S. Value of surgical resection and timing of therapy in patients with pancreatic cancer at high risk for positive margins. *ESMO Open*. 2018;3(1):e000282.

## 2.4 Prognostische Bedeutung direkter Tumorinfiltration regionaler Lymphknoten im Vergleich zu regionaler Lymphknotenmetastasierung ohne Tumorkontakt bei resektablen exokrinen Pankreaskarzinomen (Originalarbeit 4)

Die folgende Originalarbeit untersucht den prognostischen Einfluss des Mechanismus der Lymphknoteninvasion an Operationsresektaten resezierter exokriner Pankreaskarzinome. Somit fügt sie der **Originalarbeit 3** ein weiteres prognostisches Merkmal aus der postoperativen pathologischen Aufarbeitung chirurgischer Operationsresektate hinzu.

Fiona Speichinger, Mihnea P. Dragomir, Simon Schallenberg, **Florian N. Loch**, Claudius E. Degro, Ann-Kathrin Baukloh, Lisa Hartmann, Ioannis Pozios, Christian Schineis, Georgios A. Margonis, Johannes C. Lauscher, Katharina Beyer, Carsten Kamphues.

Rethinking the TNM Classification Regarding Direct Lymph Node Invasion in Pancreatic Ductal Adenocarcinoma. *Cancers*. **2021**; 14: 201.

Der nachfolgende Text entspricht dem Originalabstract der o.g. Publikation *Rethinking the TNM Classification Regarding Direct Lymph Node Invasion in Pancreatic Ductal Adenocarcinoma* übersetzt durch den Koautor Florian N. Loch:

*„Die Mechanismen der Lymphknoteninvasion scheinen eine prognostische Rolle zu spielen beim PDAC nach der Resektion. Dieser Aspekt wird von der achten Edition der TNM-Klassifikation des American Joint Committee on Cancer (AJCC) jedoch nicht erfasst. Ziel dieser Studie war es, die prognostische Rolle der unterschiedlichen Mechanismen der Lymphknoteninvasion des PDAC zu analysieren. 122 Patient:innen mit reseziertem PDAC wurden untersucht. Wir unterschieden drei Gruppen: direkt (per continuitatem, Nc) von dem Primärtumor, Metastasierung (Nm) ohne jeglichen Kontakt zum Primärtumor und ein gemischter Mechanismus (Ncm). Anschließend wurde der prognostische Einfluss der unterschiedlichen Gruppen hinsichtlich des Gesamtüberlebens untersucht. Insgesamt zeigten 20 Patient:innen direkte Lymhpknoteninvasion (Nc=16,4%), 44 wurden als Nm (36,1%) klassifiziert und 21 wurden als Ncm klassifiziert (17,2%). Der Unterschied im Gesamtüberleben zwischen N0 (keine Lymphknotenmetastasen, n=37) und Nc war nicht statistisch signifikant (p=0.134), während Nm ein schlechteres Gesamtüberleben hatte als N0 (p<0.001). Direkte Invasion allein hatte keinen statistisch signifikanten Effekt auf das Gesamtüberleben (p=0.885). Die Neudefinition des N0 Stadiums durch*

*Einschluss von Nc Patient:innen zeigte eine präzisere Vorhersage des Gesamtüberlebens unter den N-Stadien (p=0.001 vs. p=0.002).*

*Nc war ähnlicher zu N0 als zu Nm; demzufolge empfehlen wir ein Überdenken der TNM-Klassifikation auf der Grundlage des Mechanismus der Lymphknotenmetastasierung beim PDAC. Insgesamt ist diese neuartige Klassifikation präziser.“*

cancers

MDPI

*Article*

# Rethinking the TNM Classification Regarding Direct Lymph Node Invasion in Pancreatic Ductal Adenocarcinoma

**Fiona Speichinger [1,*], Mihnea P. Dragomir [2,3,4], Simon Schallenberg [2], Florian N. Loch [1], Claudius E. Degro [1], Ann-Kathrin Baukloh [1], Lisa Hartmann [1], Ioannis Pozios [1], Christian Schineis [1], Georgios Antonios Margonis [5], Johannes C. Lauscher [1], Katharina Beyer [1] and Carsten Kamphues [1]**

1 Charité–Universitätsmedizin Berlin, Corporate Member of Freie Universität Berlin and Humboldt–Universität zu Berlin, Department of General and Visceral Surgery, Hindenburgdamm 30, 12203 Berlin, Germany; florian.loch@charite.de (F.N.L.); claudius-erwin.degro@charite.de (C.E.D.); ann-kathrin.baukloh@charite.de (A.-K.B.); lisa.hartmann@charite.de (L.H.); ioannis.pozios@charite.de (I.P.); christian.schineis@charite.de (C.S.); johannes.lauscher@charite.de (J.C.L.); katharina.beyer2@charite.de (K.B.); carsten.kamphues@charite.de (C.K.)

2 Charité-Universitätsmedizin Berlin, Freie Universität Berlin, Humboldt-Universität zu Berlin and Berlin Institute of Health, Institute of Pathology, 10117 Berlin, Germany; mihnea.dragomir@charite.de (M.P.D.); simon.schasllenberg@charite.de (S.S.)

3 German Cancer Consortium (DKTK), Partner Site Berlin, German Cancer Research Center (DKFZ), 69210 Heidelberg, Germany

4 Berlin Institute of Health, Anna-Louisa-Karsch-Straße 2, 10178 Berlin, Germany

5 Department of Surgery, The Johns Hopkins University School of Medicine, 600 N. Wolfe Street, Blalock 688, Baltimore, MD 21287, USA; margonig@mskcc.org

* Correspondence: fiona.speichinger@charite.de

check for updates

**Citation:** Speichinger, F.; Dragomir, M.P.; Schallenberg, S.; Loch, F.N.; Degro, C.E.; Baukloh, A.-K.; Hartmann, L.; Pozios, I.; Schineis, C.; Margonis, G.A.; et al. Rethinking the TNM Classification Regarding Direct Lymph Node Invasion in Pancreatic Ductal Adenocarcinoma. *Cancers* **2022**, *14*, 201. https://doi.org/10.3390/cancers14010201

Academic Editor: Amit Mahipal

Received: 23 November 2021
Accepted: 29 December 2021
Published: 31 December 2021

**Publisher's Note:** MDPI stays neutral with regard to jurisdictional claims in published maps and institutional affiliations.



**Simple Summary:** Due to the rising burden of pancreatic cancer and poor outcomes, a precise, post-operative cancer staging for further and individualized therapy is needed. In the latest cancer classification system, the lymph node invasion mechanism is not addressed. Due to different outcomes regarding the lymph node invasion, we suggest a rethinking of the current system.

**Abstract:** Mechanisms of lymph node invasion seem to play a prognostic role in pancreatic ductal adenocarcinoma (PDAC) after resection. However, the 8th edition of the TNM classification of the American Joint Committee on Cancer (AJCC) does not consider this. The aim of this study was to analyse the prognostic role of different mechanisms of lymph node invasion on PDAC. One hundred and twenty-two patients with resected PDAC were examined. We distinguished three groups: direct (per continuitatem, Nc) from the main tumour, metastasis (Nm) without any contact to the main tumour, and a mixed mechanism (Ncm). Afterwards, the prognostic power of the different groups was analysed concerning overall survival (OS). In total, 20 patients displayed direct lymph node invasion (Nc = 16.4%), 44 were classed as Nm (36.1%), and 21 were classed as Ncm (17.2%). The difference in OS was not statistically significant between N0 (no lymph node metastasis, $n = 37$) and Nc ($p = 0.134$), while Nm had worse OS than N0 ($p < 0.001$). Direct invasion alone had no statistically significant effect on OS ($p = 0.885$). Redefining the N0 stage by including Nc patients showed a more precise OS prediction among N stages ($p = 0.001$ vs. $p = 0.002$). Nc was more similar to N0 than to Nm; hence, we suggest a rethinking of TNM classification based on the mechanisms of lymph node metastases in PDAC. Overall, this novel classification is more precise.

**Keywords:** pancreatic ductal adenocarcinoma; direct lymph node invasion; TNM classification

## 1. Introduction

According to the International Agency for Research on Cancer, more than 495,000 new cases of pancreatic cancer were recorded worldwide in 2020. Moreover, pancreatic cancer is the seventh most frequent cause of cancer-related deaths [1,2]. The prognosis of patients

suffering from pancreatic ductal adenocarcinoma (PDAC) is very poor, with high lethality rates, leading to a five-year survival rate of less than 10% [1,2]. The most powerful predictor of survival after surgery is lymph node status [3–6]. Previous studies [7–12] have analysed the mechanisms of lymph node invasion and compared the prognosis of direct lymph nodes from the main tumour through cancer related angiogenesis and immunosuppression via crosstalk between the cancer endothelium and the surrounding microenvironment and lymph node metastasis without any contact with the main tumour [13,14]. These small studies showed that the mechanisms underlying lymph node invasion may have effects on the survival rate, however, the data are contradictory [7–12]. In addition, the latest TNM classification—the 8th edition of the American Joint Committee on Cancer (AJCC) with changes to the T and N categories—does not consider the mechanisms of lymph node involvement [15–19].

Our study provides data that support a redefinition of the N stage by including the mechanism of lymph node involvement [12]. We believe that this could lead to a more precise description of lymph node status, providing an individualized prognosis of PDAC patients compared with the current TNM classification.

## 2. Materials and Methods

### 2.1. Patients and Clinical Data

A total of 136 patients who underwent pancreatic resection at the Department of General and Visceral Surgery at the Charité University Hospital, Campus Benjamin Franklin, Berlin, Germany, between 2008 and 2021, were retrospectively analyzed. Thirteen patients with 30-day mortality (9.6% overall postoperative mortality) and one patient with carcinoma of the duodenum were excluded. Overall, 122 patients suffering from PDAC were included in this study. All patients underwent pancreatic surgery (pylorus-preserving pancreaticoduodenectomy = PPPD/Whipple procedure or left-sided pancreatic resection) according to the current guidelines, after the indication for surgery and chemotherapy was confirmed by an interdisciplinary tumour board. Clinicopathological characteristics such as age, sex, follow-up, and recurrence-free survival were collected for each patient (Table 1). The study was approved by the Ethics Committee of the Charité University Medical Department in Berlin (EA4/020/19).

**Table 1.** Clinicopathologics arranged by the different lymph node types.

| | | N0 ($n$ = 37) | Nc ($n$ = 20) | Nm ($n$ = 44) | Ncm ($n$ = 21) | Total ($n$ = 122) | $p$-Value |
|---|---|---|---|---|---|---|---|
| Median Age (range) | | 70.3 (35.4–84.4) | 70.3 (52.6–83) | 71.6 (36.8–84.5) | 69.2 (41.8–86.7) | 70.3 (35.4–86.7) | 0.402 |
| Gender | | | | | | | 0.459 |
| | female | 20 | 10 | 19 | 7 | 56 (45.9) | |
| | male | 17 | 10 | 25 | 14 | 66 (54.1) | |
| T stage | | | | | | | 0.693 |
| | T1 | 4 | 1 | 2 | 2 | 9 (7.4) | |
| | T2 | 13 | 10 | 24 | 9 | 56 (45.9) | |
| | T3 | 20 | 9 | 18 | 10 | 57 (46.7) | |
| | T4 | 0 | 0 | 0 | 0 | 0 | |
| N stage | | | | | | | <0.001 |
| | N0 | 37 | 0 | 0 | 0 | 37 (30.3) | |
| | N1 | 0 | 20 | 27 | 7 | 54 (44.3) | |
| | N2 | 0 | 0 | 17 | 14 | 31 (25.4) | |
| Resection | | | | | | | 0.340 |
| | R0 | 29 | 18 | 35 | 14 | 96 (78.7) | |
| | R1 | 8 | 2 | 9 | 7 | 26 (21.3) | |

**Table 1.** *Cont.*

| | | N0 ($n$ = 37) | Nc ($n$ = 20) | Nm ($n$ = 44) | Ncm ($n$ = 21) | Total ($n$ = 122) | $p$-Value |
|---|---|---|---|---|---|---|---|
| Grade | | | | | | | 0.090 |
| | G1 | 5 | 0 | 0 | 0 | 5 (4.1) | |
| | G2 | 20 | 11 | 21 | 11 | 63 (51.6) | |
| | G3 | 12 | 9 | 22 | 10 | 53 (43.4) | |
| | G4 | 0 | 0 | 1 | 0 | 1 (0.8) | |
| Location | | | | | | | 0.035 |
| | head | 24 | 17 | 41 | 19 | 101 (82.8) | |
| | corpus | 3 | 1 | 0 | 1 | 5 (4.1) | |
| | tail | 10 | 2 | 3 | 1 | 16 (13.1) | |
| Invasion | | | | | | | |
| | ALI | 1 | 8 | 28 | 14 | 51 (41.8) | <0.001 |
| | VNI | 3 | 6 | 9 | 7 | 25 (20.5) | 0.115 |
| | PNI | 17 | 14 | 31 | 16 | 78 (63.9) | 0.486 |

N0: node negative; Nc: direct node invasion (per continuitatem); Nm: regional lymph node metastasis; Ncm: mixed node invasion; ALI: angiolymphatic invasion; VNI: venous invasion; PNI: perineural invasion. Percentage in brackets.

### *2.2. Histopathological Assessment: Grossing, Histological Examination and Reexamination of Lymph Node Metastases*

Resected specimens were fixed in 10% buffered formalin before grossing. After overnight fixation, the specimens were stained before preparation (anterior margin yellow, medial margin blue, posterior margin black, bile duct green and pancreas parenchyma red). As a first step, resection margins of oral and aboral duodenum, biliary duct and pancreas parenchyma were identified and were completely embedded. As a second step, the axial method was used, slicing the specimen from apical to caudal in 5-mm-thick slices. Next, the tumour was detected, described and measured, including the minimum distance to all relevant anatomical structures and the previously stained circumferential soft tissue margins. We next embedded the tumour in closest relation to the ampulla, pancreatic duct, duodenum, bile duct, pancreas parenchyma resection margin and to the anterior, posterior, medial circumferential soft tissue margins.

Regarding lymph node grossing, according to our protocol, we embedded all macroscopic detectable lymph nodes, minimally 12, and if this number was not achieved, we embedded the peripancreatic fat completely. If the surgeons submitted other regional lymph nodes separately, these were completely sampled. On average, per case, we embedded 18 blocks.

Histological examination was done according to the 8th edition of the TNM classification (AJCC) and included: defining the cancer subtype, grading, pTNM-classification, vascular, lymphatic, and perineural invasion, detection of precursor lesions and R-status analysis. R-status, at our institution, is defined as direct invasion of the tumour in the resection margins/circumferential soft tissue margins (0 mm).

Two pathologists independently re-evaluated the histology slides for the lymph node metastases reclassification. Lymph nodes were categorized according to the mechanism/presence of invasion: direct (Nc), metastasis (Nm), mixed mechanism (Ncm), and node-negative (N0). Nc was defined as direct lymph node invasion by the tumour (Figure 1A), Nm was defined as regional lymph node metastasis without any contact to the tumour (Figure 1B) as previously described [7–12], and Ncm was defined as a combination of both (Figure 1C). If discrepancies existed between the two pathologists, these were resolved by extensively discussing the case and if no consensus was met, the opinion of a third pathologist was asked.

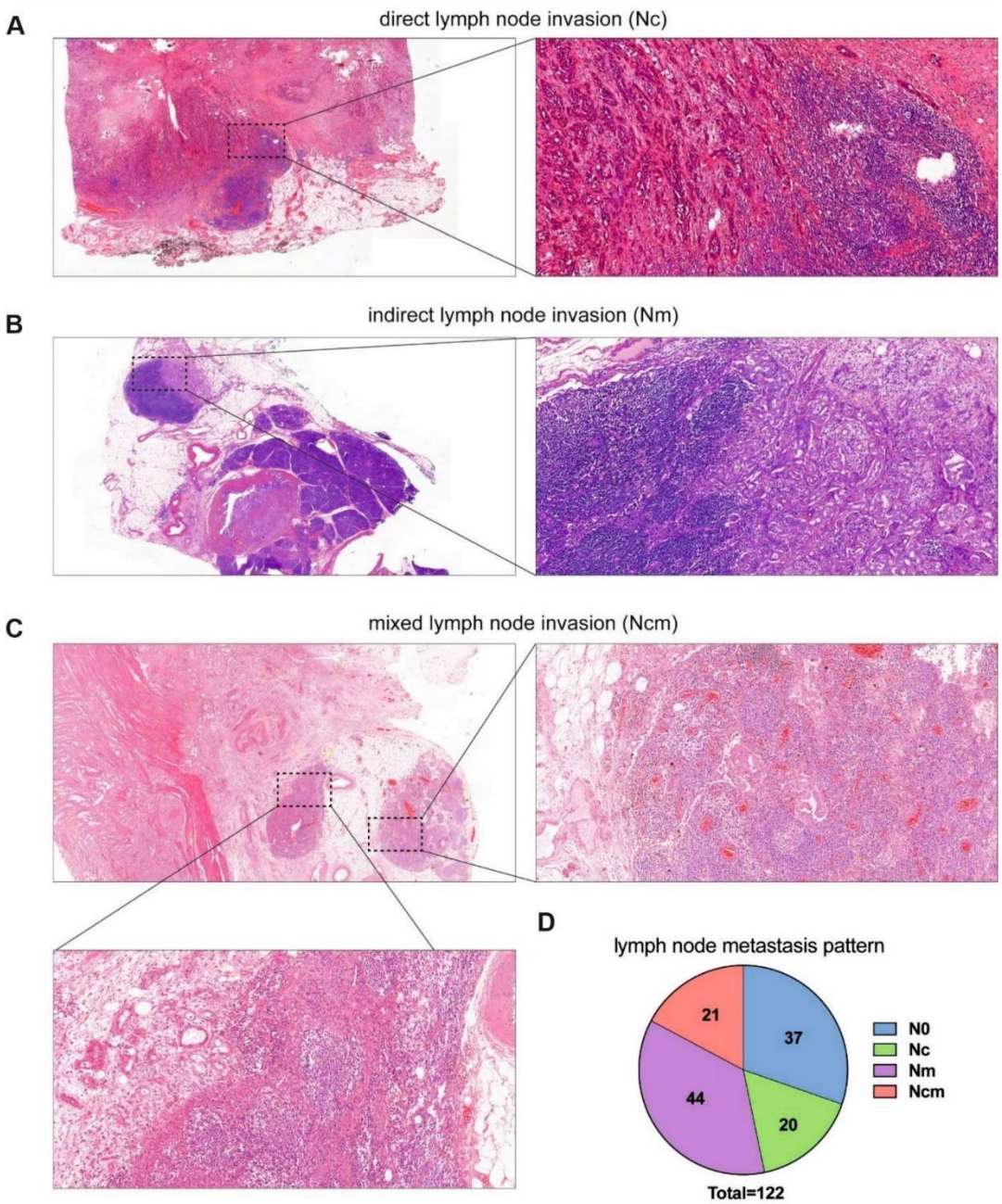


**Figure 1.** Histological sections with haematoxylin–eosin staining (at 20x magnification and the zoom-in cassettes at 100x magnification) of the different types of lymph node invasion in pancreatic ductal adenocarcinoma: (**A**) direct lymph node invasion by the main tumour per continuitatem, Nc; (**B**) indirect lymph node invasion without any contact to the main tumour, Nm; (**C**) Mixed lymph node invasion, Ncm; (**D**) pattern of the different lymph node types in our study.

### *2.3. Statistical Analysis*

For the statistical analyses, we used SPSS version 27.0 (IBM). Overall (OS) were plotted as Kaplan–Meier curves and survival differences were calculated using the log-rank

test. Clinicopathologic characteristics were compared using the Pearson–chi-quadrant test. Significant univariate variables ($p < 0.10$) in the Cox proportional hazards regression model were proofed of proportional hazards assumption and further analysed in the multivariate model. For comparison of the results from the other groups, we analysed a weighted median of OS. A $p$-value of <0.05 was considered as a statistically significant difference. Graphics were designed using CorelDRAW®Graphic Suite 2021 (Corel Corporation, Ottawa, ON, Canada).

## 3. Results

### 3.1. Demographics

Table 1 shows the clinicopathological characteristics for the different lymph node invasion types of the 122 patients with PDAC after radical resection. In total, 56 patients (45.9%) were female. The median age of the patients was 70.3 (35.4–86.7) years. In 101 (82.8%) patients, the tumour was located mainly in the pancreatic head, and 96 (78.7%) of the resections were R0. According to the 8th Edition of the TNM classification, 57 tumours (46.7%) were stage T3, followed by 56 tumours at T2 (45.9%), 9 tumours at T1 (7.4%), and no tumours at T4; further, 37 (30.3%) patients were node-negative (N0), 54 (44.3%) were N1, and 31 (25.4%) were N2, while 51 (41.8%) patients had angiolymphatic invasion, 25 (20.5%) had venous invasion, and 78 (63.9%) had perineural invasion. According to the involved lymph node mechanisms, we found 20 (16.4%) patients with direct lymph node invasion (Nc), 44 (36.1%) patients with lymph node metastasis without any contact with the tumour (Nm), and 21 (17.2%) patients showing mixed lymph node invasion (Ncm) (Figure 1). The median number of analysed lymph nodes per patient was 15 (range 3–50) for all groups, 11 (range 3–50) for N0 patients, 12 (range 4–46) for Nc, 15 (range7–43) for Nm, and 20 (range 8–43) for patients with a mixed lymph node invasion. Statistically, more lymph nodes were analysed in the Ncm group compared with the N0 group ($p = 0.035$) as well as in the Nc group ($p = 0.04$). Interestingly no statistically significant difference was seen in the lymph node Ratio (LNR) between the groups (Table 2). In total, we analysed 2079 lymph nodes. In total, 334 lymph nodes were positive, and direct invasion was found in 73 lymph nodes (21.9%)—on average, 1–5 lymph nodes with direct invasion per patient. Statistically significant difference between the groups were only seen in the N stage ($p < 0.001$), tumour location ($p = 0.035$), and angiolymphatic invasion ($p < 0.001$).

**Table 2.** Univariate and multivariate analysis of prognostic factors.

| | Univariate | | | Multivariate | | |
|---|---|---|---|---|---|---|
| | HR | CI 95% | *p*-Value | HR | CI 95% | *p*–Value |
| age (<65/>65 years) | 01.217 | 0.708–2.091 | 0.478 | | | |
| sex (male/female) | 0.671 | 0.411–1.097 | 0.112 | | | |
| T stage (T1/T3) | 1.539 | 0.645–3.674 | 0.331 | | | |
| resection (R0/R1) | 2.706 | 1.507–4.859 | 0.001 | 1.627 | 0.838–3.160 | 0.151 |
| grade (G2/G3) | 1.481 | 0.901–2.435 | 0.121 | | | |
| PNI (no/yes) | 2.250 | 0.891–5.683 | 0.86 | | | |
| VI (no/yes) | 2.387 | 1.336–4.266 | 0.003 | 2.504 | 1.384–4.515 | 0.002 |
| ALI (no/yes) | 2.378 | 1.420–3.983 | 0.001 | 1.6 | 0.861–2.973 | 0.137 |
| LNR (>0-<0.2/≥0.4) | 2.138 | 0.910–5.024 | 0.081 | | | |
| Mechanism of lymph node invasion | | | | | | |
| Nc (no/yes) | 0.952 | 0.484–1.869 | 0.885 | | | |
| N0-R(N0 + Nc)/Nm + Ncm | 2.567 | 1.511–4.359 | <0.001 | 3.024 | 1.709–5.352 | <0.001 |

HR: hazard ratio; CI: confidence interval; ALI: angiolymphatic invasion; VNI: venous invasion; PNI: perineural invasion; N0: node negative; Nc: direct node invasion (per continuitatem); Nm: regional lymph node metastasis; Ncm: mixed node invasion.

### 3.2. Survival Analysis

The median overall survival of the entire cohort was 21.6 months with a 95% confidence interval (CI) from 14.3 to 28.8 months and the recurrence-free survival was 13

(8.4–17.6, 95% CI) months. The one-year survival of all patients was 61.9%, the three-year survival 31.6%, and the five-year survival was 24.3%.

3.2.1. Analysis by the Mechanism of Lymph Node Invasion

According to the invasion mechanisms of lymph nodes, the one-year survival of the different groups showed 74.8% in N0, 52.1% in Nc, 61.6% in Nm, and 47.7% in Ncm. The three-year survival was 62.1% in N0, 38% in Nc, 12.8% in Nm, and no patient lived after three years in the Ncm group. The five-year survival of the different groups showed 50.2% in N0, 38% in Nc, and no patient survived five years or more in the Nm and Ncm groups.

The median OS of the N0 group could not be calculated since less than 50% of the patients in the N0 group died. The median OS of the other groups was 13.5 (0–37.1, 95% CI) months for Nc, 18.2 (11–25.5, 95% CI) months for Nm patients, and 9.2 (1.4–16,9, 95% CI) months for the Ncm group (Figure 2).

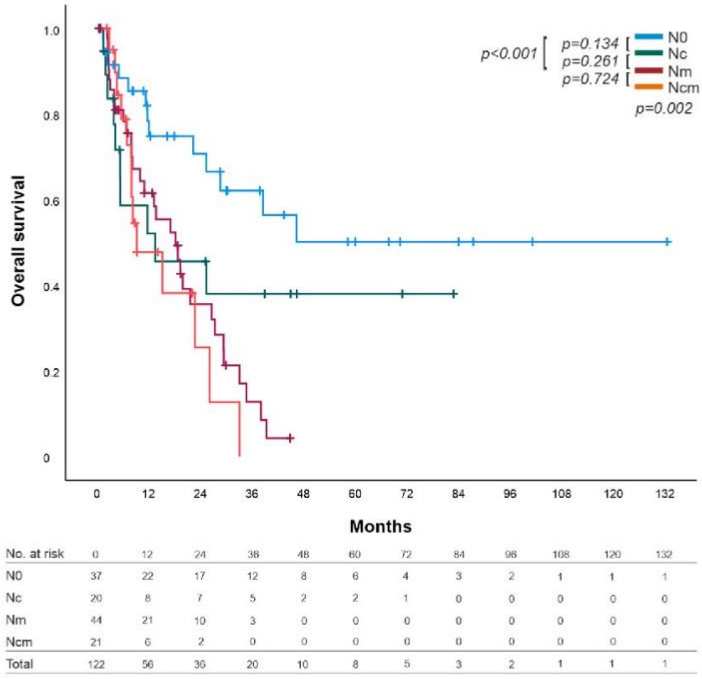


| No. at risk | 0 | 12 | 24 | 36 | 48 | 60 | 72 | 84 | 96 | 108 | 120 | 132 |
|---|---|---|---|---|---|---|---|---|---|---|---|---|
| N0 | 37 | 22 | 17 | 12 | 8 | 6 | 4 | 3 | 2 | 1 | 1 | 1 |
| Nc | 20 | 8 | 7 | 5 | 2 | 2 | 1 | 0 | 0 | 0 | 0 | 0 |
| Nm | 44 | 21 | 10 | 3 | 0 | 0 | 0 | 0 | 0 | 0 | 0 | 0 |
| Ncm | 21 | 6 | 2 | 0 | 0 | 0 | 0 | 0 | 0 | 0 | 0 | 0 |
| Total | 122 | 56 | 36 | 20 | 10 | 8 | 5 | 3 | 2 | 1 | 1 | 1 |

**Figure 2.** Overall survival (OS) of patients with PDAC distinguished by node-negative (N0), per continuitatem (Nc), lymph node metastasis (Nm), and combination of per continuitatem and lymph node metastasis (Ncm). Overall statistical significance difference was $p = 0.002$; no statistical significance difference between N0 and Nc ($p = 0.134$); a significant statistically difference between N0 and Nm was found ($p \leq 0.001$); Nc and Nm showed no statistically significant difference, but their curves diverged strongly ($p = 0.261$). No statistically significant difference between Nm and Ncm was found ($p = 0.724$).

Overall comparison of OS by the mechanisms of lymph node invasion indicated a statistical significance ($p = 0.002$). Paired comparisons of the two groups showed no statistically significant difference between N0 and Nc (13.5 months; $p = 0.134$), however, a statistically significant difference between N0 and Nm (18.2 months; $p < 0.001$), as well as between N0 and Ncm (9.2 months; $p = 0.01$) was found. Nc showed no statistically significant difference with Ncm (13.5 vs. 9.2 months; $p = 0.458$) or Nm (13.5 vs. 18.2 months; $p = 0.261$), but their curves diverged strongly. No statistically significant difference was found between Nm and Ncm ($p = 0.724$) (Figure 2).

#### 3.2.2. Overall Survival by TNM Classification and UICC Stages

As we determined no impact on survival by direct lymph node invasion alone (Table 2), we defined a reviewed N stage by combining the N0 group with the Nc group as a reviewed N0 stage (N0-R = N0 + Nc; Figure 3B). The overall comparison in our reviewed N stage showed greater statistically significant difference ($p = 0.001$) in contrast to the current N stage of the 8th edition of the AJCC ($p = 0.002$; Figure 3A) concerning OS.

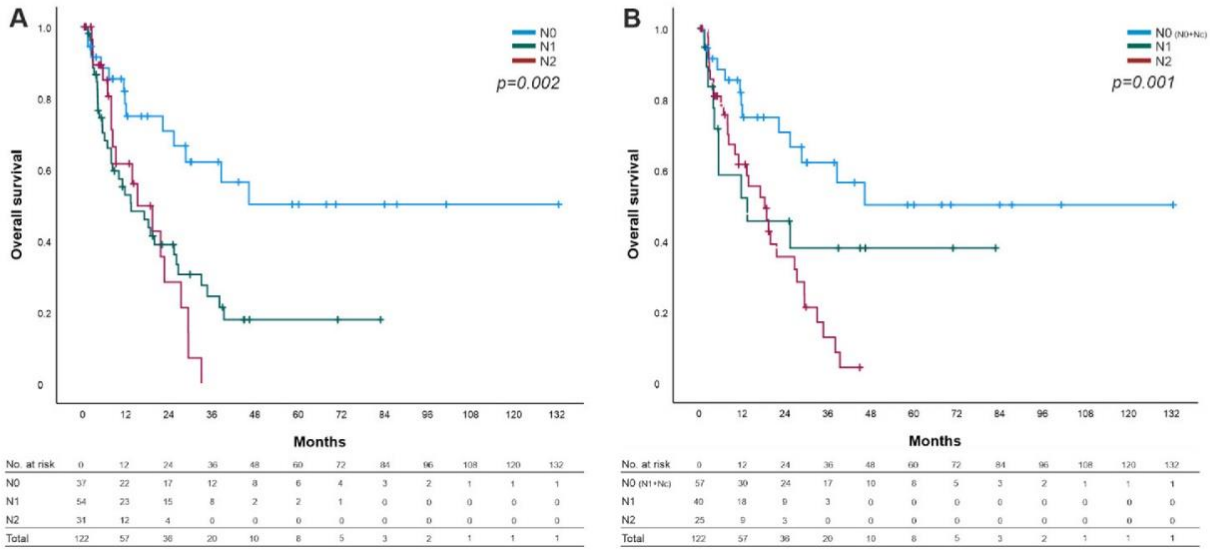


**Figure 3.** Overall survival (OS) sorted by N categories. (**A**) OS of the 8th edition of the AJCC Cancer Staging Manual for PDAC. (**B**) Revised N categories (N0-R = N0 + Nc) with statistically significant difference compared with the actual N categories ($p$= 0.002 vs. $p$= 0.001).

The same observations were identified for the UICC stages between the current system and the reviewed stages ($p = 0.009$ vs. $p = 0.008$). As described above, we combined the group of direct lymph node invasion (Nc) with the node-negative group. (data not shown).

### *3.3. Prognosis Factors*

Resection margin status venous, and angiolymphatic invasion, as well as our revised N stage (N0-R = N0 + Nc/Nm + Ncm) showed a statistically significant difference in the overall survival in the univariate analysis using the Cox proportional hazards regression model and seemed to be predictors of shorter OS (Table 2). To determine the lymph node ratio (LNR) we build three groups with different cut offs (1: >0 and <0.2; 2: ≥0.2 and <0.4; 3: ≥0.4), as described before [20–22] with no statistically significant difference. After proofing the proportional hazards assumption, further analysis of these variables in the multivariate analysis indicated venous invasion (VI) as well N0-R as predictors for overall survival. Direct node invasion (Nc) alone is not a prognostic factor of worse survival ($p = 0.885$).

### *3.4. Contribution of Disease Recurrence by Node Invasion Mechanism*

Overall, 71 (58.2%) patients suffered a disease recurrence. Thereof, 19 (26.8%) patients were in the N0 group, 8 (11.3%) were in the Nc, 29 (40.8%) were in the Nm, and 15 (21.1%) patients were in the Ncm group. No statistical differences were detected in disease recurrence patients compared with patients without disease recurrence ($p = 0.164$). In total, we counted 20 (28.2%) patients with a local disease recurrence, 37 (52.1%) with a systemic disease recurrence and 14 (19.7%) patients with a combination of both. No differences were seen between the groups based on localization ($p = 0.118$).

Direct invasion (Nc + Ncm vs. N0 + Nm) alone had no effect on disease recurrence ($p = 1.0$). No differences were seen between N0 and Nc ($p = 0.562$) nor between Nc and Nm ($p = 0.089$).

## 4. Discussion

Since lymph node status is the strongest predictor of survival in PDAC [3–6], a more detailed classification of the N stage is needed regarding the different mechanisms of lymph node invasion for an individualized therapy after resection. No distinction is made among the local proliferation of the tumour by infiltrating lymph nodes externally per continuitatem through angiogenesis and immunosuppression [13,14] and "real" lymphogenic spread in the current TNM classification system—despite the assumption that a local proliferation differs from a systemic proliferation by the lymphatic system.

Some groups have attempted to find the prognostic factors via lymph node mechanisms but have shown some contradictory data [7–12].

Thus, we discuss our data here in order to rethink TNM classification. We observed a similar patient cohort in our study concerning clinicopathologic characteristics to the other groups [7–12].

Regarding the proportions of the different lymph node types, we detected most patients with directly involved lymph nodes by the tumour (16.4% Nc) compared with the others (3.6–14.3%), as well as mixed node invasion (17.2% vs. 1.5–12.6%) (Table 3). Hoshikawa et al. [11] performed an analysis with all lymph nodes together and showed that 27.6% of lymph nodes invaded per continuitatem. In the same way, we detected almost the same (21.9%) from our analysis. Node-negative patients occur in equal amounts over all groups, except in the study by Hoshikawa et al. [11], who counted only 10 node-negative patients (10.2%). Only 36.1% of our patients showed real lymph node metastasis (Nm), and this was the lowest proportion detected in the current literature. Reversed ratios of Nc/Nm may indicate a more precise analysis of the lymph nodes in PDAC compared with former studies.

**Table 3.** Proportions of lymph node types of the latest studies.

| | Total | N0 | | Nc | | Nm | | Ncm | |
|---|---|---|---|---|---|---|---|---|---|
| | | *n* | % | *n* | % | *n* | % | *n* | % |
| Konstantinidis et al. 2010 | 336 | 168 | 50.0% | 32 | 9.5% | 131 | 39.0% | 5 | 1.5% |
| Pai et al. 2011 | 380 | 97 | 25.5% | 35 | 9.2% | 239 | 62.9% | 9 | 2.4% |
| Buc et al. 2014 | 301 | 87 | 28.9% | 19 | 6.3% | 179 | 59.5% | 16 | 5.3% |
| Williams et al. 2015 | 385 | 146 | 37.9% | 14 | 3.6% | 220 | 57.1% | 5 | 1.3% |
| Hoshikawa et al. 2019 | 98 | 10 | 10.2% | 14 | 14.3% | 66 | 67.3% | x | x |
| Byun et al. 2021 | 506 | 176 | 34.8% | 48 | 9.5% | 218 | 43.1% | 64 | 12.6% |
| Current study 2021 | 122 | 37 | 30.3% | 20 | 16.4% | 44 | 36.1% | 21 | 17.2% |

N0: node negative; Nc: direct node invasion; Nm: regional lymph node metastasis; Ncm: mixed node invasion. Total number of analysed patients; excluded patients are not considered.

Regarding the number of involved direct lymph nodes per patient, we counted 1–5 lymph nodes—similar to Byun et al. [12]. Other groups counted 1–2 [7,8] or 1–7 [10,11], and a maximum mean of 2.4 lymph nodes per continuitatem were detected in the study by Buc et al. [9].

Discrepancies in the proportions of the different types may occur due to the analysis and variable time period of the recruited patients. The first three studies [7–9] analysed patients between 1990–2009, due to rapid changes in medicine—which is a probable explanation. Furthermore, all histological sections were analysed by two different pathologists in the current study as well as in the latest studies [10–12]. Unlike in the initial studies, they did not review the sections [7,9] or, at least, not all of them [8].

Since Konstantinidis et al. and Pai et al. found only one–two invaded direct lymph nodes, they excluded all patients with more than two lymph node metastases [7] or ex-

cluded patients from a further review with three or more lymph node metastases [8]. The proportions of the Nc group are likely underestimated.

Despite the graphs diverging greatly (Figure 2) of the Nc and Nm/Ncm groups in contrast to the similar parallel curves of N0 and Nc (Figure 2) we detected no statistically significant difference of OS in the Nc group compared with Nm or Ncm. The missing statistically significant difference is probably attributed by the small group of patients supported by the worse statistically significant difference in the three- and five-year survival of the Nm and Ncm groups. Similar observations were seen in other groups [8,10,12], supporting the hypothesis that Nc might be a different entity compared with Nm and is more related to N0 (Table 4).

**Table 4.** Overall survival of lymph node types of the latest studies.

| | N0 | | Nc | | Nm | | Ncm | |
|---|---|---|---|---|---|---|---|---|
| | *n* | OS Median | *n* | OS Median | *n* | OS Median | *n* | OS Median |
| Konstantinidis et al. 2010 | 168 | 30.8 | 32 | x | 131 | x | 5 | x |
| Pai et al. 2011 | 97 | 30 | 35 | 21 * | 239 | 15 ** | 9 | 15 |
| Buc et al. 2014 | 87 | 57 | 19 | 34 ** | 179 | 33 ** | 16 | 22 |
| Williams et al. 2015 | 146 | 40.7 | 14 | 48.1 | 220 | 25.7 ** | 5 | x |
| Current study 2021 | 37 | x | 20 | 13.5 | 44 | 18.2 ** | 21 | 9.2 ** |
| Total | 535 | | 120 | | 813 | | 56 | |
| Weighted Median OS | | 30.8 | | 21 | | 25.7 | | 15 |

Modified table of Williams et al. [10]: N0: node negative; Nc: direct node invasion; Nm: regional lymph node metastasis; Ncm: mixed node invasion; x: not calculated. * Significant difference with Nm. ** Significant difference with N0. The latest study of Byun et al. was excluded as they calculated only disease-free survival, as were the results of Hoshikawa et al. [11], as they built groups of single lymph nodes and distinguished further between isolated tumour cells and between scatter type.

Pai et al. (2012) [8] analysed 308 patients and found no statistically significant difference between N0 and Nc in overall survival ($p = 0.609$) but discovered improved overall survival in Nc compared with Nm ($p = 0.001$). This result is reflected by the comparison of the five-year survival (N0 31%, Nc 36%, and Nm 8%) [8]. Williams et al. (2015) showed similar overall survival between Nc and N0 ($p = 0.719$), statistically significant differences between N0 and Nm ($p < 0.001$), however, no statistically significant difference between Nc and Nm ($p = 0.190$) was observed [10]. Supporting our results, in 2019, Hoshikawa et al. analysed 98 patients and showed similar survival between the Nc and the N0 group [11].

According to our knowledge, this study underlines the latest results in this field by Byun et al. (2021), who had also proposed a change of the N stage regarding the lymph node invasion per continuitatem. Moreover, they did not observe any statistically significant difference in the disease-free survival (DFS) of N0 and Nc ($p = 0.999$) but statistically significant difference between Nc and Nm ($p = 0.002$) as well as between Nc and Ncm ($p < 0.001$). Furthermore, they showed higher statistically significant differences in the disease-free survival of a revised TNM classification compared with the current 8th edition of the AJCC classification system ($p = 0.003$, revised $p < 0.001$) similar to our data ($p = 0.002$, N0-R (N0 + Nc)$p = 0.001$). Comparing this study with all the other studies is limited, since they analysed the disease-free survival (DFS) and showed no data regarding the overall survival [12].

In contrast, Konstantinidis et al. (2010) [7] detected a similar unfavourable overall survival of Nc and Nm patients compared with N0 patients ($p = 0.67$). However, they excluded all patients with more than two detected positive lymph nodes and the mixed type Ncm [7]. Therefore, the results are limited by this selection and do not illustrate the collective of PDAC patients, evidenced by the fact of the significantly lower five-year survival of all patients ($n = 517$) compared with the other groups inclusive of our data analysis (17.3% vs. 24.3–32%) [8–10].

Likewise, Buc et al. showed an unfavourable survival in patients with direct invasion compared with the node-negative group ($p = 0.037$). No statistically significant difference was seen between Nc and Nm ($p = 0.57$). However, statistically significant differences between Nm and N0 were found ($p < 0.001$). Interestingly, direct invasion on its own showed no impact on overall survival ($p = 0.27$), which is similar to our data ($p = 0.220$) [9].

The detected prognostic factors of survival by the different groups included margin status after resection, T stage, grade, angiolymphatic and venous invasion, and involved lymph nodes, in general, related to the current data (Table 2). Direct lymph node invasion (Nc) was not an independent prognostic factor [9,11,12] as confirmed by our observations ($p = 0.885$).

Interestingly, no statistical difference was discovered in the appearance of disease recurrence between the lymph node types as well as the location (local/systemic) of the tumour recurrence. Byun et al. published the same results in 2021 [12]. This owes to the small patient cohort size and, thus, requires further investigations in larger-scale studies.

The key strengths of our research are the histological analysis by two independent pathologists considering the 8th edition of the TNM classification of the American Joint Committee on Cancer (AJCC). The comparison of all above-mentioned studies showed that a wide range of lymph nodes invaded per continuitatem were detected [7–12]. Despite the smaller group of patients, we observed similar contributions and had, in fact, proportionally more patients with direct invasion, compared with the other studies [7–12], revealing the importance of precisely analysing the correct classification of each patient [23]. Our study supports the latest published results [12] and is, according to our knowledge, the only paper that has, so far, considered the 8th AJCC system in Europe with the highest proportion of lymph nodes per continuitatem.

Limitations, such as the small number of patients, retrospective analyses, local sampling protocols, statistically significant difference in the number of lymph nodes in the different groups, and single-institution analysis require further and larger studies with international collaborations to overcome. Especially, a statistically powered study is necessary to validate our hypothesis of rethinking the N classification. Due to cancer-related angiogenesis and immunosuppression through interactions of the cancer endothelium with immune cells, further focused studies for an individualized anti-angiogenesis and immunomodulatory therapy are urgently required [13,14].

Another limitation is that we did not find any patient in the Nc group classified N2 regarding the latest TNM classification system ($\geq$4 lymph node metastasis); however, we categorized 14 patients of the Ncm group N2. Byun et al. found 1 Nc patient and 33 Ncm patients [12]. Either PDAC has only a limited tendency of invasion of the tumour surrounding lymph nodes per continuitatem—supporting the hypothesis that Nc is similar to N0—or we underestimated the direct lymph nodes per patient due to the small groups.

All of the above results—in accordance with the latest studies—suggest that lymph node invasion per continuitatem is a different entity despite the normal N classification. Moreover, Nc seemed to be more similar to N0 lymph nodes. For a more precise prognosis of PDAC patients, we need to reconsider the TNM classification regarding the N stage.

## 5. Conclusions

In conclusion, we found similar characteristics in patients with direct lymph node invasion compared with node-negative patients after PDAC resection; hence, we suggest a redefinition of the TNM classification based on the mechanism of lymph node metastases in patients with PDAC. Overall, this novel classification has a more precise prognostic power.

**Author Contributions:** Conceptualization, C.K.; Data curation, F.S. and F.N.L.; Formal analysis, F.S. and C.K.; Methodology, C.K.; Project administration, C.K.; Resources, C.E.D., A.-K.B., L.H., I.P. and C.S.; Supervision, G.A.M., J.C.L., K.B. and C.K.; Visualization, F.S., M.P.D. and S.S.; Writing—original draft, F.S.; Writing—review and editing, F.S., M.P.D., S.S. and C.K. All authors have read and agreed to the published version of the manuscript.

**Funding:** M.P.D. is a participant in the BIH-Charité Junior Clinical Scientist Program funded by the Charité–Universitätsmedizin Berlin and the Berlin Institute of Health. S.S. was supported by a cooperation between Charité-Universitätsmedizin Berlin and Siemens Healthcare GmbH. Except his, no other external funding was received for this research.

**Institutional Review Board Statement:** The study was conducted according to the guidelines of the Declaration of Helsinki and approved by the Ethics Committee of the Charité University Medical Department in Berlin (protocol code EA4/020/19) 09.04.2019.

**Informed Consent Statement:** There is no specific patients consent required for a retrospective study in Germany. In Germany we are able to collect and analyze the data from the patients we operate. Once entering our hospital patients have to agree to a general patient consent but not for a specific study.

**Data Availability Statement:** A dataset of the present study can be requested from the corresponding author with justification.

**Conflicts of Interest:** The authors declare no conflict of interest.

## References

1. Rawla, P.; Sunkara, T.; Gaduputi, V. Epidemiology of pancreatic cancer: Global trends, etiology and risk factors. *World J. Oncol.* **2019**, *10*, 10–27. [CrossRef] [PubMed]
2. Wild, C.P.; Weiderpass, E.; Stewart, B.W. (Eds.) *World Cancer Report: Cancer Research for Cancer Prevention*; International Agency for Research on Cancer: Lyon, France, 2020. Available online: http://publications.iarc.fr/586 (accessed on 23 June 2021).
3. Berger, A.C.; Watson, J.C.; Ross, E.A.; Hoffman, J.P. The metastatic/examined lymph node ratio is an important prognostic factor after pancreaticoduodenectomy for pancreatic adenocarcinoma. *Am. Surg.* **2004**, *70*, 235.
4. Showalter, T.N.; Winter, K.A.; Berger, A.C.; Regine, W.F.; Abrams, R.A.; Safran, H.; Hoffman, J.P.; Benson, A.B.; MacDonald, J.S.; Willett, C.G. The influence of total nodes examined, number of positive nodes, and lymph node ratio on survival after surgical resection and adjuvant chemoradiation for pancreatic cancer: A secondary analysis of RTOG 9704. *Int. J. Radiat. Oncol.* **2011**, *81*, 1328–1335. [CrossRef]
5. Basturk, O.; Saka, B.; Balci, S.; Postlewait, L.M.; Knight, J.; Goodman, M.; Kooby, D.; Sarmiento, J.M.; El-Rayes, B.; Choi, H.; et al. Substaging of lymph node status in resected pancreatic ductal adenocarcinoma has strong prognostic correlations: Proposal for a revised N classification for TNM staging. *Ann. Surg. Oncol.* **2015**, *22*, 1187–1195. [CrossRef]
6. Fukuda, Y.; Asaoka, T.; Maeda, S.; Hama, N.; Miyamoto, A.; Mori, M.; Doki, Y.; Nakamori, S. Prognostic impact of nodal statuses in patients with pancreatic ductal adenocarcinoma. *Pancreatology* **2017**, *17*, 279–284. [CrossRef] [PubMed]
7. Konstantinidis, I.T.; Deshpande, V.; Zheng, H.; Wargo, J.A.; Fernandez-del Castillo, C.; Thayer, S.P.; Androutsopoulos, V.; Lauwers, G.Y.; Warshaw, A.L.; Ferrone, C.R. Does the mechanism of lymph node invasion affect survival in patients with pancreatic ductal adenocarcinoma? *J. Gastrointest. Surg.* **2010**, *14*, 261–267. [CrossRef]
8. Pai, R.K.; Beck, A.H.; Mitchem, J.; Linehan, D.C.; Chang, D.T.; Norton, J.A.; Pai, R.K. Pattern of lymph node involvement and prognosis in pancreatic adenocarcinoma: Direct lymph node invasion has similar survival to node-negative disease. *Am. J. Surg. Pathol.* **2011**, *35*, 228–234. [CrossRef] [PubMed]
9. Buc, E.; Couvelard, A.; Kwiatkowski, F.; Dokmak, S.; Ruszniewski, P.; Hammel, P.; Belghiti, J.; Sauvanet, A. Adenocarcinoma of the pancreas: Does prognosis depend on mode of lymph node invasion? *Eur. J. Surg. Oncol.* **2014**, *40*, 1578–1585. [CrossRef] [PubMed]
10. Williams, J.L.; Nguyen, A.H.; Rochefort, M.; Muthusamy, V.R.; Wainberg, Z.A.; Dawson, D.W.; Tomlinson, J.S.; Hines, O.J.; Reber, H.A.; Donahue, T.R. Pancreatic cancer patients with lymph node involvement by direct tumor extension have similar survival to those with node-negative disease. *J. Surg. Oncol.* **2015**, *112*, 396–402. [CrossRef]
11. Hoshikawa, M.; Ogata, S.; Nishikawa, M.; Kimura, A.; Einama, T.; Noro, T.; Aosasa, S.; Hase, K.; Tsujimoto, H.; Ueno, H.; et al. Pathomorphological features of metastatic lymph nodes as predictors of postoperative prognosis in pancreatic cancer. *Medicine* **2019**, *98*, e14369. [CrossRef] [PubMed]
12. Byun, Y.; Lee, K.-B.; Jang, J.-Y.; Han, Y.; Choi, Y.J.; Kang, J.S.; Kim, H.; Kwon, W. Peritumoral lymph nodes in pancreatic cancer revisited; is it truly equivalent to lymph node metastasis? *J. Hepatobiliary Pancreat. Sci.* **2021**, *28*, 893–901. [CrossRef]
13. Argentiero, A.; De Summa, S.; Di Fonte, R.; Iacobazzi, R.M.; Porcelli, L.; Da Vià, M.; Brunetti, O.; Azzariti, A.; Silvestris, N.; Solimando, A.G. Gene expression comparison between the lymph node-positive and-negative reveals a peculiar immune microenvironment signature and a theranostic role for WNT targeting in pancreatic ductal adenocarcinoma: A pilot study. *Cancers* **2019**, *11*, 942. [CrossRef] [PubMed]
14. Solimando, A.G.; De Summa, S.; Vacca, A.; Ribatti, D. Cancer-Associated angiogenesis: The endothelial cell as a checkpoint for immunological patrolling. *Cancers* **2020**, *12*, 3380. [CrossRef] [PubMed]
15. Ueno, M.; Morizane, C.; Ikeda, M.; Okusaka, T.; Ishii, H.; Furuse, J. A review of changes to and clinical implications of the eighth TNM classification of hepatobiliary and pancreatic cancers. *Jpn. J. Clin. Oncol.* **2019**, *49*, 1073–1082. [CrossRef] [PubMed]

16. Roalsø, M.; Aunan, J.R.; Søreide, K. Refined TNM-staging for pancreatic adenocarcinoma-Real progress or much ado about nothing? *Eur. J. Surg. Oncol.* **2020**, *46*, 1554–1557. [CrossRef]
17. Morales-Oyarvide, V.; Rubinson, D.A.; Dunne, R.F.; Kozak, M.M.; Bui, J.L.; Yuan, C.; Qian, Z.R.; Babic, A.; Da Silva, A.; Nowak, J.A.; et al. Lymph node metastases in resected pancreatic ductal adenocarcinoma: Predictors of disease recurrence and survival. *Br. J. Cancer* **2017**, *117*, 1874–1882. [CrossRef]
18. Allen, P.J.; Kuk, D.; Castillo, C.F.-D.; Basturk, O.; Wolfgang, C.L.; Cameron, J.L.; Lillemoe, K.D.; Ferrone, C.R.; Morales-Oyarvide, V.; He, J.; et al. Multi-institutional validation study of the american joint commission on cancer (8th Edition) changes for T and N staging in patients with pancreatic adenocarcinoma. *Ann. Surg.* **2017**, *265*, 185–191. [CrossRef]
19. van Roessel, S.; Kasumova, G.G.; Verheij, J.; Najarian, R.M.; Maggino, L.; de Pastena, M.; Malleo, G.; Marchegiani, G.; Salvia, R.; Ng, S.C.; et al. International validation of the eighth edition of the American joint committee on cancer (AJCC) TNM staging system in patients with resected pancreatic cancer. *JAMA Surg.* **2018**, *153*, e183617. Available online: https://www.ncbi.nlm.nih.gov/pmc/articles/PMC6583013/ (accessed on 23 June 2021). [CrossRef]
20. Slidell, M.B.; Chang, D.C.; Cameron, J.L.; Wolfgang, C.; Herman, J.M.; Schulick, R.D.; Choti, M.A.; Pawlik, T.M. Impact of total lymph node count and lymph node ratio on staging and survival after pancreatectomy for pancreatic adenocarcinoma: A large, population-based analysis. *Ann. Surg. Oncol.* **2007**, *15*, 165–174. [CrossRef]
21. Hartwig, W.; Hackert, T.; Hinz, U.; Gluth, A.; Bergmann, F.; Strobel, O.; Büchler, M.W.; Werner, J. Pancreatic cancer surgery in the new millennium: Better prediction of outcome. *Ann. Surg.* **2011**, *254*, 311–319. [CrossRef]
22. Pyo, J.-S.; Kim, N.Y.; Son, B.K.; Chung, K.H. Prognostic implication of pN stage subdivision using metastatic lymph node ratio in resected pancreatic ductal adenocarcinoma. *Int. J. Surg. Pathol.* **2020**, *28*, 245–251. [CrossRef] [PubMed]
23. House, M.G.; Gönen, M.; Jarnagin, W.R.; D'Angelica, M.; DeMatteo, R.P.; Fong, Y.; Brennan, M.F.; Allen, P.J. Prognostic significance of pathologic nodal status in patients with resected pancreatic cancer. *J. Gastrointest. Surg.* **2007**, *11*, 1549–1555. [CrossRef] [PubMed]

## 2.5 Genauigkeit und Kriterien des regionalen Lymphknotenstaging resektabler exokriner Pankreaskopfkarzinome durch Computertomographie sowie der Magnetresonanztomographie (Originalarbeit 5)

Neben Analysen des prognostischen Einflusses exprimierter Proteine **der Originalarbeiten 1 und 2** sowie den aus der postoperativen pathologischen Aufarbeitung chirurgischer Operationsresektate hervorgehenden Merkmalen der **Originalarbeiten 3 und 4** ist eine weitere wichtige methodische Säule der prognostischen Risikostratifikation resektabler exokriner Pankreaskarzinome die präoperative radiologische Ausbreitungsdiagnostik. Die **Originalarbeit 5** ergänzt die **Originalarbeiten 1-4** um eine weitere differenzierte Analyse eines prognostischen Merkmals resektabler exokriner Pankreaskarzinome unter Einbeziehung dieser weiteren methodischen Ebene. Hierbei untersucht die **Originalarbeit 5** die diagnostische Genauigkeit verschiedener bildmorphologischer Kriterien von Lymphknoten in der präoperativen Schnittbildgebung, um das lokoregionäre Lymphknotenstaging zu erweitern.

**Florian N. Loch**, Patrick Asbach, Matthias Haas, Hendrik Seeliger, Katharina Beyer, Christian Schineis, Claudius E. Degro, Georgios A. Margonis, Martin E. Kreis, Carsten Kamphues.

Accuracy of various criteria for lymph node staging in ductal adenocarcinoma of the pancreatic head by computed tomography and magnetic resonance imaging. *World Journal of Surgical Oncology*. **2020**; 18:213.

Der nachfolgende Text entspricht dem Originalabstract der o.g. Publikation *Accuracy of various criteria for lymph node staging in ductal adenocarcinoma of the pancreat-ic head by computed tomography and magnetic resonance imaging* übersetzt durch den Erstautor Florian N. Loch:

***„Hintergrund***

*Das Lymphknotenstaging des PDAC des Pankreaskopfes durch Schnittbildgebung ist eingeschränkt. Ziel dieser Studie ist es, die diagnostische Genauigkeit erweiterter Kriterien des Lymphknotenstaging bei Patient:innen mit einem PDAC zu untersuchen.*

***Methoden***

*Es wurden 66 Patient:innen mit histologisch bestätigtem PDAC, welche eine primäre Tumorresektion erhielten, in diese monozentrische Studie eingeschlossen, nach Zustimmung der lokalen Ethikkomission. CT- und MRT-Untersuchungen wurden durch einen bezüglich der Histopathologie verblindeten Radiologen beurteilt. Die Anzahl der Lymphknoten sowie ihre Größe (kurzer Achsendurchmesser) wurden bestimmt und die Lymphknoten charakterisiert in Bezug auf die morphologischen Kriterien Kontur (spikuliert, lobuliert und unscharf) und Textur (homogen oder inhomogen). Sensitivitäten und Spezifitäten wurden berechnet mit der Histopathologie als Referenzstandard.*

***Ergebnisse***

*Bei 48 von 66 Patient:innen (80%) lagen histologisch nachgewiesene regionale Lymphknotenmetastasen vor (pN+). Sensitivität, Spezifität und Youden-Index waren für das Kriterium „Größe“ 44,2%, 82,4% und 0,27, für das Kriterium „inhomogene Signalintensität“ 25,6%, 94,1% und 0,20 und für das Kriterium „Kontur“ 62,7%, 52,9% und 0,16. Es gab eine statistisch signifikante Assoziation zwischen der Anzahl in der CT präoperativ erkennbaren Lymphknoten und pathologischer Lymphknotenmetastasierung (pN+, p=0,031).*

***Schlussfolgerung***

*Das Lymphknotenstaging des PDAC ist hauptsächlich eingeschränkt durch eine niedrige Sensitivität in der Erkennung von Metastasen. Die Anwendung erweiterter morphologischer Kriterien anstelle des Kriteriums Größe hat nicht zu einer Verbesserung des regionalen Lymphknotenstaging geführt, da die Sensitivität niedrig bleibt. Die Kombination einzelner Kriterien erhöht die Sensitivität während Spezifität und positiver prädiktiver Wert hoch bleiben.“*

Loch et al. World Journal of Surgical Oncology (2020) 18:213
https://doi.org/10.1186/s12957-020-01951-3

World Journal of Surgical Oncology

RESEARCH Open Access

# Accuracy of various criteria for lymph node staging in ductal adenocarcinoma of the pancreatic head by computed tomography and magnetic resonance imaging

Florian N. Loch[1*], Patrick Asbach[2], Matthias Haas[2], Hendrik Seeliger[1], Katharina Beyer[1], Christian Schineis[1], Claudius E. Degro[1], Georgios A. Margonis[3], Martin E. Kreis[1] and Carsten Kamphues[1]

## Abstract

**Background:** Lymph node staging of ductal adenocarcinoma of the pancreatic head (PDAC) by cross-sectional imaging is limited. The aim of this study was to determine the diagnostic accuracy of expanded criteria in nodal staging in PDAC patients.

**Methods:** Sixty-six patients with histologically confirmed PDAC that underwent primary surgery were included in this retrospective IRB-approved study. Cross-sectional imaging studies (CT and/or MRI) were evaluated by a radiologist blinded to histopathology. Number and size of lymph nodes were measured (short-axis diameter) and characterized in terms of expanded morphological criteria of border contour (spiculated, lobulated, and indistinct) and texture (homogeneous or inhomogeneous). Sensitivities and specificities were calculated with histopathology as a reference standard.

**Results:** Forty-eight of 66 patients (80%) had histologically confirmed lymph node metastases (pN+). Sensitivity, specificity, and Youden's Index for the criterion "size" were 44.2%, 82.4%, and 0.27; for "inhomogeneous signal intensity" 25.6%, 94.1%, and 0.20; and for "border contour" 62.7%, 52.9%, and 0.16, respectively. There was a significant association between the number of visible lymph nodes on preoperative CT and lymph node involvement (pN+, $p = 0.031$).

**Conclusion:** Lymph node staging in PDAC is mainly limited due to low sensitivity for detection of metastatic disease. Using expanded morphological criteria instead of size did not improve regional nodal staging due to sensitivity remaining low. Combining specific criteria yields improved sensitivity with specificity and PPV remaining high.

**Keywords:** Ductal adenocarcinoma of the pancreatic head, Staging, Lymph nodes, Computed tomography, Magnetic resonance imaging, Cross-sectional imaging, Neoadjuvant therapy

* Correspondence: Florian.Loch@charite.de
[1]Charité – Universitätsmedizin Berlin, corporate member of Freie Universität Berlin, Humboldt-Universität zu Berlin, and Berlin Institute of Health, Department of Surgery, Campus Benjamin Franklin, Hindenburgdamm 30, 12203 Berlin, Germany
Full list of author information is available at the end of the article

## Background

Pancreatic cancer remains one of the most lethal malignancies being the fourth leading cause of cancer death in the USA and predicted to be the second leading cause of cancer death by 2020 [1]. The overall 5-year survival after diagnosis is 7% [2], and at the time of diagnosis, the main proportion of patients has advanced-stage disease leaving only 15–20% qualified for resective surgery [3]. Pancreatic cancer is located in the head of the pancreas in 75% of the cases [4]. Even after successful resective surgery in patients with cancer of the pancreatic head, the 5-year survival remains as low as 21% [5]. These data underline the importance of establishing multimodal therapeutic concepts for patients with pancreatic cancer as per other entities of abdominal cancer.

Apart from the potential to increase the resectability rate of pancreatic cancer by neoadjuvant therapy [6, 7], there is evidence that patients which are successfully downstaged from node-positive disease (cN1) to node-negative disease (ypN0) prior to surgery benefit in terms of higher 5-year survival rate [8]. This would qualify nodal involvement as a sufficient basis for indicating neoadjuvant therapy. Yet, even given advanced imaging technologies, identifying lymph node metastasis remains challenging. Consequently, the indication of a potentially effective neoadjuvant therapy (cN+) with side effects in lymph node-positive patients (cN+) is mainly based on unreliable clinical staging.

The established criterion for lymph node involvement in pancreatic cancer is size. Using the size underlies the assumption that tumor spread to regional lymph nodes leads to an enlargement of the respective lymph node. The usual cut-off value is a short-axis diameter of 10 mm [3, 9–12]. It has been shown though that lymph nodes of ≥ 10 mm are not seen more frequently in patients with histopathological lymph node involvement (pN+) [13]. In various other tumor entities, expanded morphological criteria such as texture and border contour of lymph nodes are used for the assessment of lymph node malignancy on both computed tomography (CT) and magnetic resonance (MR) imaging. This is utilized in order to improve the accuracy of lymph node staging [14–16]. By applying morphological criteria instead of Brown et al. size criterion alone, the sensitivity was improved from 42 to 85% and the specificity from 87 to 97% in lymph node staging of rectal cancer [16].

Thus, the aim of this study was to determine the accuracy of lymph node staging in patients with ductal adenocarcinoma of the pancreatic head by both computed tomography and magnetic resonance imaging using size and expanded morphological criteria.

## Material and methods

### Patients

In this retrospective single-center study approved by the local ethics committee, consecutive patients with histologically proven ductal adenocarcinoma of the pancreatic head that underwent primary surgery between February 2013 and November 2018 at the Department of Surgery, Campus Benjamin Franklin, Charité—University Medicine Berlin, Germany, were included. Patients were retrieved from the database of our pancreatic cancer center certified by the German Cancer Society (n = 80). Inclusion criteria were primary oncologic tumor resection and the presence of preoperative cross-sectional imaging of sufficient quality (see below). Exclusion criteria were neoadjuvant therapy, presence of a potential simultaneous cause of lymphadenopathy of the upper abdominal region (e.g. abdominal lymphoma, neuroendocrine tumor), and main tumor mass located outside the pancreatic head on histopathology. The process of patient selection with the respective reasons for inclusion and exclusion is shown in Fig. 1.

### Cross-sectional imaging

All images were retrospectively analyzed for the purpose of this study by a single abdominal radiologist, with more than 12 years of experience in staging of tumors of the visceral organs, blinded to the results of histopathology.

All cross-sectional imaging studies were assessed for sufficient image quality by the radiologist prior to commencement. For CT imaging, the minimum quality was defined as either thin-section CT (≤ 2 mm reconstructed slice thickness) or contrast-enhanced CT with a slice thickness of ≤ 5 mm. For MRI, minimum quality was defined as availability of an axial T2-weighted sequence with fat suppression (slice thickness ≤ 5 mm) in combination with a venous phase post-contrast 3D gradient-echo sequence (slice thickness ≤ 3 mm).

For lymph node assessment, all visible regional lymph nodes in the field of view were recorded on a score chart and the total number of visible lymph nodes per patient was calculated. Then, for each patient, all lymph nodes were characterized in terms of size (long- and short-axis diameter in millimeters) and the expanded morphological criteria border contour (lobulated, spiculated, indistinct, or unaltered) and texture (homogeneous or inhomogeneous, Fig. 2 based on Kim et al. [17]).

Regional lymph nodes of the pancreas are defined as the following lymph node station numbers: 5, 6, 7, 8a, 8p, 9, 10, 11p, 11d, 12a, 12b, 12p,13a, 13b,14p,14d, 17a, 17b, and 18 [17]. In all cases in which a lymph node was not definitively regional, correlation with postoperative cross-sectional imaging was performed to assess whether the lymph node was resected or not. Only resected lymph nodes were analyzed in this study.

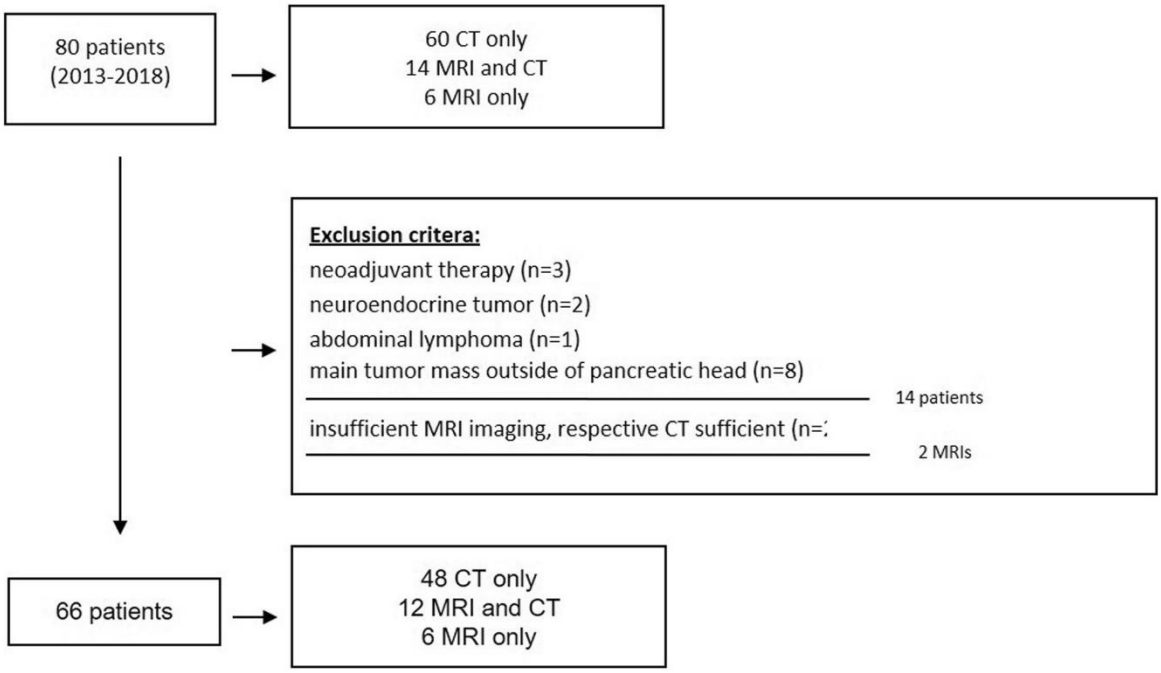


**Fig. 1** Flowchart of patient recruitment. The process of patient selection with the respective reasons for inclusion and exclusion is shown

A second radiologist with more than 5 years of experience in staging of tumors of the visceral organs, also blinded to the results of histopathology, evaluated the CT examinations of a representative subgroup of 20 patients for evaluation of interobserver agreement.

### Surgery

All patients underwent primary, oncologic pylorus-preserving pancreaticoduodenectomy or Whipple procedure with complete lymphadenectomy of the regional lymph nodes mentioned above.

### Histopathology

For the study, the original histopathological reports using formalin-embedded surgical specimens were reviewed. Cancer of the pancreatic head was defined as a malignant tumor located within the pancreas to the right of the superior mesenteric vein and portal vein. Each patient with histologically proven lymph node metastases was classified as node-positive (pN+) regardless of the number of metastatic lymph nodes. Patients without any metastatic lymph nodes were classified as node-negative (pN-). The ratio of metastatic lymph nodes vs. the total number of retrieved lymph nodes was documented in

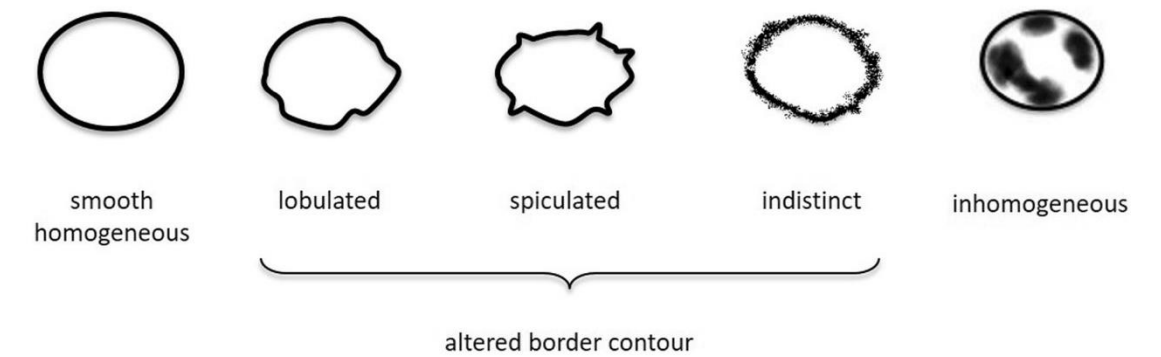


**Fig. 2** Morphological characterization of lymph nodes based on Kim et al. [16]. The morphological criteria for lymph node assessment used in this study are shown. Smooth and homogeneous lymph nodes were considered normal

the histopathological report (e.g., 0/14 or 3/23). Tumors were classified according to their respective TNM stage using the 8th Edition of TNM Classification of Malignant Tumors [18].

### Comparison of cross-sectional imaging and histopathology

Sensitivity, specificity, and positive predictive value of the nodal status using CT and MRI, with histopathology as a reference standard, were calculated for lymph node involvement using size and morphological criteria. Specifically, nodal involvement criteria were based on either size (short-axis diameter), altered border contour (lobulated, spiculated or indistinct), and inhomogeneous signal intensity (Fig. 2). CT and MRI examinations were considered node-positive (cN+), if at least one lymph node met one of the respective criteria used for involvement. If no lymph node with the respective criteria was seen on CT or MRI, then the examination was considered node-negative (cN-).

### Statistical analysis

Sensitivities, specificities, and positive predictive value (PPV) for the size criterion, and all morphological criteria were calculated for their respective cut-off values. An index summarizing the sensitivity and specificity for Youden's Index was calculated (Sensitivity + Specificity − 1) [19]. The number of lymph nodes visible on CT and MR images in the group with (pN+) and without (pN-) nodal metastases was compared using the Mann-Whitney U test. When calculating the association between CT and MRI criteria and lymph node positivity, the $\chi 2$-test was used. Interobserver agreement was calculated using Cohen's Kappa statistic. A p value of $\leq 0.05$ was considered to indicate a statistically significant difference.

## Results

### Patients

Sixty-six patients were included in the study (Fig. 1) with the characteristics of the patients presented in Table 1. Sixty of these patients were staged by preoperative CT, twelve of which had additional staging by MRI, and six patients were staged by only MRI. In two patients, the MRI examinations were excluded due to insufficient imaging quality. Both patients had sufficient staging by CT and were therefore included in the study. Of the 66 patients, 10 patients received preoperative biliary drainage. Eight of them were staged by CT only and two by MRI only.

### Computed tomography (CT)

Lymph nodes were detected by CT in 96.7% (58/60) of the patients. The median number of visible lymph nodes was 5 (range 0–15). The smallest visible lymph node was 2.0 mm of size whereas the largest measured 18 mm (short-axis diameter). The mean time between CT and surgery was 7 days with a median of 6 days (range 1–43). The slice thickness in 61 of the 66 CT examinations (92.4%) was 3 mm or less. In five CT examinations (7.6%), slice thickness was 5 mm.

**Table 1** Demographic data of patients with ductal adenocarcinoma of the pancreatic head undergoing primary tumor resection

| Patients | n = 66 |
|---|---|
| **Age** | |
| Median age (years) | 73 |
| Age range (years) | 44–86 |
| **Sex** | |
| Female | 28 (42%) |
| Male | 38 (58%) |
| **Cross-sectional imaging** | |
| CT only | 48 (73%) |
| CT and MRI | 12 (18%) |
| MRI only | 6 (9%) |
| **Histopathological staging** | |
| pN+ | 48 (73%) |
| pN- | 18 (27%) |
| pT1 | 5 (8%) |
| pT2 | 39 (59%) |
| pT3 | 22 (33%) |

### Size criterion for lymph node involvement on preoperative CT

Figure 3 shows the percentage of patients with (pN+) and without (pN-) lymph node metastases in which a lymph node of the respective size was visible (5–11 mm). In Table 2, sensitivity, specificity, and Youden's Index are presented for the respective cut-off values. Lymph nodes of small and medium size (5–9 mm) were visible in patients with (51–95%; 22–41/43, pN+) and without lymph node metastases (41–100%; 7–17/17, pN-) in even frequency. Large lymph nodes (10–11 mm) were seen more frequently in the lymph node-positive group (35–44%; 15–19/43, pN+) than in the lymph node-negative group (12–18%; 2–3/17, pN-). The maximum value of Youden's Index for the size criterion was J = 0.27 (95% CI; 0.00, 0.45) when a cut-off value of 10 mm was applied, yielding a sensitivity of 44% and specificity of 82%. Additionally, the presence of lymph nodes greater than 10 mm on preoperative CT, and the histopathological confirmation of a lymph node metastasis (pN+), showed a trend towards significance (p = 0.076).

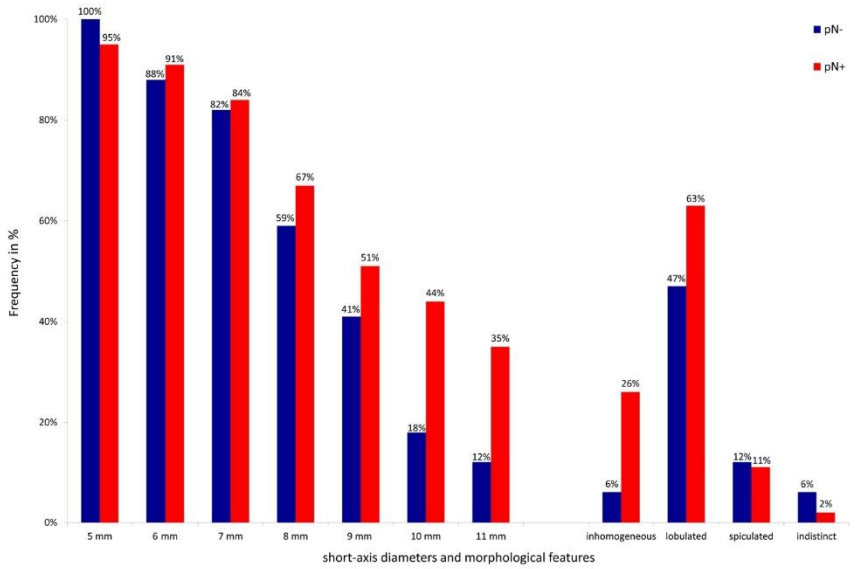


**Fig. 3** Graph showing lymph node size and morphological criteria of lymph node-positive and -negative patients. Frequency of regional lymph nodes of the pancreatic head in percent (x-axis) with different short-axis diameters and morphological features (y-axis) in patients with (pN+, red bars) or without histologically proven lymph node metastases (pN-, blue bars) on preoperative CT imaging

### Expanded morphological criteria for lymph node involvement on preoperative CT

Figure 3 shows the percentage of patients with (pN+) and (pN-) without lymph node metastases in which a lymph node of the respective morphological criterion was visible and Table 2 shows the sensitivity, specificity, and Youden's Index of the respective criterion.

Lymph nodes of lobulated border contour were visible with a similar frequency in patients with (63%; 27/60, pN+) and without lymph node metastases (47%; 7/17, pN-). Lymph nodes of spiculated or indistinct border contour were only occasionally detected in both groups (11%; 5/43 vs. 2%; 1/43 in the lymph node-positive group (pN+) and 12%; 2/17 vs. 12% 2/17 in the lymph node-negative group (pN-)).

Lymph nodes of inhomogeneous signal intensity were detected in only one patient of the lymph node-negative group (6%; 1/17, pN-) and more frequently in patients of the lymph node-positive group (26%; 11/43, pN+) resulting in the maximum value of Youden's Index for the morphological criteria J = 0.20 (95% CI; 0.04, 0.35), consisting of a sensitivity of 26% and a specificity of 94%. The PPV was 91.7%.

### Comparison of size with expanded morphological criteria

The maximum value of the Youden's Index of the "size" criterion was J = 0.27 (95% CI; 0.00, 0.45; cut-off 10 mm) which is not inferior to the maximum value of the morphological criteria J = 0.20 (95% CI; 0.04, 0.35; inhomogeneous signal intensity). Figure 4 displays respective CT images of patients with and without lymph node metastases.

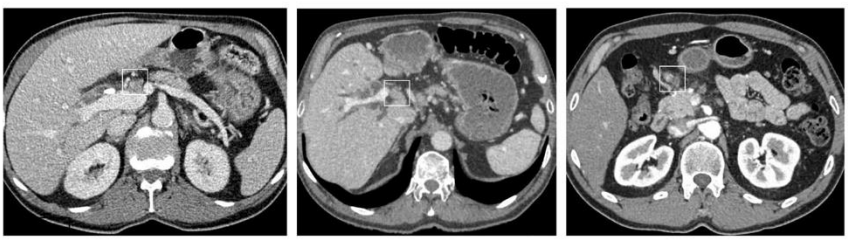

**Fig. 4** CT images of patients with and without lymph node metastases. **a** Patient with enlarged suspicious lymph node adjacent to the portal vein and hepatic artery who had no lymph node metastases on pathology. **b** Patient with enlarged suspicious lymph node adjacent to the hepatic artery who had lymph node metastases on pathology. **c** Patient with multiple suspicious lymph nodes based on size and inhomogeneity who had lymph node metastases on pathology

**Table 2** Sensitivity, specificity, PPV, and Youden's Index for cut-off values and morphological criteria by CT and MRI

| | Sensitivity | Specificity | PPV | Youden's Index |
|---|---|---|---|---|
| **CT** | | | | |
| **Size, cut-off value** | | | | |
| 4 mm | 95.3% | 0% | 70.7% | − 0.05 |
| 5 mm | 95.3% | 0% | 70.7% | − 0.05 |
| 6 mm | 90.7% | 11.7% | 72.2% | − 0.02 |
| 7 mm | 83.7% | 17.6% | 72.0% | 0.01 |
| 8 mm | 67.4% | 41.2% | 74.4% | 0.08 |
| 9 mm | 51.1% | 58.8% | 75.9% | 0.10 |
| 10 mm | **44.2%** | **82.4%** | **86.4%** | **0.27** |
| 11 mm | 34.9% | 88.2% | 88.2% | 0.23 |
| **Morphological criterion** | | | | |
| Lobulated | 62.7% | 52.9% | 77.1% | 0.16 |
| Spiculated | 11.6% | 88.2% | 71.4% | − 0.00 |
| Indistinct | 2.3% | 94.1% | 50.0% | − 0.04 |
| **Inhomogeneous** | **25.6%** | **94.1%** | **91.7%** | **0.20** |
| **MRI** | | | | |
| **Size, cut-off value** | | | | |
| 7 mm | 75.0% | 0% | 60.0% | − 0.25 |
| **8 mm** | **58.3%** | **83.3%** | **87.5%** | **0.42** |
| 9 mm | 58.3% | 66.7% | 77.8% | 0.25 |
| **10 mm** | **58.3%** | **83.3%** | **87.5%** | **0.42** |
| 11 mm | 25.0% | 83.3% | 75.0% | 0.08 |
| 12 mm | 16.7% | 83.3% | 66.7% | 0.00 |
| 13 mm | 16.7% | 83.3% | 66.7% | 0.00 |
| 14 mm | 8.3% | 83.3% | 50.0% | − 0.08 |
| 15 mm | 8.3% | 83.3% | 50.0% | − 0.08 |
| **Morphological criterion** | | | | |
| Lobulated | 16.7% | 66.7% | 50.% | − 0.17 |
| Spiculated | 8.3% | 100% | 35.3% | 0.08 |
| Indistinct | Not visible | | | |
| Inhomogeneous | Not visible | | | |

### Number of visible lymph nodes

There was a significant association between number of visible lymph nodes seen on preoperative CT and histopathological lymph node involvement (pN+, p = 0.031).

Seven or more lymph nodes were seen on preoperative CT in 32.6% (14/43) of patients with lymph node metastases (pN+) and in 5.9% (1/17) of patients without lymph node metastasis (pN-, p = 0.046). This resulted in a specificity of 94.1%, Youden's Index of 0.27, and PPV of 93.3%.

### Combination of number, size, and expanded morphologic criteria on preoperative CT

Combining the size criterion and the morphological criterion with the respective highest Youden's Index (cut-off 10 mm and "inhomogeneous signal intensity") and the criterion "visible lymph nodes n ≥ 7" was significantly associated with nodal metastases (pN+, p = 0.004). For this combined criterion, specificity was 82%, sensitivity 61%, PPV 90%, and Youden's Index 0.43 (95% CI; 0.15, 0.60).

### Interobserver agreement

Interobserver agreement was calculated for 20 patients (pN+, 75% pN+ vs. 25% pN-) for the criteria size, morphology, and number of visible lymph nodes with the respective highest Youden's Index. Interobserver agreement was substantial for size (10 mm cut-off, κ = 0.8, p = 0.001), moderate for the presence of seven or more lymph nodes (κ = 0.571, p = 0.032), and fair for the morphological criterion inhomogeneous signal intensity (κ = 0.306, p = 0.202).

### Magnetic resonance imaging (MRI)

Lymph nodes were detected in 88.9% (16/18) of patients on preoperative MRI. The median number of visible lymph nodes was 3 (range 0–6). There was no significant association between number of visible lymph nodes seen on preoperative MRI and histopathological lymph node involvement (pN+, p = 0.682).

The smallest visible lymph node was 3.0 mm of size, whereas the largest measured 16 mm (short-axis diameter). The mean time between MRI and surgery was 11 days with a median of 7 days (range 1–38).

The cut-off values of the highest diagnostic value were 8 mm or 10 mm for the "size" criterion (sensitivity 58.3%, specificity 83.3%, Youden's Index = 0.42). The presence of a lymph node of these sizes was not associated with lymph node metastases (pN+, p = 0.152). Lobulated and spiculated lymph nodes were only seen in a few patients (n = 4 and n = 1), and indistinct and inhomogeneous lymph nodes were not seen at all (Table 2).

## Discussion

In this retrospective single-center study on lymph node staging by CT in ductal adenocarcinoma of the pancreatic head, we could show that the morphologic criteria "inhomogeneous signal intensity" and "size" are specific for regional nodal metastatic disease. Replacing the size criterion by morphologic criteria, however, did not improve diagnostic accuracy due to sensitivity remaining low. Combining specific criteria yields improved sensitivity with specificity remaining high.

By CT, lymph nodes of 4–9 mm in short-axis diameter were seen just as often in patients with and without

lymph node metastases resulting in poor discrimination. Larger lymph nodes (> 9 mm) had a higher prevalence in the lymph node-positive group leading to high specificity. However, these lymph nodes (10 mm or 11 mm) were seen infrequently resulting in a rather low sensitivity. The maximum value of the Youden's Index for the size criterion of 0.27 was achieved when a cut-off value of 10 mm was applied, consisting of a specificity of 82.4% and sensitivity of 44.2%, yielding a PPV of 84.6%.

As for morphologic criteria, lymph nodes of lobulated border contour were seen in about half of the patients of both groups (pN+, 63% and pN-, 47%), and therefore is a criterion that is not suitable to differentiate between the groups. Lymph nodes of spiculated and indistinct border contour were seen in few cases in both patient groups only (pN+ 11% and 2% versus pN- 12% and 6%) making them poor diagnostic criteria. However, lymph nodes of inhomogeneous signal intensity were visible in 26% of patients with lymph node metastases (pN+) and only in 6% of the patients without lymph node metastases (pN-), resulting in a Youden's Index of 0.20, which was the maximum value for the morphological criteria, and a PPV of 91.7%.

Ideally, a good discriminator for nodal metastases is negative in patients without nodal involvement and positive for tumors with lymph node metastases. In our study, each criterion, i.e., size as well as different morphological features, only met one of these prerequisites. The size criterion (10 mm) as well as the presence of a lymph node of inhomogeneous signal intensity as morphological criterion turned out to be negative in patients without nodal involvement (pN-) and therefore highly specific. Yet, lymph nodes of the respective characteristic were not positive in a sufficiently high number of tumors with lymph node metastases (pN+) to reach high levels of sensitivity and consequently did not have a significant diagnostic value.

The maximum value of the Youden's Index for the size criterion was 0.27 when a cut-off value of 10 mm was applied and 0.20 for the morphological criteria, when the criterion "inhomogeneous signal intensity" was used, showing that morphologic criteria do not yield in higher diagnostic value than lymph node size in adenocarcinoma of the pancreatic head (PDAC) patients. This is contrary to the findings of Brown et al. in rectal cancer [16]. One reason might be that Brown et al. used MRI to assess morphologic criteria which has a higher soft tissue contrast compared to CT which was used in most patients in our study.

Interestingly, we could show that with preoperative CT, the presence of seven or more lymph nodes was seen more often in patients with lymph node metastasis (pN+) than in those without metastasis (pN-, $p = 0.046$). When applying this as a sole criterion (cN) for lymph node metastasis (pN), this led to a sensitivity of 32.6%, a specificity of 94.1%, PPV of 93.3%, and Youden's Index of 0.27.

In diagnostic test analysis, criteria can be combined in mainly two ways: sensitive criteria can be taken together to improve specificity or specific criteria can be accumulated to improve sensitivity. When combining the highly specific criteria size (cut-off value 10 mm), inhomogeneous signal intensity, and number of visible lymph nodes $n \geq 7$, a highly significant association with nodal metastases (pN+, $p = 0.004$) was found. Consequently, the CT examination was considered node-positive (cN+) when at least one of these criteria was met. The application of this criterion improved the sensitivity to 60% with a remaining specificity of 82% and PPV 90% resulting in an also improved Youden's Index of 0.43.

The results of the MRI examinations must be viewed in a rather descriptive manner since the sample size was limited ($n = 18$). Lymph nodes were detected in the majority (88.9%) of examinations generally allowing the evaluation of lymph nodes by MRI as well. Upper abdominal MRI generally has a lower spatial resolution, but a higher soft tissue contrast compared to CT. For the size criterion a cut-off value of 8 mm or 10 mm led to the best diagnostic results (sensitivity 58.3%, specificity 83.3%, Youden's Index = 0.42). Lymph nodes of abnormal morphological criteria were seen in only very few patients (Table 2).

The main limitation of this study is the retrospective study design in which a node-by-node comparison of cross-sectional imaging with histopathology was not possible. This was of minor importance, though, since low sensitivity was the main factor that led to compromised diagnostic performance in our study. We were also able to correlate with postoperative cross-sectional imaging in all cases in which it was unclear whether a lymph node had been resected during surgery or not. Also, in our cohort, only patients who had subsequent surgery were included, presuming lower tumor stage as compared to the average patient who undergoes imaging for presurgical workup.

The strength of our single-center study is reinforced by a defined number of surgeons, a high standardization of the CT technique, and an experienced radiologist who performed the analysis.

The results of our study are consistent with recent and initial data demonstrating that clinical staging, by low sensitivity, underestimates histopathological lymph node involvement (pN+) [6, 20–22]. However, by adding the criterion "inhomogeneous signal intensity" and "number of visible lymph nodes" to the size criterion, we were able to increase the sensitivity to 60% in comparison to previous findings (14%, Roche et al.; 37% Nanashima

et al.; and 46.2%, Cao et al.) with specificity remaining sufficient.

An additional imaging modality that has shown the potential to improve the sensitivity of detecting metastatic disease is positron emission tomography-computed tomography (PET/CT) [23]. However, a beneficial role of PET/CT in locoregional nodal staging could not be established to date. The majority of initial as well as recent studies show very limited sensitivities for nodal status between 10 and 61% [24–29]. The PET-PANC study evaluated the incremental diagnostic accuracy and impact of PET/CT in addition to multidetector CT in patients with suspected pancreatic cancer in a prospective multicenter study that included 550 patients. In this study, significantly more patients with stage IIb disease (pN+) were correctly staged by PET/CT than by multidetector CT ($p = 0.002$), but this only led to a moderate sensitivity of 38% for PET/CT versus 22% for multidetector CT [30].

Endoscopic ultrasonography (EUS) is a well-established diagnostic procedure in pancreatic cancer with the benefit of a dynamic diagnostic examination that allows fine-needle aspiration for cytologic diagnosis. Two meta-analyses evaluating diagnostic accuracy of EUS for locoregional nodal staging the pooled sensitivities and specificities were 0.62 and 0.74 (Li et al 2014, 14 studies, n = 516 patients) [31] and 69% and 81% (Nawaz et al., 16 studies, n = 512 patients) [32]. Advanced techniques such as contrast-enhanced EUS (CH-EUS) and EUS elastography are currently in evaluation [33].

To date, CT remains the standard staging imaging modality recommended by NCCN guidelines for locoregional staging of pancreatic cancer [34]. Neither PET/CT nor EUS yields reliable diagnostic accuracy for nodal staging.

An advantageous effect on resectability and overall survival (OS) in unresectable cases (including both borderline resectable and unresectable) of PDAC by multimodality therapy including neoadjuvant therapy has already been described in several studies [35].

The benefit of neoadjuvant therapy in cases of primarily resectable disease at diagnosis is yet less revealed. Several phase II trials showed that patients who completed neoadjuvant chemoradiation without progressive disease at restaging had a higher chance of achieving R0 resection and, consequently, higher median and OS when compared to historical data [36]. As seen in other tumor entities, a potential benefit of neoadjuvant therapy on the basis of positive nodal status (cN+) is strongly implied. Cao et al. found that the 38% of patients that were successfully downstaged from node-positive disease (cN1) to node-negative disease (ypN0) by neoadjuvant therapy benefit in terms of higher rates of 5-year survival (ypN0 27.2% vs ypN1 12.3%, $p < 0.001$) [8]. This is consistent with the findings of Portuondo et al. (5-year survival ypN0 12.4% vs. ypN1 6.0%, $p < 0.0001$) [37]. The NCCN guidelines for pancreatic adenocarcinoma appreciates these results by stating that consideration can be given to neoadjuvant therapy for selected patients with resectable tumor but poor prognostic features such as large regional lymph nodes, markedly elevated CA 19-9, large primary tumors, extreme pain, and excessive weight loss [34]. Further clarification on this matter is expected to come from the ongoing NEONAX trial (NCT02047513), a phase II study comparing neoadjuvant plus adjuvant with only adjuvant nab-paclitaxel plus gemcitabine therapy for resectable pancreatic cancer. The ongoing phase III NEOPA trial (NCT01900327) compares neoadjuvant chemoradiotherapy with upfront surgery of resectable pancreatic head cancer. A subgroup analysis in terms of nodal status would present reliable data.

Given the suggested benefit of neoadjuvant therapy based on lymph node staging, there is an urgent need to find criteria and modalities to further improve the diagnostic value of lymph node staging by pretherapeutic cross-sectional imaging in patients with ductal adenocarcinoma of the pancreatic head. To date, none of the existing modalities and criteria accomplishes reliable nodal staging. Larger, prospective studies are ongoing and necessary to get a more precise idea of the prognostic advantage of neoadjuvant therapy in patients with regional lymph node metastasis (cN+) of PDAC in pretherapeutic staging.

## Conclusions

Lymph node staging in PDAC patients when using CT morphological criteria such as border contour or homogeneity compared to diameter cut-off values does not lead to reliable diagnostic value. Diagnostic accuracy is limited due to low sensitivity for detection of metastatic disease. Combining specific criteria yields improved sensitivity with specificity and PPV remaining high. These results suggest an attentive interpretation of the results of pretherapeutic lymph node staging, particularly in cases in which lymph node metastases are absent.

### Abbreviations

PDAC: Adenocarcinoma of the pancreatic head; CT: Computed tomography; MRI: Magnetic resonance imaging; pN+: Histopathologically involved lymph nodes; pN-: Histopathologically no involved lymph nodes; cN+: Clinically involved lymph nodes; cN-: Clinically no involved lymph nodes; PPV: Positive predictive value; PET/CT: Positron emission tomography-computed tomography; EUS: Endoscopic ultrasonography; CH-EUS: Contrast-enhanced endoscopic ultrasonography; OS: overall survival

### Acknowledgements

We acknowledge support from the German Research Foundation (DFG) and the Open Access Publication Funds of Charité – Universitätsmedizin Berlin.

### Authors' contributions

All authors were involved in data acquisition and manuscript revision. The conception of the design of the study and drafting of the manuscript was

done by FN Loch, C Kamphues, and P Asbach. Image analysis was performed by P Asbach and assisted by FN Loch. Image analysis of the subgroup for analysis of interobserver agreement was performed by M Haas. All authors have approved the submitted version of the manuscript and account for their own contribution and the accuracy as well as the integrity of the work presented.

**Funding**
The study was not funded.

**Availability of data and materials**
The datasets used during the current study are available from the corresponding author on reasonable request.

**Ethics approval and consent to participate**
The study was approved by the local ethics committee of the Charité, University Medicine Berlin. Informed consent of participation was waived by the IRB given the retrospective study design (IRB No. EA4/114/18).

**Consent for publication**
Consent for publication is not applicable for this study.

**Competing interests**
The authors declare that they have no competing interests.

**Author details**
[1]Charité – Universitätsmedizin Berlin, corporate member of Freie Universität Berlin, Humboldt-Universität zu Berlin, and Berlin Institute of Health, Department of Surgery, Campus Benjamin Franklin, Hindenburgdamm 30, 12203 Berlin, Germany. [2]Charité – Universitätsmedizin Berlin, corporate member of Freie Universität Berlin, Humboldt-Universität zu Berlin, and Berlin Institute of Health, Department of Radiology, Campus Benjamin Franklin, Hindenburgdamm 30, 12203 Berlin, Germany. [3]The Johns Hopkins University School of Medicine, Department of Surgery, 600 N. Wolfe Street, Blalock 688, Baltimore, MD 21287, USA.

Received: 12 December 2019 Accepted: 7 July 2020
Published online: 18 August 2020

**References**

1. Pietryga JA, Morgan DE. Imaging preoperatively for pancreatic adenocarcinoma. J Gastrointest Oncol. 2015;6:343–57.
2. Howlader N, Noone AM, Krapcho M, Garshell J, Miller D, Altekruse SF et al. SEER Cancer Statistics Review, 1975-2012, National Cancer Institute. Bethesda, MD, https://seer.cancer.gov/archive/csr/1975_2012/, based on November 2014 SEER data submission, posted to the SEER web site, April 2015. Section 22, page 8.
3. Du T, Bill KA, Ford J, Barawi M, Hayward RD, Alame A, et al. The diagnosis and staging of pancreatic cancer: A comparison of endoscopic ultrasound and computed tomography with pancreas protocol. Am J Surg. 2018;215:472–5.
4. Zhang Q, Zeng L, Chen Y, Lian G, Qian C, Chen S, et al. Pancreatic cancer epidemiology, detection, and management. Gastroenterol Res Pract. 2016;2016:1–10.
5. Yeo CJ, Cameron JL, Lillemoe KD, Sitzmann JV, Hruban RH, Goodman SN, et al. Pancreaticoduodenectomy for cancer of the head of the pancreas. 201 patients. Ann Surg. 1995;221:721–33.
6. Asano T, Hirano S, Nakamura T, Okamura K, Tsuchikawa T, Noji T, et al. Survival benefit of conversion surgery for patients with initially unresectable pancreatic cancer who responded favorably to nonsurgical treatment. J Hepato-Biliary-Pancreat Sci. 2018;25:342–50.
7. Endo Y, Kitago M, Aiura K, Shinoda M, Yagi H, Kitagawa Y, et al. Efficacy and safety of preoperative 5-fluorouracil, cisplatin, and mitomycin C in combination with radiotherapy in patients with resectable and borderline resectable pancreatic cancer: a long-term follow-up study. World J Surg Onc. 2019;17:145–152 27.
8. Cao HST, Zhang Q, Sada YH, Silberfein EJ, Hsu C, Van Buren G, et al. Value of lymph node positivity in treatment planning for early stage pancreatic cancer. Surgery. 2017;162:557–67.
9. Zeman RK, Cooper C, Zeiberg AS, Kladakis A, Silverman PM, Marshall JL, et al. TNM staging of pancreatic carcinoma using helical CT. Am J Roentgenol. 1997;169:459–64.
10. Müller MF, Meyenberger C, Bertschinger P, Schaer R, Marincek B. Pancreatic tumors: evaluation with endoscopic US, CT, and MR imaging. Radiology. 1994;190:745–51.
11. Midwinter MJ, Beveridge CJ, Wilsdon JB, Bennett MK, Baudouin CJ, Charnley RM. Correlation between spiral computed tomography, endoscopic ultrasonography and findings at operation in pancreatic and ampullary tumours. Br J Surg. 1999;86:189–93.
12. Rösch T, Braig C, Gain T, Feuerbach S, Siewert JR, Schusdziarra V, et al. Staging of pancreatic and ampullary carcinoma by endoscopic ultrasonography: Comparison with conventional sonography, computed tomography, and angiography. Gastroenterology. 1992;102:188–99.
13. Prenzel KL, Hölscher AH, Vallböhmer D, Drebber U, Gutschow CA, Mönig SP, et al. Lymph node size and metastatic infiltration in adenocarcinoma of the pancreatic head. Eur J Surg Oncol. 2010;36:993–6.
14. Rollvén E, Blomqvist L, Öistämö E, Hjern F, Csanaky G, Abraham-Nordling M. Morphological predictors for lymph node metastases on computed tomography in colon cancer. Abdom Radiol. 2019;44:1712–21.
15. Brown G, Richards CJ, Bourne MW, Newcombe RG, Radcliffe AG, Dallimore NS, et al. Morphologic predictors of lymph node status in rectal cancer with use of high-spatial-resolution MR imaging with histopathologic comparison. Radiology. 2003;227:371–7.
16. Kim JH, Beets GL, Kim MJ, Kessels AGH, Beets-Tan RGH. High-resolution MR imaging for nodal staging in rectal cancer: are there any criteria in addition to the size? Eur J Radiol. 2004;52:78–83.
17. Isaji S, Murata Y, Kishiwada M. New Japanese classification of pancreatic cancer. In: Neoptolemos J, Urrutia R, Abbruzzese J, Büchler MW, editors. Pancreatic Cancer. New York: Springer; 2017. p. 1–17.
18. Brierley JD, Gospodarowicz MK, Wittekind C. UICC: TNM Classification of Malignant Tumours. 8th ed. Oxford: Wiley-Blackwell; 2017. p. 93–6.
19. Youden WJ. Index for rating diagnostic tests. Cancer. 1950;3:32–5.
20. Swords DS, Firpo MA, Johnson KM, Boucher KM, Scaife CL, Mulvihill SJ. Implications of inaccurate clinical nodal staging in pancreatic adenocarcinoma. Surgery. 2017;162:104-111. 28.
21. Nanashima A, Sakamoto I, Hayashi T, Tobinaga S, Araki M, Kunizaki M, et al. Preoperative diagnosis of lymph node metastasis in biliary and pancreatic carcinomas: Evaluation of the combination of multi-detector CT and serum CA19-9 level. Dig Dis Sci. 2010;55:3617–26.
22. Roche CJ, Hughes ML, Garvey CJ, Campbell F, White DA, Jones L, et al. CT and pathologic assessment of prospective nodal staging in patients with ductal adenocarcinoma of the head of the pancreas. AJR Am J Roentgenol. 2003;180:475–80.
23. Farma JM, Santillan AA, Melis M, Walters J, Belinc D, Chen DT, et al. PET/CT fusion scan enhances CT staging in patients with pancreatic neoplasms. Ann Surg Oncol. 2008;15:2465–71.
24. Kauhanen SP, Komar G, Seppänen MP, Dean KI, Minn HR, Kajander SA, et al. A prospective diagnostic accuracy study of 18F-fluorodeoxyglucose positron emission tomography/computed tomography, multidetector row computed tomography, and magnetic resonance imaging in primary diagnosis and staging of pancreatic cancer. Ann Surg. 2009;250:957–63.
25. Lemke AJ, Niehues SM, Hosten N, Amthauer H, Boehmig M, Stroszczynski C, et al. Retrospective digital image fusion of multidetector CT and 18F-FDG PET: clinical value in pancreatic lesions—a prospective study with 104 patients. J Nucl Med. 2004;45:1279–86.
26. Heinrich S, Goerres GW, Schäfer M, Sagmeister M, Bauerfeind P, Pestalozzi BC, et al. Positron emission tomography/computed tomography influences on the management of resectable pancreatic cancer and its cost-effectiveness. Ann Surg. 2005;242:235.
27. Joo I, Lee JM, Lee DH, Lee ES, Paeng JC, Lee SJ, et al. Preoperative assessment of pancreatic cancer with FDG PET/MR imaging versus FDG PET/CT plus contrast-enhanced multidetector CT: a prospective preliminary study. Radiology. 2017;282:149–59.
28. Asagi A, Ohta K, Nasu J, Tanada M, Nadano S, Nishimura R, et al. Utility of contrast-enhanced FDG-PET/CT in the clinical management of pancreatic cancer: impact on diagnosis, staging, evaluation of treatment response, and detection of recurrence. Pancreas. 2013;42:11–9.
29. Kim HR, Seo M, Nah YW, Park HW, Park SH. Clinical impact of fluorine-18-fluorodeoxyglucose positron emission tomography/computed tomography

in patients with resectable pancreatic cancer: diagnosing lymph node metastasis and predicting survival. Nucl Med Commun. 2018;39(7):691–8.
30. Ghaneh P, Hanson R, Titman A, Lancaster G, Plumpton C, Lloyd-Williams H, et al. PET-PANC: multicentre prospective diagnostic accuracy and health economic analysis study of the impact of combined modality 18fluorine-2-fluoro-2-deoxy-d-glucose positron emission tomography with computed tomography scanning in the diagnosis and management of pancreatic cancer. Health Technol Assess. 2018;22:1–114.
31. Li JH, He R, Li YM, Cao G, Ma QY, Yang WB. Endoscopic ultrasonography for tumor node staging and vascular invasion in pancreatic cancer: a meta-analysis. Digest Surg. 2014;31:297–305.
32. Nawaz H, Yi-Fan C, Kloke J, Khalid A, McGrath K, Landsittel D, et al. Performance characteristics of endoscopic ultrasound in the staging of pancreatic cancer: a meta-analysis. JOP. 2013;14:484.
33. Kitano M, Yoshida T, Itonaga M, Tamura T, Hatamaru K, Yamashita Y. (2019). Impact of endoscopic ultrasonography on diagnosis of pancreatic cancer. J Gastroenterol. 2019;54:19–32.
34. Network NCC. NCCN guidelines version 1.2020. Pancreatic Adenocarcinoma. https://www.nccn.org/professionals/physician_gls/pdf/pancreatic.pdf.
35. Laurence JM, Tran PD, Morarji K, Eslick GD, Lam VWT, Sandroussi C. A systematic review and meta-analysis of survival and surgical outcomes following neoadjuvant chemoradiotherapy for pancreatic cancer. J Gastrointest Surg. 2011;15:2059–69.
36. Lim KH, Chung E, Khan A, Cao D, Linehan D, Ben-Josef E, et al. Neoadjuvant therapy of pancreatic cancer: the emerging paradigm? Oncologist. 2012;17:192–200.
37. Portuondo JI, Massarweh NN, Zhang Q, Chai CY, Cao HST. Nodal downstaging as a treatment goal for node-positive pancreatic cancer. Surgery. 2019;165:1144–50.

## Publisher's Note

## 3. Diskussion

Ziel der in dieser Schrift präsentierten Originalarbeiten war es Merkmale prognostischer Heterogenität herauszuarbeiten sowie ihre Identifikation zu Präzisieren und so die prognostische Risikostratifikation der Gruppe der Patient:innen mit einem resektablen exokrinen Pankreaskarzinom weiterzuentwickeln. Hierbei wurden perioperative Möglichkeiten der prognostischen Risikostratifikation untersucht: Die **Originalarbeit 1 und 2** beschäftigten sich mit der Identifikation von Proteinen prognostischer Relevanz, die von Tumorzellen resektabler exokriner Pankreaskarzinome exprimiert werden. Die **Originalarbeit 3 und 4** beschäftigten sich mit den aus der postoperativen pathologischen Aufarbeitung von Operationsresektaten hervorgehenden prognostischen Merkmalen der operativen Resektionsränder sowie des Mechanismus der Lymphknoteninvasion. Inhalt der **Originalarbeit 5** war die Evaluation und Erweiterung von präoperativen Bildgebungskriterien des etablierten prognostischen Risikofaktors der regionalen Lymphknotenmetastasierung.

Die in malignen Tumoren vorhandenen Änderungen bzw. Mutationen des Zellgenoms führen zu Veränderung der Expression von Proteinen in Tumorzellen.[55] Frühe Analysen zum prognostischen Einfluss dieser Veränderungen existieren bereits seit Jahrzehnten.[56, 57] Ein fest etabliertes Beispiel für eine suffiziente prognostische Risikostratifikation von Tumoren anhand der Analyse der Proteinexpression ist die Quantifizierung der Expression von Ki-67 in Tumorzellen neuroendokriner Tumore. Als prognostischer Gewebemarker hat Ki-67 einen größeren Einfluss auf das Gesamtüberleben bei Patient:innen mit neuroendokrinen Tumoren des Pankreas als das Tumorstadium, ist wesentlicher Bestandteil der prognostischen Risikostratifikation und hierbei eine wesentliche Grundlage für Therapieentscheidungen.[8, 58] Für das resektable exokrine Pankreaskarzinom bedarf es aktuell an etablierten Gewebemarkern, die eine solche zuverlässige prognostische Risikostratifikation zulassen.

Die Gesamtgenomsequenzierung exokriner Pankreaskarzinome hat regelmäßige Alterationen der zu den Proteinen K-Ras, p16, p53 und SMAD4 korrespondieren Gene festgestellt.[59] Die Veränderungen von K-Ras sind hierbei vor allem funktioneller Natur und kommen in nahezu allen exokrinen Pankreaskarzinomen vor, weswegen quantitative Expressionsanalysen des Proteins zur prognostischen Risikostratifikation keine wesentliche Aufmerksamkeit zukommt.[60, 61] Die Änderungen in den zu p16, p53 und SMAD4 korrespondieren Genen führen durchaus zu einer ausgelöschten bzw. aberranten Expression der jeweiligen Proteine.[62] Die

Analyse des Einflusses der Expression von p16, p53 und SMAD4 auf die Prognose von Patient:innen mit exokrinen Pankreaskarzinomen hinterlässt eine aktuell ambivalente Studienlage, aus der heraus für SMAD4 einige Hinweise für eine prognostische Relevanz bestehen und für p53 eine Tendenz zu einem ausbleibenden Einfluss.[62, 63, 64, 65, 66, 67, 68]

Darüber hinaus existierende Untersuchungen analysieren den prognostischen Einfluss einer Vielzahl von durch exokrine Pankreaskarzinome exprimierte Proteinen, die beteiligt sind an der gesteigerten Reproduktionsrate, Apoptoseresistenz, Tumorinvasion und -metastasierung, ausdauernden Angiogenese, Immunevasion und dem Chemotherapiemetabolismus der Tumore.[24] Hierbei arbeiten existierende Metaanalysen den potentiellen prognostischen Wert der Expression weiterer Proteine wie BAX, Bcl-2, E-Cadherin, Ki-67, p27 und CD34 für das exokrine Pankreaskarzinom heraus. Aus dieser gegenwärtigen Studienlage heraus konnte sich bis dato trotz der gegebenen Notwendigkeit für das resektable exokrine Pankreaskarzinom kein Gewebemarker zur zuverlässigen prognostischen Risikostratifikation heraus etablieren.[9, 69] Die **Originalarbeiten 1 und 2** erweitern diese hierzu existierenden Studienlage. Hierbei konnten durch die **Originalarbeit 1** als auch **Originalarbeit 2** Proteine identifiziert werden mit prognostischen Implikationen. In der **Originalarbeit 1** war das vermehrte Vorhandensein von Kollagen-Typ 2α1, Kollagen-Typ 6α3, Aktin (zytoplasmatisch-1), Valosin-haltigem Protein, Filamin B, Histon H1.3, Spektrin beta (nicht-erythrozytär 1) und Vinculin mit einer Lymphgefäßinvasion (pL+) assoziiert. Das vermehrte Vorhandensein von Kollagen-Typ 2α1 und Myosin-11 war mit einer Gefäßinvasion assoziiert (pV+) und eine niedrigere Intensität von Histon H1.3 mit einer regionalen Lymphknotenmetastasierung (pN+). In der **Originalarbeit 2** wurde die prognostische Bedeutung von Proteinen untersucht, die zu der Gruppe der Immuncheckpoints gehören. Für TIM3, IDO, B7H4 und LAG3 zeigte sich hier kein Einfluss auf das Gesamtüberleben ($p>0.05$). Für sowohl VISTA als auch PD-L1 zeigte sich ein negativer Einfluss auf das Gesamtüberleben ($p<0.05$). Die relative 5-Jahres-Überlebensraten in Abwesenheit von VISTA und PD-L1 war 27%, bei Vorhandensein einer der beiden Immuncheckpoints 13-15% und bei Vorhandensein beider Marker betrug die relative Überlebensrate bereits nach drei Jahren 0%.

Eine bevorzugte Methode für die Untersuchung des prognostischen Einfluss von durch exokrine Pankreaskarzinome exprimierte Proteinen ist die konventionelle Immunhistochemie.[62, 63, 64, 65, 66, 67, 68] Trotz des breiten Einsatzes und Nutzen dieser Methode ist eine Einschränkung, dass die konventionelle Immunhistochemie die Expression einzelner zuvor ausgewählter Proteine untersucht und somit einen eingeschränkt explorativen Analyseansatz darstellt.[70] In der **Originalarbeit 2** fand sie Anwendung, da hier die prognostische Bedeutung der Expression

konkreter Proteine von Tumorzellen exokriner Pankreaskarzinome untersucht werden sollte, die durch bereits existierende Arbeiten mechanistisch mit einer potentiellen Immunevasion von Tumoren und somit einer potentiellen prognostischen Bedeutung in Zusammenhang gebracht wurden.[71] Das in der **Originalarbeit 1** zur Proteinanalyse angewandte Verfahren war MALDI-MSI. In der Proteinexpressionsanalyse hat dieses explorative Verfahren den Vorteil, dass keine a priori Kenntnis der untersuchten Proteine notwendig ist, weil das Verfahren Proteine identifiziert und quantifiziert.[72] Da das Verfahren an mit Formalin-fixiertem Paraffin-eingebettetem Gewebe erfolgen kann, ist auch keine gesonderte Gewebefixierung außerhalb der klinischen Routine notwendig und die retrospektive Analyse vom im klinischen Alltag herkömmlich fixiertem Gewebe bzw. von TMAs möglich.[44] Neben anderen massenspektrometrischen und elektrophoretischen Methoden oder Protein-Micoarrays als explorative Verfahren der Proteinanalyse hat MALDI-MSI den Vorteil, dass die Analyse direkt auf dem Gewebe erfolgt.[73] Hierdurch bleibt die Integrität des Gewebes durch das Analyseverfahren erhalten und es ist eine räumliche Auflösung der Proteinanalysen sowie der direkte Vergleich mit HE-Färbungen analysierter Areale möglich (siehe auch Abbildung 1 in 1.4.3). Die Proteinanalysen können somit zusätzlich zu klinischen Parametern, wie in der **Originalarbeit 1,** unmittelbar mit histopathologischen Eigenschaften des untersuchten Gewebes korreliert werden.[44] Die **Originalarbeit 1** stellt eine Machbarkeitsstudie der Anwendung dieses innovativen, explorativen Verfahrens dar für die Analyse von Formalin-fixiertem Paraffin-eingebettetem Tumorgewebe von Patient:innen mit exokrinen Pankreaskarzinomen. In Bezug auf zukünftige Untersuchungen sollte die Kombination solch explorativer Untersuchungsverfahren und gezielter Validierungsverfahren Anwendung finden. Hochwertige explorative Längsschnttstudien, die ausreichend große Kollektive an Patient:innen einschließen, könnten Ergebnisse liefern, die strukturiert an Subgruppen validiert werden können.

Bei der postoperativen pathologischen Aufarbeitung von Operationsresektaten resezierter exokriner Pankreaskarzinome steht zunächst die Feststellung des pathologischen TNM-Stadiums im Mittelpunkt. Diese Parameter haben einen stark etablierten, gesicherten prognostischen Einfluss bei Patient:innen mit einem exokrinem Pankreaskarzinom.[9, 74] Das sich hieraus zusammensetzende UICC-Stadium (Union for International Cancer Control) ist nach kurativ intendierter Tumorresektion der wichtigste prognostische Faktor betroffener Patient:innen.[9] So beträgt das relative 5-Jahres-Überleben im UICC-Stadium 67-71%, im Stadium II 40-52%, im Stadium III 18-20% und im Stadium IV (3-5%).[2] Dass die TNM-Klassifikation einen solchen

prognostischen Wert hat ist kein Zufall, sondern ein dezidiertes Ziel der Einteilung: Die jeweilige Stadieneinteilung soll Subgruppen anhand ihrer Prognose stratifizieren. Die wesentliche Grundlage hierfür ist das anatomische Ausmaß der Erkrankung. Auf der Basis von Erkenntnissen neuer Prognosedaten hierzu erschien 2017 die aktualisierte 8. Auflage der TNM-Klassifikation.[75] So erfolgt die Einteilung der Stadien T1-T3 seither auf der Grundlage der Tumorgröße unabhängig von einer Invasion peripankreatischen Gewebes. Die N-Klassifikation geht über die Stadien N0 und N1 hinaus und wird differenzierter eingeteilt anhand der Anzahl betroffener Lymphknoten in N0 (kein regionaler Lymphknotenbefall), N1 (1-3 befallene regionale Lymphknoten) und N2 (≥4 befallene regionale Lymphknoten).[75] Validierungsstudien bestätigen, dass diese neuen Klassifikationskriterien zu einer präziseren prognostischen Stratifikation von Subgruppen nach Resektion exokriner Pankreaskarzinome geführt haben im Vergleich zu ihren Vorgängern.[76] Auch in Zukunft sollten die in die TNM-Klassifikation einfließenden Aspekte weiter differenziert und präzisiert werden, um ihr Ziel einer exakten prognostischen Stratifikation zu erreichen und weiterzuentwickeln.

Um die prognostischen Bedeutung einer Beteiligung regionaler Lymphknoten (N-Stadium) durch Tumore weiter zu differenzieren und zu präzisieren, erfolgte in der **Originalarbeit 4** die systematische Analyse des Einflusses des Mechanismus der Lymphknoteninvasion auf das Gesamtüberleben von Patient:innen nach Resektion exokriner Pankreaskarzinome. Hierbei wurden der Mechanismus der direkten Lymphknoteninvasion per continuitatem durch den Tumor (Nc), das Vorhandensein von Lymphknotenmetastasen ohne Tumorkontakt (Nm) sowie das Vorhandensein beider Formen der Lymphknoteninvasion gleichzeitig (Ncm) untersucht. Sowohl Patient:innen mit Lymphknotenmetastasen ohne Tumorkontakt (Nm) als auch Patient:innen mit beiden Formen der Lymphknoteninvasion gleichzeitig (Ncm) zeigten ein signifikant kürzeres Gesamtüberleben verglichen mit Patient:innen ohne Lymphknotenbefall (N0, $p \leq 0.05$). Dieses Ergebnis entspricht den Resultaten konventioneller Analysen in Bezug auf den prognostischen Einfluss regionaler Lymphknotenmetastasierung, die diese als prognostischen Risikofaktor etabliert haben.[22, 30] Zwischen Patient:innen mit ausschließlichem Befall von Lymphknoten durch Lymphknoteninvasion per continuitatem durch den Tumor (Nc) und Patient:innen ohne Lymphknotenmetastasen (N0) hingegen bestand kein Unterschied im Gesamtüberleben in der **Originalarbeit 4** ($p > 0.05$). Anhand dieser Ergebnisse der **Originalarbeit 4** entspricht ein Lymphknotenbefall, der isoliert durch eine Lymphknoteninvasion per continuitatem durch den Tumor (Nc) erfolgt, nicht dem etablierten prognostischen Risikofaktor einer regionalen Lymphknotenmetastasierung. Vergleichbare Studien bestärken das Ergebnis, dass das Gesamtüberleben von Patient:innen mit einer isolierten per continuitatem Invasion von Lymphknoten

dem von Patient:innen ohne Lymphknotenmetastasen (N0) entspricht nach Resektion exokriner Pankreaskarzinome.[77, 78, 79] Dies ist ein Aspekt, der von der gegenwärtig aktuellen 8. Auflage der TNM-Klassifikation nicht erfasst wird und zukünftig Beachtung finden sollte.

Auch die Beteiligung der chirurgischen Resektionsränder am Operationsresektat gilt als gesicherter prognostischer Parameter und wurde als solcher in Form der R-Klassifikation (R0, R1, R2) bereits in 1980er Jahren in die TNM-Klassifikation maligner Tumoren aufgenommen.[9, 74, 80, 81] Hierbei wurde anfänglich universell R0 als kein Tumorresiduum, R1 als DMI eines Resektionsrandes und R2 als makroskopisches Tumorresiduum definiert.[81] Im Verlauf hat sich für andere gastrointestinale Tumorentitäten gezeigt, dass ein mikroskopisches Tumorresiduum im Abstand von ≤ 1 mm ebenfalls eine prognostische Relevanz. So gilt für das Rektumkarzinom eine Tumor nur noch als R0 reseziert, wenn der Abstand > 1 mm zum zirkumferentiellen Resektionsrand beträgt.[82] Für das exokrine Pankreaskarzinom ist die Bedeutung eines mikroskopischen Tumorzellnachweißes über eine DMI hinaus sowie der potentielle Einfluss der Lokalisation noch nicht abschließend geklärt.[9, 21, 28, 82] Die **Originalarbeit 3** soll hierzu einen Beitrag leisten. Auch in der **Originalarbeit 3** hatte das klassische R1-Kriterium der DMI eines Resektionsrandes einen negativen Einfluss auf Gesamtüberleben nach erfolgreicher Tumorresektion (p=0.02). Der Fokus der Arbeit über den etablierten Risikofaktor der DMI hinaus war, den prognostische Einfluss von Tumorzellen im Abstand von ≤ 1 mm von Resektionsrändern zu untersuchen und ob prognostische Unterschiede in Bezug auf die Lokalisation der Resektionsrandbeteiligung durch den Tumor bestehen. Das Vorhandensein von Tumorzellen im Abstand von ≤ 1 mm eines Resektionsrandes zeigte eine Tendenz für einen negativen Einfluss auf Gesamtüberleben (p=0.09). In der individuellen Analyse der einzelnen untersuchten Resektionsränder zeigte sich in der **Originalarbeit 3** ein signifikant negativer Einfluss auf das Gesamtüberleben für die Pankreasabsetzungsebene, sowohl für eine DMI als auch das Vorhandensein von Tumorzellen im Abstand von ≤ 1 mm des Resektionsrandes (p≤0.05). Dieser signifikante prognostische Effekt auf das Gesamtüberleben blieb für die individuelle Analyse der übrigen untersuchten Resektionsränder aus.

Die **Originalarbeiten 3 und 4** fügen so Merkmalen, die aus der postoperativen pathologischen Aufarbeitung von Operationsresektaten hervorgehen, wertvolle Informationen hinzu und leisten einen Beitrag zu einer potentiellen Erweiterung der aktuellen TNM-Klassifikation. Über das TNM-Stadium und die R-Klassifikation hinaus wurde auch das histologische Tumorgrading (G1-4) aufgrund seiner prognostischen Bedeutung der 7. Auflage der TNM-Klassifikation hinzugefügt und ist nun fester Bestandteil der postoperativen pathologischen Aufarbeitung von

Operationsresektaten exokriner Pankreaskarzinome.[9, 83,84] Zudem sollten auch eine Blutgefäßinvasion, eine Lymphgefäßinvasion und eine Perineuralscheideninfiltration Bestandteil der Aufarbeitung sein. Für diese Parameter gibt es Hinweise auf eine negative prognostische Bedeutung, die weitere Validierung finden sollten.[9, 85, 86, 87]

Die Hauptsäule der prätherapeutischen Risikostratifikation exokriner Pankreaskarzinome bildet aktuell das Staging in Form der radiologischen Ausbreitungssdiagnostik von Tumoren, wofür zunächst die CT das etablierteste Verfahren ist.[12, 32] Bei diesem Staging sind die wesentlichsten initial zu beurteilenden Aspekte, ob Fernmetastasen vorliegen und der Tumor anatomisch primär resektabel, borderline resektabel oder lokal fortgeschritten (anatomisch nicht resektabel) ist (siehe auch Kapitel 1.3). Bei resektablen exokrinen Pankreaskarzinomen sollte noch eine Leber-MRT mit Diffusionswichtung zum Ausschluss von Lebermetastasen erfolgen.[9] Die häufigsten Lokalisationen von Metastasen exokriner Pankreaskarzinome ist die Leber.[88] Für das Erkennen von Lebermetastasen liegen Sensitivität und Spezifität der CT bei 75% und 94% und für die MRT bei 85% und 98%.[89] Für die Einordnung der Resektabilität exokriner Pankreaskarzinome ist für die CT eine Sensitivität von bis zu 88% und Spezifität bis zu 86% beschrieben.[90] Ergibt die Ausbreitungsdiagnostik ein resektables exokrine Pankreas ohne Fernmetastasierung ist die Beurteilung des prognostischen Risikofaktors der regionalen Lymphknotenmetastasierung von besonderem Wert, da es aktuell das einzige bildmorphologische Kriterium ist, das eine Grundlage für die Indikation einer neoadjuvanten Therapie eines primär resektablen Pankreaskarzinoms darstellt. Aufgrund der niedrigen diagnostischen Genauigkeit der CT mit einer Sensitivität von 17-37% ist hierfür jedoch aktuell der Nachweis von einer regionalen Lymphknotenmetastasierung durch eine zusätzliche diagnostische Modalität in Form einer PET-CT oder Biopsie gefordert.[9, 20, 32, 33] Der bildmorphologische Aspekt der regionalen Lymphknotenmetatasierung zur prognostischen Risikostratifikation primär resektabler exokriner Pankreaskarzinome mit seiner unmittelbaren potentiellen therapeutischen Bedeutung ist somit in dem etablierten lokoregionären Staging mittels CT deutlich verbesserungswürdig.

Aus diesem Grund wurde in der **Originalarbeit 5** die diagnostische Genauigkeit der präoperativen Beurteilung regionaler Lymphknoten resektabler exokriner Pankreaskopfkarzinome mittels CT evaluiert. Zudem wurden erweiterte Kriterien untersucht mit dem Ziel das lokoregionäre Lymphknotenstaging mittels CT zu verbessern. Zunächst wurde hierbei die diagnostische Genauigkeit des herkömmlichen Kriteriums Größe von Lymphknoten (kurzer Achsendurch-

messer) berechnet. Dann wurden zusätzlich zum Größenkriterium die morphologischen Kriterien Lymphknotenkontur und –homogenität untersucht. Durch die Einführung dieser morphologischen Kriterien in der präoperativen Beurteilung von Lymphknoten wurde für das Rektumkarzinom eine deutliche Verbesserung der diagnostischen Genauigkeit der MRT beschrieben.[91] In der **Originalarbeit 5** zeigte sich eine Sensitivität, Spezifität und ein Youden-Index für das Kriterium Größe (≥10 mm kurzer Achsendurchmesser) von 44%, 82% und 0,27 und für das morphologischen Kriterium mit dem höchsten Youden-Index, inhomogene Signalintensität, 26%, 94% und 0,20. Eine spikulierte Lymphknotenkontur war ein zwar spezifisches Kriterium (88%) mit jedoch niedriger Sensitivität (12%, Youden-Index 0,00). Durch die Kombination der Kriterien Größe (≥10 mm kurzer Achsendurchmesser), inhomogene Signalintensität und eine Anzahl sichtbarer Lymphknoten ≥ 7 konnte die diagnostische Genauigkeit durch eine Erhöhung der Sensitivität etwas verbessert werden mit einer Sensitivität, Spezifität und einem Youden-Index von 61%, 82% und 0.43.

Der durchschnittliche kurze Achsendurchmesser metastatischer Lymphknoten beträgt 4,3 mm – ein weiterer deutlicher Hinweis darauf, dass das alleinige Kriterium Größe im präoperativen Lymphknotenstaging deutliche Einschränkungen aufweist.[92] Der Nutzen von Kombinationskriterien zeigt sich auch in dem Aufkommen strukturierter Befundungssysteme mit der Bildung eines Punktewertes für jeden einzelnen Lymphknoten, der durch die Kriterien Größe sowie morphologische Kriterien gebildet wird.[93] Auch der Einsatz von Radiomics wird aktuell untersucht.[35] Berichtete Sensitivitäten des Lymphknotenstaging von Pankreaskarzinomen in der PET-CT sind ebenfalls eingeschränkt mit 21-61%.[94, 95] Es sollte Inhalt zukünftiger Studien sein, das lokoregionäre Lymphknotenstaging exokriner Pankreaskarzinome systematisch und standardisiert zu untersuchen und zu verbessern.

Auch über die aktuell existierenden Ansprüche an die prätherapeutische Bildgebung hinaus ist es wichtiger Gegenstand aktueller Forschung, weitere Merkmale und Methoden der initialen radiologischen Ausbreitungsdiagnostik mittels CT zur prognostischen Risikostratifikation exokriner Pankreaskarzinome zu etablieren. Diese könnten neben der regionalen Lymphknotenmetastasierung weitere Indikationsgrundlagen für eine neoadjuvante Therapie primär resektabler Tumore darstellen. So gibt es bereits Hinweise darauf, dass eine niedrigere Kontrastierung von Tumoren in der venösen Kontrastmittelphase einen weiteren negativen prognostischen Parameter in Bezug auf das Gesamtüberleben darstellt.[90] Es existieren auch anfängliche Ansätze für die erfolgreiche Anwendung künstlicher Intelligenz mit maschinellem Lernen zur

Vorhersage des Gesamtüberlebens anhand präoperativer CT-Untersuchungen resektabler exokriner Pankreaskarzinome.[96]

Die **Originalarbeiten 1-5** identifizieren Subgruppen von Patient:innen resezierter exokriner Pankreaskarzinome prognostischer Heterogenität auf unterschiedlichen methodischen Ebenen. Zusätzlich zu dieser prognostischen Risikostratifikation haben die Ergebnisse auch unmittelbares therapeutisches Potential.

Sowohl durch **Originalarbeit 1** als auch **Originalarbeit 2** wurden Proteine identifiziert mit prognostischen Implikationen. Die Untersuchung solcher Gewebemarker in Tumorzellen kann grundsätzlich an (prätherapeutischen) Biopsien sowie postoperativ an Tumorresektaten erfolgen. Zusätzlich zu einer prognostischen Bedeutung können so identifizierte Proteine auch als potentielle therapeutische Ziele einer gezielten Therapie dienen. Hemmstoffe des Valosin-haltigen Proteins werden bereits in klinischen Studien als Wirkstoff zur gezielten Tumortherapie untersucht.[97] Die Anwendung von PD-L1/PD-1 gerichteten Antikörper, die eine Interaktion dieser Membranproteine hemmen, sind bereits zugelassen als Immuntherapie multipler solider Tumore wie Plattenepithelkarzinomen im Kopf-Hals-Bereich oder dem Lungenkarzinom und ergänzen hier die Regime der medikamentösen Tumortherapie. Grund hierfür ist, dass sie das Gesamtüberleben verlängern können.[98] Cohen at al. beobachteten in diesem Kontext, dass ein günstiger Effekt auf das Gesamtüberleben durch PD-1-Antikörper (Pembrolizumab) bei bestimmten Indikationen von der PD-L1-Expression abhängt. So wurde ein positiver Effekt auf das Gesamtüberleben in der univariaten Analyse bei membranständiger PD-L1-Expression ≥50 % in der Tumorzellen verzeichnet, nicht aber bei <50%.[99] Auch eine Anti-VISTA-Antikörpertherapie in der Therapie solider Tumoren ist Gegenstand aktueller klinischer Studien.[100] Eine Anti-VISTA-Antikörpertherapie hat das Überleben tumortragender Mäuse verlängert bei Überexpression verbessert, nicht aber bei Kontrollgruppe ohne Überexpression.[101] Zum einen bietet die Risikostratifikation durch Identifikation von Gewebemarker mit negativen prognostischen Eigenschaften somit in der Therapie des exokrinen Pankreaskarzinoms eine potentielle Perspektive als Indikationsgrundlage einer neoadjuvanten Therapie (siehe auch 1.5). Zur prätherapeutischen Identifikation von Gewebemarkern ist eine Biopsie möglich. Die NCCN empfiehlt die Durchführung einer Biopsie vor Beginn einer neoadjuvanten Therapie.[12] Zusätzlich haben so identifizierte Gewebemarker das direkte Potential Wirkansatzpunkte einer gezielten Tumortherapie darzustellen, welche eine Ergänzung neoadjuvanter Therapieregime bedeuten könnte. Selbiges gilt für die Untersuchung von Operationsresektaten postoperativ in Bezug

auf eine adjuvante Therapie. Expressionsanalysen könnten Aufschluss darüber geben, welche konkrete gezielte Therapie Anwendung finden kann.

In der **Originalarbeit 3 und 4** wurden Operationsresektate resezierter exokriner Pankreaskarzinome untersucht. Die Ergebnisse der **Originalarbeit 3** zeigten einen negativen Einfluss auf das Gesamtüberleben einer DMI als für auch das Vorhandensein von Tumorzellen im Abstand von ≤ 1 mm an der Pankreasabsetzungsebene bei resezierten Pankreaskopfkarzinomen. Bei Pankreaskopfresektionen erfolgt in der Regel intraoperativ die Beurteilung der Pankreasabsetzungsebene mittels histopathologischer Schnellschnittuntersuchung. Bei DMI der Pankreasabsetzungsebene kann eine Nachresektion die Prognose verbessern durch einen positiven Effekt auf Gesamtüberleben.[102] Als therapeutische Perspektive sprechen die Ergebnisse der **Originalarbeit 3** dafür, dass hier die Erweiterung dieser Schnellschnittuntersuchung von einer DMI auf die Untersuchung von Tumorzellen im Abstand von bis zu 1 mm von der Pankreasabsetzungsebene die Prognose verbessern könnte. Es sollte Inhalt zukünftiger Studien sein, diesen Aspekt zu untersuchen.

Die **Originalarbeit 4** gibt Hinweise darauf, dass eine isolierte Lymphknoteninvasion per continuitatem prognostisch nicht wie das Vorhandensein von Lymphknotenmetastasen ohne Tumorkontakt einzuordnen ist. Andere Arbeiten bestärken dieses Ergebnis. Die Differenzierung dieser Subgruppen kann perspektivisch bei dieser Entscheidung zur Indikation einer neoadjuvanten Therapie auf der Grundlage des Lymphknotenstatus einfließen und muss auch bildmorphologisch in zukünftigen Studien untersucht werden.

Eine zuverlässige Verbesserung des lokoregionären Lymphknotenstaging mittels präoperativer Bildgebung würde eine suffiziente Basis zur Indikation einer neoadjuvanten Therapie auf der Grundlage des Lymphknotenstatus bieten, die aktuell nicht existiert. Eine Präzisierung der Staging-CT hierbei würde zudem dazu führen, dass diese Einschätzung in der aktuell etablierten klinischen Routine erfolgt ohne das explizite Hinzuziehen weiterer Diagnostik. In der **Originalarbeit 5** führte die Kombination der Kriterien Größe (≥10 mm kurzer Achsendurchmesser), inhomogene Signalintensität und Anzahl sichtbarer Lymphknoten ≥ 7 zu einer Erhöhung der Sensitivität und des Youden-Index des regionalen Lymphknotenstaging in der der präoperativen CT.

Trotz der präsentierten Ergebnisse haben die in diese Schrift eingeschlossenen Originalarbeiten Limitationen. So bestand eine Heterogenität der in die Studien eingeschlossenen Gruppen von

Patient:innen in Bezug die Lokalisation exokriner Pankreaskarzinome. **Originalarbeiten 1,2 und 4** schlossen Karzinome des Pankreaskopfes, -korpus und -schwanzes eine, wohingegen in die **Originalarbeiten 3 und 5** ausschließlich Patient:innen mit Tumoren des Pankreaskopfes eingeschlossen wurden. Bei der **Originalarbeit 3** ist dies dadurch begründet, dass hier explizit der prognostische Einfluss der Resektionsränder in Abhängigkeit der dort befindlichen Anatomie unter Einschluss der Gefäßrinne der oberen Mesenterialgefäße untersucht werden sollte. Das Pankreaskopfkarzinom ist die mit Abstand häufigste Tumorlokalisation resezierter duktaler Pankreaskarzinome (78,6% in Winer et al.)[103] Dies spiegelt sich auch in den Ergebnissen der **Originalarbeiten 1,2 und 4** (77-83%) wieder. Es hat jedoch nach Resektion eine schlechtere Prognose im Vergleich zu im Pankreaskorpus oder –schwanz lokalisierten Befunden.[103] Somit empfiehlt sich grundsätzlich durchaus eine differenzierte Analyse prognostischer Risikofaktoren von Subgruppen in Abhängigkeit der Lokalisation. Diese ist in den **Originalarbeiten 1,2 und 4** nicht erfolgt.

Zudem besteht eine Heterogenität der eingeschlossenen Originalarbeiten in Bezug auf Patient:innen, welche eine neoadjuvante Therapie erhalten haben. In die **Originalarbeit 1** wurden leidglich primär operierte Patient:innen eingeschlossen. In die **Originalarbeit 2 und 3** wurden vereinzelte Patient:innen mit einer Resektion nach neoadjuvanter Therapie eingeschlossen (2-3%). In der **Originalarbeit 4** hat keine Charakterisierung der Patient:innen in Bezug auf den Erhalt einer neoadjuvanten Therapie stattgefunden. In der **Originalarbeit 5** war eine neoadjuvante Therapie ein Ausschlusskriterium aufgrund potentieller Veränderung der bildmorphologischen Erscheinung von Lymphknoten in der präoperativen Bildgebung. Letztlich ist dies eine grundsätzliche Herausforderungen gegenwärtiger und zukünftiger Studien, die prognostische Risikofaktoren resektabler exokriner Pankreaskarzinome untersuchen. Der Einfluss einer neoadjuvanten Therapie auf die Prognose in Abhängigkeit spezifischer Risikofaktoren sollte zukünftig differenziert untersucht werden. Voraussetzung hierfür ist das Vorhandensein ausreichend großer Subgruppen von Patient:innen, die eine neoadjuvante Therapie erhalten haben.

Insgesamt sind die eingeschlossenen Gruppengrößen der in die jeweiligen Originalarbeiten eingeschlossenen Patient:innen erweiterbar. Die **Originalarbeit 1** ist mit 17 eingeschlossenen Patient:innen als Pilotstudie zu betrachten. Die **Originalarbeiten 2-5** schlossen 66-122 Patient:innen ein. Eine höhere Anzahl eingeschlossener Patient:innen würde die Power der einzelnen Studien erhöhen sowie die Anzahl von Patient:innen der in den jeweiligen Studien gebildeten

Subgruppen. Auch die Bildung neuer Subgruppen mit einer für Subgruppenanalysen ausreichenden Anzahl an Patient:innen wäre so möglich, z. B. in Abhängigkeit der Tumorlokalisation und Durchführung einer neoadjuvanten Therapie.

Insgesamt bestätigen die Ergebnisse in dieser Schrift präsentierter Originalarbeiten eine prognostische Heterogenität des resektablen exokrinen Pankreaskarzinoms. Die präsentierten Originalarbeiten konnten einen Beitrag zur Herausarbeitung und Präzisierung prognostischer Merkmale leisten. Bei der Behandlung des exokrinen Pankreaskarzinoms kommen bereits multimodale Therapiekonzepte zum Einsatz, die zunehmend eine neoadjuvante Therapie einschließen, vor allem bei Patient:innen mit borderline resektablen und lokal fortgeschrittenen Tumoren.[104] Die Applikation neoadjuvanter Therapie des primär resektablen Pankreaskarzinoms ist Gegenstand aktueller Untersuchungen.[105] Eine prätherapeutische Biopsie lässt die Charakterisierung von prognostischen Gewebemarkern zu und kann perspektivisch potentiell zu der Indikationsstellung einer neoadjuvanten Therapie beitragen. Auch Modifizierungen des intraoperativen Vorgehens sowie der adjuvanten Therapie auf der Grundlage von differenzierten Untersuchungen von Operationsresektaten bilden eine potentielle Perspektive.[49, 54] Im Rahmen der schlechten Prognose sowie der gegebenen Morbidität onkologischer Resektionen sollten maximal differenzierte Konzepte die Zukunftsperspektive der Risikostratifikation und Therapie des exokrinen Pankreaskarzinoms bilden.

## 4. Zusammenfassung

Die häufigsten malignen Tumoren des Pankreas sind exokrine Pankreaskarzinome.[7] Betroffene Patient:innen haben nach wie vor eine stark eingeschränkte Prognose[2] und lediglich ein Bruchteil ist zum Zeitpunkt der Diagnosestellung operabel.[3, 4] Die operative Resektion stellt weiterhin die einzige kurative Therapiemöglichkeit dar.[9, 12] Auch nach erfolgreicher onkologischer Resektion bleibt die Prognose der betroffenen Patient:innen stark eingeschränkt.[5, 6] Innerhalb der Gruppe resektabler Pankreaskarzinome besteht jedoch eine prognostische Heterogenität. [10, 21, 22, 23] Im Rahmen multimodaler Therapiekonzepte bildet eine prognostische Risikostratifikation die Grundlage für die Wahl des geeigneten Therapiekonzeptes.[9] Die Präzisierung dieser Risikostratifikation bildet somit eine potentielle Grundlage für eine exaktere Indikationsstellung des geeigneten Therapiekonzeptes. Im Kontext der stark eingeschränkten Prognose des exokrinen Pankreaskarzinoms und der Morbidität onkologischer Resektionen ist die exakte prognostische Risikostratifikation essenziel für die bestmögliche Behandlung betroffener Patient:innen. Ziel der vorliegenden Arbeit ist die Herausarbeitung von Merkmalen prognostischer Heterogenität sowie die Präzisierung ihrer Identifizierung und somit die Weiterentwicklung dieser prognostischen Risikostratifikation bei Patient:innen mit resektablem exokrinen Pankreaskarzinom.

Die **Originalarbeiten 1 und 2** untersuchen hierbei in exokrinen Pankreaskarzinomen exprimierte Proteine mit prognostischem Einfluss. In der **Originalarbeit 1** konnte mittels MALDI-TOF-MS-Analyse eine Assoziation der Expression von Kollagen-Typ 2α1, Kollagen-Typ 6α3, Aktin (zytoplasmatisch-1), Valosin-haltigem Protein, Filamin B, Histon H1.3, Spektrin beta (nicht-erythrozytär 1), Myosin-11 und Vinculin mit prognostisch relevanten histopathologischen Merkmalen resezierter exokriner Pankreaskarzinome gezeigt werden. In der **Originalarbeit 2** konnte ein negativer Einfluss der Immuncheckpoints PD-L1 und VISTA auf das Gesamtüberleben von Patient:innen mit exokrinem Pankreaskarzinom nach erfolgter onkologischer Resektion gezeigt werden. Die relative 5-Jahres-Überlebensraten in Abwesenheit von VISTA und PD-L1 war 27%, bei Vorhandensein einer der beiden Immuncheckpoints 13-15% und bei Vorhandensein beider Marker betrug die relative Überlebensrate bereits nach drei Jahren 0%.

Die **Originalarbeit 3 und 4** untersuchten prognostische Merkmale aus der pathologischen Aufarbeitung von Operationsresektaten von Patient:innen mit exokrinem Pankreaskarzinom nach operativer onkologischer Tumorentfernung. In der **Originalarbeit 3** erfolgte die systematische Analyse des Einflusses der Entfernung und Lokalisation von Tumorzellen zu Resektionsrän-

dern auf das Gesamtüberleben sowie die Entstehung von Fernmetastasen. Hier zeigte eine direkte mikroskopische Infiltration (DMI) eines Resektionsrandes einen negativen Einfluss auf das Gesamtüberleben (Median 5 vs. 19 Monate, p=0.02). In der Analyse individueller Resektionsränder hatte eine DMI als auch das Vorhandensein von Tumorzellen im Abstand von ≤ 1 mm an der Pankreasabsetzungsebene einen negativen Einfluss auf das Gesamtüberleben (Median 4 vs. 19 Monate und 6 vs. 19 Monate, p≤0.05). Das Vorhandensein von Tumorzellen im Abstand von ≤ 1 mm ausschließlich an der Gefäßrinne ging mit einer kürzeren Zeit bis zur Entwicklung von Lebermetastasen einher (50% vs. 5% der Patientinnen vier Monate nach Resektion, p=0.05). In der **Originalarbeit 4** wurde der Einfluss des Mechanismus der Lymphknoteninvasion auf das Gesamtüberleben bei Patient:innen mit exokrinem Pankreaskarzinom untersucht. Hierbei wurde differenziert zwischen der direkten Lymphknoteninvasion durch den Tumor per continuitatem (Nc), dem Vorhandensein von Lymphknotenmetastasen ohne Tumorkontakt (Nm) und dem Vorhandensein beider Formen der Lymphknoteninvasion gleichzeitig (Ncm). Das Gesamtüberleben von N0 und Nc unterschied sich nicht signifikant (p=0,13). Das Gesamtüberleben von N0 und Nm als auch von N0 und Ncm hingegen unterschied sich signifikant (p≤0.05). Diese Ergebnisse sprechen dafür, dass ein isolierter Lymphknotenbefall durch eine Lymphknoteninvasion per continuitatem durch den Tumor (Nc) nicht gleichzusetzen ist mit dem etablierten prognostischen Risikofaktor der regionalen Lymphknotenmetastasierung (pN+).

In der **Originalarbeit 5** wurde die diagnostische Genauigkeit der präoperativen Beurteilung des prognostischen Risikofaktors der regionalen Lymphknotenmetastasierung resezierter exokriner Pankreaskarzinome mittels Computertomographie untersucht. Hierbei wurde zunächst die diagnostische Genauigkeit des konventionellen Kriteriums Lymphknotengröße untersucht, welches eine Sensitivität, Spezifität und einen Youden-Index von 44%, 82% und 0,27 aufwies. Als Erweiterung des Kriteriums Größe wurde die diagnostische Genauigkeit der morphologischen Kriterien Lymphknotenkontur und –homogenität untersucht. Das Kriterium einer inhomogenen Signalintensität hatte eine Sensitivität, Spezifität und einen Youden-Index von 26%, 94% und 0,20. Eine spikulierte Lymphknotenkontur war ein sehr ebenfalls sehr spezifisches Kriterium mit einer Spezifität von 88.2%, jedoch lediglich einer Sensitivität von 12% (Youden-Index 0.00). Durch die Kombination unterschiedlicher Kriterien konnte die Sensitivität erhöht werden bei hoch bleibender Spezifität und somit die diagnostische Genauigkeit: Die Kombination der Kriterien Größe, inhomogene Signalintensität und Anzahl sichtbarer Lymphknoten n ≥ 7 zeigte eine Sensitivität, Spezifität und einen Youden-Index von 61%, 82% und 0,43.

Insgesamt bestätigt die vorliegende Arbeit eine prognostische Heterogenität des resektablen exokrinen Pankreaskarzinoms. Die Ergebnisse der Originalarbeiten dieser Schrift sind ein Beitrag zu der Herausarbeitung von Merkmalen prognostischer Heterogenität sowie der Präzisierung ihrer Identifizierung und somit zu der Weiterentwicklung der prognostischen Risikostratifikation des resektablen exokrinen Pankreaskarzinoms.

## 5. Literaturangaben


[1] Sung H, Ferlay J, Siegel RL, Laversanne M, Soerjomataram I, Jemal A, et al. Global Cancer Statistics 2020: GLOBOCAN Estimates of Incidence and Mortality Worldwide for 36 Cancers in 185 Countries. CA Cancer J Clin. 2021; 71:209-49.

[2] Robert Koch Insitut. Krebs in Deutschland für 2017/2018. 2021. https://www.krebsdaten.de/Krebs/DE/Content/Publikationen/Krebs_in_Deutschland/kid_2021/krebs_in_deutschland_2021.pdf?__blob=publicationFile. Zugriff 31.10.2024.

[3] Vincent A, Herman J, Schulick R, Hruban RH, Goggins M. Pancreatic cancer. Lancet. 2011; 378:607-20.

[4] Du T, Bill KA, Ford J, Barawi M, Hayward RD, Alame A, et al. The diagnosis and staging of pancreatic cancer: A comparison of endoscopic ultrasound and computed tomography with pancreas protocol. Am J Surg. 2018; 215:472–75.

[5] Lewis R, Drebin JA, Callery MP, Fraker D, Kent TS, Gates J, et al. A contemporary analysis of survival for resected pancreatic ductal adenocarcinoma. HPB (Oxford). 2013; 15:49-60.

[6] Belfiori G, Crippa S, Francesca A, Pagnanelli M, Tamburrino D, Gasparini G, et al. Long-Term Survivors after Upfront Resection for Pancreatic Ductal Adenocarcinoma: An Actual 5-Year Analysis of Disease-Specific and Post-Recurrence Survival. Ann Surg Oncol. 2021; 28:8249-60.

[7] Haeberle L, Esposito I. Pathology of pancreatic cancer. Transl Gastroenterol Hepatol. 2019; 4:50.

[8] Deutsche Gesellschaft für Gastroenterologie, Verdauungs- und Stoffwechselkrankheiten, S2k-Leitlinie Neuroendokrine Tumore, Langfassung Version 1.0, März 2018, verfügbar unter: https://register.awmf.org/assets/guidelines/021-026l_S2k_Neuroendokrine_Tumore_2018-07-abgelaufen.pdf (Zugriff am 31.10.2023).

[9] Deutsche Gesellschaft für Gastroenterologie, Verdauungs- und Stoffwechselkrankheiten, S3-Leitlinie zum exokrinen Pankreaskarzinom, Langversion 2.0, Dezember 2021, verfügbar unter: https://www.leitlinienprogramm-onkologie.de/fileadmin/user_upload/Downloads/Leitlinien/Pankreaskarzinom/Version_2/LL_Pankreaskarzinom_Langversion_2.0.pdf (Zugriff am 31.10.2023).

[10] Wagner M, Redaelli C, Lietz M, Seiler CA, Friess H, Büchler MW. Curative resection is the single most important factor determining outcome in patients with pancreatic adenocarcinoma. Br J Surg. 2004; 91:586-94.

[11] Shrikhande SV, Kleeff J, Reiser C, Weitz J, Hinz U, Esposito I, et al. Pancreatic resection for M1 pancreatic ductal adenocarcinoma. Ann Surg Oncol. 2007; 14:118-27.

[12] National Comprehensive Cancer Network. NCCN Clinical Practice Guidelines in Oncology (NCCN Guidelines®): Pancreatic Adenocarcinoma, Version 2.2023, Juni 2023, verfügbar unter: https://www.nccn.org/professionals/physician_gls/pdf/pancreatic.pdf (Zugriff am

31.10.2023).

[13] Takada T, Yasuda H, Amano H, Yoshida M, Uchida T. Simultaneous hepatic resection with pancreato-duodenectomy for metastatic pancreatic head carcinoma: does it improve survival? Hepatogastroenterology. 1997;44:567-73.

[14] Gebauer F, Damanakis AI, Bruns C. Oligometastasis in pancreatic cancer : Current state of knowledge and spectrum of local therapy. Chirurg. 2018;89:510-515.

[15] Takaori K, Bassi C, Biankin A, Brunner TB, Cataldo I, Campbell F, et al. International Association of Pancreatology (IAP)/European Pancreatic Club (EPC) consensus review of guidelines for the treatment of pancreatic cancer. Pancreatology. 2016; 16:14-27.

[16] Al-Hawary MM, Francis IR, Chari ST, Fishman EK, Hough DM, Lu DS, et al. Pancreatic ductal adenocarcinoma radiology reporting template: consensus statement of the Society of Abdominal Radiology and the American Pancreatic Association. Radiology. 2014; 270:248-60.

[17] Versteijne E, Vogel JA, Besselink MG, Busch ORC, Wilmink JW, Daams JG, et al.; Dutch Pancreatic Cancer Group. Meta-analysis comparing upfront surgery with neoadjuvant treatment in patients with resectable or borderline resectable pancreatic cancer. Br J Surg. 2018; 105:946-58.

[18] Gilbert JW, Wolpin B, Clancy T, Wang J, Mamon H, Shinagare AB, et al. Borderline resectable pancreatic cancer: conceptual evolution and current approach to image-based classification. Ann Oncol. 2017; 28:2067-76.

[19] Hackert T, Sachsenmaier M, Hinz U, Schneider L, Michalski CW, Springfeld C, et al. Locally Advanced Pancreatic Cancer: Neoadjuvant Therapy With Folfirinox Results in Resectability in 60% of the Patients. Ann Surg. 2016; 264:457-63.

[20] Isaji S, Mizuno S, Windsor JA, Bassi C, Fernández-Del Castillo C, Hackert T, et al. International consensus on definition and criteria of borderline resectable pancreatic ductal adenocarcinoma 2017. Pancreatology. 2018; 18:2-11.

[21] Chang DK, Johns AL, Merrett ND, Gill AJ, Colvin EK, Scarlett CJ, et al. Margin clearance and outcome in resected pancreatic cancer. J Clin Oncol. 2009; 27:2855-62.

[22] Allen PJ, Kuk D, Castillo CF, Basturk O, Wolfgang CL, Cameron JL, et al. Multi-institutional Validation Study of the American Joint Commission on Cancer (8th Edition) Changes for T and N Staging in Patients With Pancreatic Adenocarcinoma. Ann Surg. 2017 ;265:185-91.

[23] Bergquist JR, Puig CA, Shubert CR, Groeschl RT, Habermann EB, Kendrick ML, et al. Carbohydrate Antigen 19-9 Elevation in Anatomically Resectable, Early Stage Pancreatic Cancer Is Independently Associated with Decreased Overall Survival and an Indication for Neoadjuvant Therapy: A National Cancer Database Study. J Am Coll Surg. 2016; 223:52-65.

[24] Jamieson NB, Carter CR, McKay CJ, Oien KA. Tissue biomarkers for prognosis in pancreatic ductal adenocarcinoma: a systematic review and meta-analysis. Clin Cancer Res. 2011; 17:3316-31.

[25] Winter JM, Yeo CJ, Brody JR. Diagnostic, prognostic, and predictive biomarkers in pancreatic cancer. J Surg Oncol. 2013; 107:15-22.

[26] LH Sobin, Wittekind LH. International Union Against Cancer. TNM classification of malignant tumours. 5th edition. New York, Wiley–Liss; 1997.

[27] Kimbrough CW, St. Hill CR, Martin RC, McMasters KM, Scoggins CR. Tumor-positive resection margins reflect an aggressive tumor biology in pancreatic cancer. J Surg Oncol. 2013; 107:602-7.

[28] Strobel O, Hank T, Hinz U, Bergmann F, Schneider L, Springfeld C, et al. Pancreatic Cancer Surgery: The New R-status Counts. Ann Surg. 2017; 265:565-73.

[29] Ghaneh P, Kleeff J, Halloran CM, Raraty M, Jackson R, Melling J, et al. The impact of positive resection margins on survival and recurrence following resection and adjuvant chemotherapy for pancreatic ductal adenocarcinoma. Ann Surg. 2019; 269:520-9.

[30] Morales-Oyarvide V, Rubinson DA, Dunne RF, Kozak MM, Bui JL, Yuan C, et al. Lymph node metastases in resected pancreatic ductal adenocarcinoma: predictors of disease recurrence and survival. Br J Cancer. 2017; 117:1874-82.

[31] Lee ES, Lee JM. Imaging diagnosis of pancreatic cancer: a state-of-the-art review. World J Gastroenterol. 2014; 20:7864-77.

[32] Pietryga JA, Morgan DE. Imaging preoperatively for pancreatic adenocarcinoma. J Gastrointest Oncol. 2015; 6:343-57.

[33] Roche CJ, Hughes ML, Garvey CJ, Campbell F, White DA, Jones L, et al. CT and pathologic assessment of prospective nodal staging in patients with ductal adenocarcinoma of the head of the pancreas. AJR Am J Roentgenol. 2003; 180:475-80.

[34] Soriano A, Castells A, Ayuso C, Ayuso JR, de Caralt MT, Ginès MA, et al. Preoperative staging and tumor resectability assessment of pancreatic cancer: prospective study comparing endoscopic ultrasonography, helical computed tomography, magnetic resonance imaging, and angiography. Am J Gastroenterol. 2004; 99:492-501.

[35] Mirza-Aghazadeh-Attari M, Madani SP, Shahbazian H, Ansari G, Mohseni A, Borhani A, et al. Predictive role of radiomics features extracted from preoperative cross-sectional imaging of pancreatic ductal adenocarcinoma in detecting lymph node metastasis: a systemic review and meta-analysis. Abdom Radiol (NY). 2023; 48:2570-84.

[36] Pai RK, Beck AH, Mitchem J, Linehan DC, Chang DT, Norton JA, et al. Pattern of lymph node involvement and prognosis in pancreatic adenocarcinoma: direct lymph node invasion has similar survival to node-negative disease. Am J Surg Pathol. 2011; 35:228-34.

[37] Konstantinidis IT, Deshpande V, Zheng H, Wargo JA, Fernandez-del Castillo C, Thayer SP, et al. Does the mechanism of lymph node invasion affect survival in patients with pancreatic ductal adenocarcinoma? J Gastrointest Surg. 2010; 14:261-7.

[38] Goonetilleke KS, Siriwardena AK. Systematic review of carbohydrate antigen (CA 19-9) as a biochemical marker in the diagnosis of pancreatic cancer. Eur J Surg Oncol. 2007; 33:266-70.

[39] Luo G, Jin K, Deng S, Cheng H, Fan Z, Gong Y, et al. Roles of CA19-9 in pancreatic cancer: Biomarker, predictor and promoter. Biochim Biophys Acta Rev Cancer. 2021; 1875:188409.

[40] Hartwig W, Strobel O, Hinz U, Fritz S, Hackert T, Roth C, et al. CA19-9 in potentially resectable pancreatic cancer: perspective to adjust surgical and perioperative therapy. Ann Surg Oncol. 2013; 20:2188-96.

[41] Yoon KW, Heo JS, Choi DW, Choi SH. Factors affecting long-term survival after surgical resection of pancreatic ductal adenocarcinoma. J Korean Surg Soc. 2011; 81:394-401.

[42] Azizian A, Rühlmann F, Krause T, Bernhardt M, Jo P, König A, et al. CA19-9 for detecting recurrence of pancreatic cancer. Sci Rep. 2020; 10:1332.

[43] Alaiya A, Al-Mohanna M, Linder S. Clinical cancer proteomics: promises and pitfalls. J Proteome Res. 2005; 4:1213-22.

[44] Casadonte R, Caprioli RM. Proteomic analysis of formalin-fixed paraffin-embedded tissue by MALDI imaging mass spectrometry. Nat Protoc. 2011; 6:1695-709.

[45] Al-Batran SE, Homann N, Pauligk C, Goetze TO, Meiler J, Kasper S, et al.; FLOT4-AIO Investigators. Perioperative chemotherapy with fluorouracil plus leucovorin, oxaliplatin, and docetaxel versus fluorouracil or capecitabine plus cisplatin and epirubicin for locally advanced, resectable gastric or gastro-oesophageal junction adenocarcinoma (FLOT4): a randomised, phase 2/3 trial. Lancet. 2019; 393:1948-57.

[46] Tepper J, Krasna MJ, Niedzwiecki D, Hollis D, Reed CE, Goldberg R, et al. Phase III trial of trimodality therapy with cisplatin, fluorouracil, radiotherapy, and surgery compared with surgery alone for esophageal cancer: CALGB 9781. J Clin Oncol. 2008; 26:1086-92.

[47] Fathi A, Christians KK, George B, Ritch PS, Erickson BA, Tolat P, et al. Neoadjuvant therapy for localized pancreatic cancer: guiding principles. J Gastrointest Oncol. 2015; 6:418-29.

[48] Varadhachary GR, Tamm EP, Abbruzzese JL, Xiong HQ, Crane CH, Wang H, et al. Borderline resectable pancreatic cancer: definitions, management, and role of preoperative therapy. Ann Surg Oncol. 2006; 13:1035-46.

[49] Turpin A, El Amrani M, Bachet JB, Pietrasz D, Schwarz L, Hammel P. Adjuvant Pancreatic Cancer Management: Towards New Perspectives in 2021. Cancers (Basel). 2020; 12:3866.

[50] van Roessel S, van Veldhuisen E, Klompmaker S, Janssen QP, Abu Hilal M, Alseidi A, et al. Evaluation of Adjuvant Chemotherapy in Patients With Resected Pancreatic Cancer After Neoadjuvant FOLFIRINOX Treatment. JAMA Oncol. 2020; 6:1733–40.

[51] Sharma P, Allison JP. The future of immune checkpoint therapy. Science. 2015; 348:56-61.

[52] Topalian SL, Taube JM, Pardoll DM. Neoadjuvant checkpoint blockade for cancer immunotherapy. Science. 2020; 367:eaax0182.

[53] Johansson H, Andersson R, Bauden M, Hammes S, Holdenrieder S, Ansari D. Immune checkpoint therapy for pancreatic cancer. World J Gastroenterol. 2016; 22:9457-76.

[54] Birgin E, Rasbach E, Téoule P, Rückert F, Reissfelder C, Rahbari NN. Impact of intraoperative margin clearance on survival following pancreatoduodenectomy for pancreatic cancer: a systematic review and meta-analysis. Sci Rep. 2020; 10:22178.

[55] Reva B, Antipin Y, Sander C. Predicting the functional impact of protein mutations: application to cancer genomics. Nucleic Acids Res. 2011; 39:e118.

[56] Maehara Y, Tomoda M, Hasuda S, Kabashima A, Tokunaga E, Kakeji Y, et al. Prognostic value of p53 protein expression for patients with gastric cancer--a multivariate analysis. Br J Cancer. 1999; 79:1255-61.

[57] Lipponen P, Ji H, Aaltomaa S, Syrjänen S, Syrjänen K. p53 protein expression in breast cancer as related to histopathological characteristics and prognosis. Int J Cancer. 1993; 55:51-6.

[58] Martin-Perez E, Capdevila J, Castellano D, Jimenez-Fonseca P, Salazar R, Beguiristain-Gomez A, et al. Prognostic factors and long-term outcome of pancreatic neuroendocrine neoplasms: Ki-67 index shows a greater impact on survival than disease stage. The large experience of the Spanish National Tumor Registry (RGETNE). Neuroendocrinology. 2013; 98:156-68.

[59] Cancer Genome Atlas Research Network. Integrated Genomic Characterization of Pancreatic Ductal Adenocarcinoma. Cancer Cell. 2017; 32:185–203.e13.

[60] Luo J. KRAS mutation in pancreatic cancer. Semin Oncol. 2021; 48:10-18.

[61] Mizrahi JD, Surana R, Valle JW, Shroff RT. Pancreatic cancer. Lancet. 2020; 395:2008-20.

[62] Oshima M, Okano K, Muraki S, Haba R, Maeba T, Suzuki Y, et al. Immunohistochemically detected expression of 3 major genes (CDKN2A/p16, TP53, and SMAD4/DPC4) strongly predicts survival in patients with resectable pancreatic cancer. Ann Surg. 2013; 258:336-46

[63] Tascilar M, Skinner HG, Rosty C, Sohn T, Wilentz RE, Offerhaus GJ, et al. The SMAD4 protein and prognosis of pancreatic ductal adenocarcinoma. Clin Cancer Res. 2001; 7:4115-21.

[64] Shugang X, Hongfa Y, Jianpeng L, Xu Z, Jingqi F, Xiangxiang L, et al. Prognostic Value of SMAD4 in Pancreatic Cancer: A Meta-Analysis. Transl Oncol. 2016; 9:1-7.

[65] Smith RA, Tang J, Tudur-Smith C, Neoptolemos JP, Ghaneh P. Meta-analysis of immunohistochemical prognostic markers in resected pancreatic cancer. Br J Cancer. 2011; 104:1440-51.

[66] Zhao H, Wang Q, Wang X, Zhu H, Zhang S, Wang W, et al. Correlation Between RAB27B and p53 Expression and Overall Survival in Pancreatic Cancer. Pancreas. 2016; 45:204-10.

[67] Iwatate Y, Hoshino I, Ishige F, Itami M, Chiba S, Arimitsu H, et al. Prognostic significance of p16 protein in pancreatic ductal adenocarcinoma. Mol Clin Oncol. 2020; 13:83-91.

[68] Bold RJ, Hess KR, Pearson AS, Grau AM, Sinicrope FA, Jennings M, et al. Prognostic factors in resectable pancreatic cancer: p53 and bcl-2. J Gastrointest Surg. 1999; 3:263-77.

[69] Wang Y, Zhong X, Zhou L, Lu J, Jiang B, Liu C, et al. Prognostic Biomarkers for Pancreatic Ductal Adenocarcinoma: An Umbrella Review. Front Oncol. 2020; 10:1466.

[70] Tan WCC, Nerurkar SN, Cai HY, Ng HHM, Wu D, Wee YTF, et al. Overview of multiplex immunohistochemistry/immunofluorescence techniques in the era of cancer immunotherapy. Cancer Commun (Lond). 2020; 40:135-53.

[71] Wang M, Liu Y, Cheng Y, Wei Y, Wei X. Immune checkpoint blockade and its combination therapy with small-molecule inhibitors for cancer treatment. Biochim Biophys Acta Rev Cancer. 2019; 1871:199-224.

[72] Goodwin RJ, Pennington SR, Pitt AR. Protein and peptides in pictures: imaging with MALDI mass spectrometry. Proteomics. 2008; 8:3785-800.

[73] Gemoll T, Roblick UJ, Habermann JK. MALDI mass spectrometry imaging in oncology (Review). Mol Med Rep. 2011; 4:1045-51.

[74] Hermanek P. Chirurgische Pathologie des Pankreaskarzinoms. In: Trede M., Saeger H.D., Hrsg. Aktuelle Pankreaschirurgie: 1. Auflage. Berlin Heidelberg, Springer; 1990. S. 3-12.

[75] Tumoren des Verdauungstraktes, Pankreas. In: Wittekind C. Hrsg. TNM-Klassifikation maligner Tumoren: 8. Auflage. Weinheim, Wiley-VCH; 2020 S.126-9.

[76] van Roessel S, Kasumova GG, Verheij J, Najarian RM, Maggino L, de Pastena M, et al. International Validation of the Eighth Edition of the American Joint Committee on Cancer (AJCC) TNM Staging System in Patients With Resected Pancreatic Cancer. JAMA Surg. 2018; 153:e183617.

[77] Williams JL, Nguyen AH, Rochefort M, Muthusamy VR, Wainberg ZA, Dawson DW, et al. Pancreatic cancer patients with lymph node involvement by direct tumor extension have similar survival to those with node-negative disease. J Surg Oncol. 2015; 112:396-402.

[78] Pai RK, Beck AH, Mitchem J, Linehan DC, Chang DT, Norton JA, et al. Pattern of lymph node involvement and prognosis in pancreatic adenocarcinoma: direct lymph node invasion has similar survival to node-negative disease. Am J Surg Pathol. 2011; 35:228-34.

[79] Hashimoto D, Satoi S, Ishida M, Nakagawa K, Kotsuka M, Takagi T, et al. Does direct invasion of peripancreatic lymph nodes impact survival in patients with pancreatic ductal adenocarcinoma? A retrospective dual-center study. Pancreatology. 2021; 21:884-91.

[80] Wittekind C, Compton C, Quirke P, Nagtegaal I, Merkel S, Hermanek P, et al. A uniform residual tumor (R) classification: integration of the R classification and the circumferential margin status. Cancer. 2009; 115:3483-8.

[81] P Hermanek, LH Sobin. TNM Classification of Malignant Tumors. 4th ed. Berlin, Springer; 1987.

[82] Pollheimer MJ, Langner C. Pathologie der R1-Klassifikation in der viszeralonkologischen Chirurgie. Chirurg. 2017; 88:731-9.

[83] Wasif N, Ko CY, Farrell J, Wainberg Z, Hines OJ, Reber H, et al. Impact of tumor grade on prognosis in pancreatic cancer: should we include grade in AJCC staging? Ann Surg Oncol. 2010; 17:2312-20.

[84] Sobin LH, Gospodarowicz MK, Wittekind C. TNM classification of malignant tumours. 7th edition. Hoboken, John Wiley & Sons; 2011.

[85] Karamitopoulou E, Zlobec I, Born D, Kondi-Pafiti A, Lykoudis P, Mellou A, et al. Tumour budding is a strong and independent prognostic factor in pancreatic cancer. Eur J Cancer. 2013; 49:1032-9.

[86] Bilici A. Prognostic factors related with survival in patients with pancreatic adenocarcinoma. World J Gastroenterol. 2014; 20:10802-12.

[87] Hartwig W, Hackert T, Hinz U, Gluth A, Bergmann F, Strobel O, et al. Pancreatic cancer surgery in the new millennium: better prediction of outcome. Ann Surg. 2011; 254:311-9.

[88] Yachida S, White CM, Naito Y, Zhong Y, Brosnan JA, Macgregor-Das AM, et al. Clinical significance of the genetic landscape of pancreatic cancer and implications for identification of potential long-term survivors. Clin Cancer Res. 2012; 18:6339-47.

[89] Hong SB, Choi SH, Kim KW, Kim SY, Kim JH, Kim S, et al. Meta-analysis of MRI for the diagnosis of liver metastasis in patients with pancreatic adenocarcinoma. J Magn Reson Imaging. 2020; 51:1737-44.

[90] Rhee H, Park MS. The Role of Imaging in Current Treatment Strategies for Pancreatic Adenocarcinoma. Korean J Radiol. 2021; 22:23-40.

[91] Brown G, Richards CJ, Bourne MW, Newcombe RG, Radcliffe AG, Dallimore NS, et al. Morphologic predictors of lymph node status in rectal cancer with use of high-spatial-resolution MR imaging with histopathologic comparison. Radiology. 2003; 227:371-7.

[92] Shin J, Shin S, Lee JH, Song KB, Hwang DW, Kim HJ, et al. Lymph node size and its association with nodal metastasis in ductal adenocarcinoma of the pancreas. J Pathol Transl Med. 2020; 54:387-95.

[93] Elsholtz FHJ, Asbach P, Haas M, Becker M, Beets-Tan RGH, Thoeny HC, et al. Introducing the Node Reporting and Data System 1.0 (Node-RADS): a concept for standardized assessment of lymph nodes in cancer. Eur Radiol. 2021; 31:6116-24.

[94] Wang XY, Yang F, Jin C, Fu DL. Utility of PET/CT in diagnosis, staging, assessment of resectability and metabolic response of pancreatic cancer. World J Gastroenterol. 2014; 20:15580-9.

[95] Kim HR, Seo M, Nah YW, Park HW, Park SH. Clinical impact of fluorine-18-fluorodeoxyglucose positron emission tomography/computed tomography in patients with resectable pancreatic cancer: diagnosing lymph node metastasis and predicting survival. Nucl Med Commun. 2018; 39:691-8.

[96] Yao J, Cao K, Hou Y, Zhou J, Xia Y, Nogues I, et al. Deep Learning for Fully Automated Prediction of Overall Survival in Patients Undergoing Resection for Pancreatic Cancer: A Retrospective Multicenter Study. Ann Surg. 2023; 278:e68-e79.

[97] Kilgas S, Ramadan K. Inhibitors of the ATPase p97/VCP: From basic research to clinical applications. Cell Chem Biol. 2023; 30:3-21.

[98] Zander H, Müller-Egert S, Zwiewka M, Groß S, van Zandbergen G, Engelbergs J. Checkpointinhibitoren in der Tumortherapie [Checkpoint inhibitors for cancer therapy]. Bundesgesundheitsblatt Gesundheitsforschung Gesundheitsschutz. 2020; 63:1322-30.

[99] Cohen EEW, Soulières D, Le Tourneau C, Dinis J, Licitra L, Ahn MJ, et al.; KEYNOTE-040 investigators. Pembrolizumab versus methotrexate, docetaxel, or cetuximab for recurrent or metastatic head-and-neck squamous cell carcinoma (KEYNOTE-040): a randomised, open-label, phase 3 study. Lancet. 2019; 393:156-67.

[100] Kilgas S, Ramadan K. Inhibitors of the ATPase p97/VCP: From basic research to clinical applications. Cell Chem Biol. 2023; 30:3-21.

[101] Mulati K, Hamanishi J, Matsumura N, Chamoto K, Mise N, Abiko K, et al. VISTA expressed in tumour cells regulates T cell function. Br J Cancer. 2019; 120:115-27.

[102] Zhang B, Lee GC, Qadan M, Fong ZV, Mino-Kenudson M, Desphande V, et al. Revision of Pancreatic Neck Margins Based on Intraoperative Frozen Section Analysis Is Associated With Improved Survival in Patients Undergoing Pancreatectomy for Ductal Adenocarcinoma. Ann Surg. 2021; 274:e134-42.

[103] Winer LK, Dhar VK, Wima K, Morris MC, Lee TC, Shah SA, et al. The Impact of Tumor Location on Resection and Survival for Pancreatic Ductal Adenocarcinoma. J Surg Res. 2019; 239:60-6.

[104] Nassour I, Parrish A, Baptist L, Voskamp S, Handoo K, Rogers S, et al. National adoption of neoadjuvant chemotherapy: paradigm shift in the treatment of pancreatic cancer. HPB (Oxford). 2023; 25:1323-8.

[105] Springfeld C, Ferrone CR, Katz MHG, Philip PA, Hong TS, Hackert T, et al. Neoadjuvant therapy for pancreatic cancer. Nat Rev Clin Oncol. 2023; 20:318-37.

**Danksagung**

Mein herzlicher Dank gilt Prof. Dr. Martin E. Kreis, der durch seine Motivation zunächst den Grundstein für diese Habilitation gelegt und im Verlauf maßgeblich zu ihrem Abschluss beigetragen hat. An dieser Stelle möchte ich mich bei ihm insbesondere auch für sein offenes Ohr, seine Geduld und seine beständige Unterstützung bedanken. Auch bei Frau Prof. Dr. Katharina Beyer bedanke ich mich herzlich. Ihrer Unterstützung verdanke ich ebenfalls maßgeblich die erfolgreiche Durchführung dieser Habilitation. Bei beiden möchte ich mich auch für die hervorragende klinische Ausbildung bedanken.

Besonders danken möchte ich Prof. Dr. Carsten Kamphues. Er hat mir die Durchführung zahlreicher Forschungsprojekte ermöglicht, sie intensiv begleitet und mich bei allen Belangen meiner wissenschaftlichen Karriere in ganz besonderem Maße unterstützt. Auch darüber hinaus war er für mich in der Zeit meiner Ausbildung durch Rat, Tat und Humor eine große Stütze. Durch seine Werte und sein Wesen ist er für mich ein wertvolles Vorbild und ein Freund geworden.

Für die interdisziplinäre Zusammenarbeit möchte ich mich insbesondere bei PD Dr. Rolf Reiter, Dr. Simon Schallenberg, Dr. Mihnea P. Dragomir, PD Dr. Jürgen Braun und Prof. Dr. Patrick Asbach bedanken, mit denen ich spannende Projekte durchführen und schöne Freizeitstunden verbringen durfte

Bei meinen Eltern, meiner Familie und meinem Freundeskreis möchte ich mich auch ganz besonders herzlich bedanken. Sie haben ebenfalls einen ganz maßgeblichen Beitrag zu dieser Habilitation geleistet durch Zuspruch, Verständnis, Verzicht und Treue.

**Erklärung**

§ 4 Abs. 3 (k) der HabOMed der Charité

Hiermit erkläre ich, dass

- weder früher noch gleichzeitig ein Habilitationsverfahren durchgeführt oder angemeldet wurde,
- die vorgelegte Habilitationsschrift ohne fremde Hilfe verfasst, die beschriebenen Ergebnisse selbst gewonnen sowie die verwendeten Hilfsmittel, die Zusammenarbeit mit anderen Wissenschaftlern/Wissenschaftlerinnen und mit technischen Hilfskräften sowie die verwendete Literatur vollständig in der Habilitationsschrift angegeben wurden,
- mir die geltende Habilitationsordnung bekannt ist.

Ich erkläre ferner, dass mir die Satzung der Charité – Universitätsmedizin Berlin zur Sicherung Guter Wissenschaftlicher Praxis bekannt ist und ich mich zur Einhaltung dieser Satzung verpflichte.

Berlin, den 21.01.2024 Dr. med. Florian Nino Loch